UNIVERSIDADE DE SANTIAGO DE COMPOSTELA
Departamento de Enxeñaría Química

Biopolymers production by *Halomonas boliviensis* in an integrated biorefinery

Memoria presentada por

María García Torreiro

Para obtar ó grado de Doutor pola
Universidade de Santiago de Compostela

Santiago de Compostela, Febreiro de 2017

UNIVERSIDADE DE SANTIAGO DE COMPOSTELA

Departamento de Enxeñaría Química

Juan M. Lema Rodicio, Catedrático de Enxeñaría Química, e Thelmo A. Lú Chau, Investigador, ámbolos dous pertencentes á Universidade de Santiago de Compostela, informan:

Que a presente memoria, titulada "Biopolymers production by *Halomonas boliviensis* in an integrated biorefinery" presentada por Dona María García Torreiro, para obtar ó grado de Doutor en Enxeñería Química no Programa de Doutoramento en Enxeñería Química e Ambiental, realizouse baixo a nosa inmediata dirección no Departamento de Enxeñaría Química da Universidade de Santiago de Compostela.

E para que así conste, firman o presente informe en Santiago de Compostela, Febreiro de 2017.

Os directores:

Juan M. Lema Rodicio Thelmo A. Lú Chau

A doutoranda:

María García Torreiro

Agradecimientos

CONTENTS

Abbreviations & Acronyms

1G: first generation
2G: second generation
3G: third generation
3HB: 3-hydroxybutyrate
3HV: 3-hydroxyvalerate
4HB: 4-hydroxybutyrate
ASTM: American Society for Testing and Materials
ATCC: American Type Culture Collection
AUC: area under the curve
BLAST: Basic Local Alignment Search Tool
BC: batch culture (media)
C: carbon
CDW: cell dry weight
CECT: Colección Española de Cultivos Tipo
CI: confident intervals
CS: corn syrup
D: dose
DDGS: distiller's dried grains with solubles
DMSO: dimethyl sulfoxide
DSC: differential scanning calorimetry
FB: fed-batch
FBC: fed-batch culture (media)
FC: flow cytometry
FID: flame ionization detector
FL1: fluorescence signal
FS: forward scattering
G: glucose
GC: gas chromatography
HHx: 3-hydroxyhexanoate
HPLC: high-performance liquid chromatography
IC: inoculum culture (media)
IC: ion chromatography
IR: infrared
LA: levulinic acid
LMD: list mode data (files)
N: nitrogen
NL: nitrogen-limiting (conditions)
NL-O_2: nitrogen -limiting with low O_2 supply (conditions)
NMR: Nuclear Magnetic Resonance
MSG: monosodium glutamate
OD: optical density
P3HB: poly(3-hydroxybutyrate)

P3HV: poly(3-hydroxyvalerate)
P(3HB-co-3HV): copolymer poly(3-hydroxybutyrate-co-3-hydroxyvalerate)
PA: polyamide
PBAT: polybutyrate adipate terephthalate
PBS: phosphate buffered saline
PCL: polycaprolactone
PCR: Polymerase Chain Reaction
PE: polyethylene
PET: polyethylene terephthalate
PHA: polyhydroxyalkanoates
PHA^+: PHA containing cells
PHA^-: PHA not containing cells
phaA: 3-ketothiolase
phaB: NADPH-dependent acetoacetyl-CoA reductase
phaC: P3HB synthase
PLA: polylatic acid
PP: polypropylene
PS: polystyrene
PTT: polytrimethylene terephtalate
RCM: residual cell mass
S: sucrose
SC: sugarcane
SD: standard deviation
SHF: separate hydrolysis and fermentation
SS: side scattering
SSF: simultaneous saccharification and fermentation
TCA: tricarboxylic acid (cycle)
TEM: transmission electron microscope
TN: total nitrogen
TOC: total organic carbon
UV: ultraviolet
VFA: volatile fatty acids
VSS: volatile suspended solids
WWTP: wastewater treatment plant

Resumen

El principal objetivo de esta tesis es desarrollar procesos que permitan integrar la producción de biopolímeros en biorrefinerías a partir de sustratos de primera y segunda generación. El cambio climático, el descenso de la disponibilidad del petróleo y el rápido crecimiento de la población motivan el desarrollo de nuevos procesos que dependan de materias primas renovables para sustituir procesos basados en síntesis petroquímicas. Además, la generación de residuos plásticos se está convirtiendo en un problema medioambiental importante debido al carácter recalcitrante de los plásticos derivados del petróleo.

Los biopolímeros, materiales biodegradables y/o obtenidos a través de un proceso renovable, son una alternativa ambientalmente sostenible frente al uso de plásticos de origen fósil. Entre los diversos tipos de biopolímeros destacan los polihidroxialcanoatos (PHA), un tipo de poliéster termoplástico, natural y biodegradable, producido por ciertos microorganismos como material de reserva. Sin embargo, a pesar de los beneficios que presentan los biopolímeros, la producción industrial de PHA se ve dificultada por unos costes de producción mas altos que el de los plásticos obtenidos a partir del petróleo. La reducción de estos costes depende del desarrollo y aplicación de nuevas estrategias de fermentación y tecnologías de recuperación del producto, así como del microorganismo y la fuente de carbono utilizadas para su obtención. En esta tesis se utilizó la bacteria halófila *Halomonas boliviensis* como microorganismo productor debido a su capacidad de acumular PHA en grandes cantidades.

En primer lugar, se llevaron a cabo una serie de experimentos para determinar los requisitos nutricionales básicos de crecimiento y producción de PHA para este microorganismo. Además, se desarrolló una metodología analítica basada en la citometría de flujo para cuantificar de manera rápida el contenido de PHA.

A continuación, se evaluaron dos materias primas de primera generación, cereal y jugo de caña, como fuente de carbono para producir PHA utilizando *H. boliviensis*. Se implementó y evaluó una novedosa configuración de proceso, basada en la estrategia de sacarificación y fermentación simultánea, para la producción de PHA a partir de cereal. Por último, se evaluó el uso de ácidos grasos volátiles derivados de corrientes residuales como fuente de carbono, ampliando de esta forma el concepto de biorrefinería.

En resumen, los resultados de esta tesis proporcionan posibles rutas para la formulación de procesos que permitan integrar la producción de biopolímeros en una biorrefinería y, particularmente, información sobre la capacidad de acumulación de PHA en *H. boliviensis*.

Palabras clave: biorrefinería, polihidroxialcanoatos, *Halomonas boliviensis*.

Resumo

O principal obxetivo desta tese é desenvolver procesos que permitan integrar a produción de biopolímeros en biorrefinerías a partir de substratos de primeira e segunda xeración. O cambio climático, o descenso da disponibilidade do petróleo e o rápido crecemento da poboación motivan o desenvolvemento de novos procesos que dependan de materias primas renovables para substituir procesos basados na síntese petroquímica. Ademais, a xeración de residuos plásticos estase a converter nun problema medioambiental importante debido ó carácter recalcitrante dos plásticos derivados do petróleo.

Os biopolímeros, materiais biodegradables e/ou obtidos a través dun proceso renovable, son unha alternativa ambientalmente sostible frente ó uso de plásticos de orixe fósil. Entre os diversos tipos de biopolímeros destacan os polihidroxialcanoatos (PHA), un tipo de poliéster termoplástico, natural e biodegradable, producido por algúns microorganismos como material de reserva. Sen embargo, a pesar dos beneficios que presentan os biopolímeros, a produción industrial de PHA vese dificultada por unhos custos de produción máis altos que os dos plásticos obtidos a partir do petróleo. A redución destos custos depende do desenvolvemento e aplicación de novas estratexias de fermentación e tecnoloxías de recuperación do producto, así como do microorganismo e a fonte de carbono utilizada para a sua obtención. Nesta tese utilizouse a bacteria halófila *Halomonas boliviensis* como microorganismo productor debido á sua capacidade de acumular PHA en grandes cantidades.

En primeiro lugar, levarónse a cabo unha serie de experimentos para determinar os requisitos nutricionais básicos de crecemento e produción de PHA para este microorganismo. Ademais, desenvolveuse unha metodoloxía analítica basada na citometría de fluxo para cuantificar de maneira rápida o contido de PHA.

A continuación, avaliaronse duas materias primas de primeira xeración, cereal e zume de cana de azucre, como fonte de carbono para producir PHA utilizando *H. boliviensis*. Implementouse e avaliouse unha novedosa configuración de proceso, basada na estratexia de sacarificación e fermentación simultáneas, na produción de PHA a partir de cereais. Por último, avaliouse o uso de ácidos grasos volátiles derivados de correntes residuais como fonte de carbono, ampliando desta forma o concepto de biorrefinería.

En resumo, os resultados desta tese proporcionan posibles rutas para a formulación de procesos que permitan integrar a produción de biopolímeros nunha biorrefinería y, particularmente, información sobre a capacidade de acumulación de PHA en *H. boliviensis*.

Palabras chave: biorrefinería, polihidroxialcanoatos, *Halomonas boliviensis*.

Abstract

The main aim of this Thesis is to develop processes that allow the integrated production of biopolymers into biorefineries, using feedstocks from first and second generation as raw materials. Climate change, the decrease of the fossil fuel resources and the rapid increase of the world population trigger the development of new processes based on the utilization of renewable raw materials for the replacement of the processes based on the petrochemical synthesis. Moreover, the generation of plastics residues is turning into an important environmental problem due to the recalcitrant feature of the plastics derived from petrol.

Biopolymers, biodegradable and/or biobased plastic-like materials, are an environmentally sustainable alternative to the use of petroleum-based plastics. Among the several types of biopolymers, polyhydroxyalkanoates (PHA) stand out. PHA is a type of thermopolyester, biobased and biodegradable, produced by certain microorganisms as a storage material. Nevertheless, despite the benefits presented by the biopolymers, the industrial production of PHA is threatened by a production costs higher than that of the petroleum-based plastics. The reduction of the PHA production costs depends on the development and application of new fermentation strategies, downstreams processes, the microorganism and carbon source used for its production. The halophilic bacterium *Halomonas boliviensis* was used in this Thesis as PHA producer organism due to its capacity to accumulate PHA in high amounts.

Firstly, experiments were carried out in order to determine the basic nutritional requirements for growth and PHA accumulation with this microorganism. Besides, an analytical methodology based on the flow cytometry was developed for a faster quantification of the PHA content.

Then, two different substrates from first generation feedstocks, cereal and sugarcane juice, were evaluated as carbon source for PHA production by *H. boliviensis*. A novel process configuration was implemented and evaluated, based on the strategy of simultaneous saccharification and fermentation, for the PHA production from cereal mash. Finally, the utilization of volatile fatty acids, derived from residual streams, was evaluated as carbon source. This allowed to upgrade the biorefinery concept.

To sum up, the results of this Thesis provide different routes for the formulation of processes that allow the integration of the biopolymers production into a biorefinery and, particularly, information about the general PHA accumulation capacity of *H. boliviensis* and its specific performance growing on complex carbon sources.

Key words: biorefinery, polyhydroxyalcanoates, *Halomonas boliviensis*.

Resumen extendido

La invención de los plásticos data del año 1869, tras el desarrollo del celuloide. Sin embargo, no es hasta el final de la Segunda Guerra Mundial cuando la producción de plásticos se dispara, llegando a alcanzar una producción mundial de 311 Mt en el año 2014. Su irremediable éxito tiene se explica por sus propiedades superiores con respecto a otros materiales y su bajo coste. Así, los plásticos se convirtieron en materiales omnipresentes y casi indispensables para nuestra vida diaria. Sin embargo, a pesar de ser uno de los mayores productos industriales del mundo, su producción tal y como se conoce se ve amenazada. La obtención de la mayor parte de los plásticos que se emplean actualmente se basa en la industria petroquímica. Debido a preocupaciones como el cambio climático, el descenso de la disponibilidad del petróleo y el rápido crecimiento de la población, se está realizando un gran esfuerzo para intentar sustituir la síntesis petroquímica de los plásticos por otros procesos que dependan de fuentes renovables. Además, la generación de residuos plásticos se está convirtiendo en un problema importante. Más de un 30% de los residuos de plástico generados al año no llegan a puntos de reciclaje, y debido a su carácter recalcitrante y a su capacidad para adsorber compuestos tóxicos en su superficie, estos residuos desencadenan un grave impacto en el medioambiente.

Los biopolímeros, materiales biodegradables y/o obtenidos por un proceso renovable, constituyen una alternativa ambientalmente sostenible al uso de plásticos de origen fósil. Entre ellos destacan los polihidroxialcanoatos (PHA), un tipo de poliéster termoplástico, natural y biodegradable; que se sintetiza y acumula en el interior de distintos microorganismos, como reserva de carbono y energía, bajo condiciones limitantes de un nutriente esencial como nitrógeno, fósforo o incluso oxígeno, y en exceso de carbono. El poli(3-hidroxibutirato) (P3HB) es uno de los PHA más conocidos y el que suele acumularse con mayor facilidad. Además, las propiedades de este biopolímero son muy semejantes a las del polipropileno.

El proceso de producción de PHA se ha escalado a nivel industrial y se han desarrollado diversos materiales y objetos a partir de este biopolímero. Sin embargo, estos materiales todavía no pueden competir con los plásticos de origen fósil debido a los altos costes de producción. La reducción de estos costes depende del desarrollo y aplicación de nuevas estrategias de fermentación y de tecnologías de recuperación del producto, así como el microorganismo y la fuente de carbono utilizadas para su obtención.

En el año 2012, los problemas ambientales y sociales derivados del uso del petróleo, así como su carácter no renovable, motivaron el desarrollo por parte de la Unión Europea de una estrategia para impulsar la economía hacia un aprovechamiento mayor y más sostenible de los recursos renovables, lo que se conoce como bioeconomía. El objetivo es alcanzar una economía basada en procesos más innovadores y con bajas emisiones, que concilie las demandas de gestión sostenible tanto de las industrias alimentarias, como las de la utilización de los recursos biológicos renovables para fines industriales, garantizando la biodiversidad y la protección del medio ambiente. En este contexto, surgen las biorrefinerías, plantas industriales en las que, a partir de materias primas de base biológica,

se obtienen una gran diversidad de nuevos compuestos, además de energía. En trabajos previos se postula que los biopolímeros tendrán un rol central en las biorrefinerías del futuro.

Halomonas boliviensis es uno de los organismos capaces de acumular PHA en grandes cantidades. Se trata de un organismo extremófilo y, por lo tanto, presenta algunas características especiales como tolerancia a altas concentraciones de sal, a pH alcalino y a temperaturas que van desde 0 hasta 45°C. Su tolerancia a altas concentraciones de sal (5% w/v NaCl) permite reducir o incluso evitar el proceso de esterilización. Por lo tanto, su uso puede suponer un menor coste energético. Esta bacteria presenta como característica importante, que deriva también de su carácter halófilo, la producción de un compuesto conocido como ectoína. Este compuesto es un tipo de soluto compatible, usado por la bacteria como protección frente al estrés osmótico causado por la alta salinidad del medio. Esta molécula está considerada como un producto de volumen de producción bajo pero de valor alto en el mercado, ya que presenta propiedades muy apreciadas en la industria farmacéutica y cosmética. De hecho, en un estudio previo sobre la viabilidad tecno-económica y ambiental de un proceso integrado de producción de bioethanol y PHA (con *Pachysolen tannophilus* y *H. boliviensis*, respectivamente) a partir de paja de trigo, se concluyó que el proceso resultaba económicamente más sostenible si se incluía la producción de ectoína.

Varios organismos halófilos, especialmente del género *Halomonas* spp., han despertado interés para su aplicación en procesos industriales debido al particular abanico de productos que se pueden obtener a partir de ellos, tales como enzimas que actúan a pH alcalino, biosurfactantes y emulsionantes, a parte de PHA o ectoína.

El principal objetivo de esta Tesis es el desarrollo de metodologías que permitan integrar la producción de biopolímeros en una biorrefinería a partir de sustratos de primera y segunda generación.

Se presenta una metodología detallada que permite la integración de un proceso de producción de biopolímeros en una biorrefinería. En este trabajo se evalúan las materias primas, tecnologías, productos y rutas de proceso para obtener la configuración optima que mejor se adecue a cada tipo de proceso.

El contenido de esta Tesis se puede dividir en dos grandes bloques temáticos. En el primero (Capítulos 3 y 4) se estudia el comportamiento de la bacteria *H. boliviensis* con el objetivo de encontrar la mejor configuración de proceso que permita incrementar la producción de PHA. En el segundo bloque (Capítulos 5, 6 y 7) se lleva a cabo la producción de PHA a partir de sustratos renovables, típicamente usados en las biorrefinerías.

En el Capítulo 2 se detallan los materiales y métodos generales usados en este trabajo. En el Capítulo 3 se presenta un estudio detallado de los requerimientos nutricionales de esta bacteria y cómo el tipo y grado de limitación de diferentes nutrientes influye sobre la acumulación del biopolímero. En el Capítulo 4, se desarrolla un método rápido y directo para cuantificar la producción de PHA, basado en la aplicación de una técnica ampliamente conocida en biotecnología como la citometría de flujo.

En los Capítulos 5 y 6 se estudia la producción de P3HB a partir de sustratos de primera generación, compuestos principalmente por carbohidratos, con el objetivo de integrar la producción de PHA en la producción actual de bioetanol a partir de azúcares. Los sustratos empleados en la producción de bioetanol de primera generación, tales como cereales y caña de azúcar, se usaron como fuente de carbono para la producción de P3HB en el Capítulo 5. A continuación, en el Capítulo 6, se desarrolla un proceso novedoso de producción de PHA basado en la fermentación y sacarificación simultáneas de mosto de maíz.

Por último, en el Capítulo 7 se propone el uso de ácidos grasos volátiles derivados de residuos como fuente de carbono para la producción de biopolímeros, ampliando de esta forma el concepto de biorrefinería. La aplicación de este tipo de proceso permite reducir los costes relacionados con la materia prima y además obtiener un co-polímero, P(3HB-co-3HV), que presenta mejores propiedades que las del homopolímero de P3HB.

La limitación de nutrientes es una de las herramientas más poderosas para dirigir el comportamiento de un cultivo bacteriano. De hecho, la disponibilidad de nutrientes ejerce una gran influencia en la composición celular y el metabolismo. La producción de PHA es uno de los mejores ejemplos para ilustrar este hecho, ya que su síntesis está normalmente inducida por la limitación de un nutriente esencial. En el Capítulo 3, se estudió el comportamiento de la bacteria *H. boliviensis* durante su cultivo en un biorreactor operado de modo discontinuo alimentado (fed-batch) y bajo diferente tipo de limitación o restricción de nutrientes. El cambio metabólico que ocurre entre las fases de crecimiento y de acumulación de PHA se determina por la limitación en uno o más nutrientes esenciales para el crecimiento bacteriano. El objetivo de este estudio es evaluar el efecto de la limitación de nutrientes como nitrógeno y la influencia de diferentes concentraciones de oxígeno en la producción de P3HB. Las limitaciones de nitrógeno y oxígeno por separado provocaron acumulaciones de P3HB del 45 y 37% P3HB/CDW, respectivamente, mientras que una limitación de nitrógeno junto con una baja adición de oxígeno incrementó la acumulación hasta el 73% P3HB/CDW. La caracterización de la bacteria *H. boliviensis*, con respecto a la producción de P3HB, permite optimizar el proceso y aportar nuevos conocimientos sobre la producción de PHA.

Por otro lado, en este tercer capítulo se estudió también la producción de ectoína y el uso de glutamato monosódico como suplemento para el medio de cultivo. El glutamato presenta una clara relación con la producción de ectoína, pero además presenta un impacto significativo en el crecimiento celular. Los resultados obtenidos en esta parte del trabajo permiten establecer las relaciones entre el consumo de glutamato, la producción de ectoína y el crecimiento bacteriano. El glutamato se considera un precursor de la ectoína y su ausencia en el medio de cultivo conllevó una reducción del 74% en la producción de ectoína y, además, un descenso en la concentración de biomasa del 54%. La síntesis de ectoína en ausencia de precursor requiere un mayor gasto de energía lo que compromete el crecimiento celular.

Existen diferentes métodos para cuantificar la producción de PHA, tales como análisis por gravimetría, varias técnicas microscópicas, UV, Raman y espectrometría de infrarrojos, métodos genéticos, NMR y cromatografía de gases o líquidos. Sin embargo, la gran mayoría de estos métodos incluyen una fase previa de extracción del PHA, dilatando

mucho el tiempo de análisis e incrementando su nivel de dificultad. La adaptación de una técnica rápida y sencilla para la cuantificación de PHA, supondría un gran avance para la implementación de este proceso a nivel industrial. La citometría de flujo, ampliamente usada en otros sectores de la biotecnología, permite cuantificar el contenido de PHA a partir de una sencilla preparación de la muestra, además de poder usarse como una técnica analítica completamente automatizada. En el Capítulo 4, se presenta un protocolo para la cuantificación del PHA acumulado por *H. boliviensis* mediante el uso de citometría de flujo. Se utilizó el fluorocromo BODIPY 493/503 como único reactivo, el cual presenta una alta afinidad por los lípidos que se encuentran formando parte de los gránulos de PHA. Introduciendo las bacterias teñidas en el citómetro de flujo, se obtiene fácilmente una señal de fluorescencia directamente proporcional a la concentración de PHA. En este capítulo se comparó la producción de PHA de diferentes cultivos de *H. boliviensis* sometidos a diferentes limitaciones nutricionales, empleando el sístema analítico el método tradicional de cromatografía de gases y comparándolo con el método de citometría de flujo. Se obtuvo una buena correlación entre los resultados de ambos métodos, que permite cuantificar de una forma más rápida y sencilla la acumulación de PHA del cultivo en cualquier momento. Además, esta técnica permite conocer de manera simultánea múltiples parámetros del cultivo que no sería posible conseguir con ninguna otra técnica de cuantificación de PHA, como por ejemplo, el porcentaje de bacterias que acumulan PHA, el tamaño de las mismas y la dinámica de la acumulación en el cultivo. De hecho, en el caso de *H. boliviensis*, fue posible distinguir dos tipos de poblaciones diferentes durante la acumulación de PHA, las bacterias acumuladoras de PHA y las no-acumuladoras, coexistiendo en el mismo biorreactor y bajo las mismas condiciones de operación.

Para mejorar la competitividad de los biopolímeros con respecto a los polímeros de origen fósil es necesario disponer de materias primas fácilmente acesibles y de bajo coste. El objetivo del Capítulo 5 es el estudio de la viabilidad de la producción de PHA mediante *H. boliviensis*, a partir de las principales fuentes de carbono usadas en la producción de bioetanol de primera generación, cereales y jugo de caña de azúcar. El uso de estos sustratos permitiría integrar la producción de bioetanol y PHA bajo un concepto de biorrefinería. Se realizó una caracterización detallada de los sustratos y se formularon medios de cultivo adaptados al crecimiento y acumulación de la bacteria *H. boliviensis*. Se analizó la acumulación de PHA usando como sustratos mosto de cereal, jugo de caña y dos medios sintéticos compuestos por glucosa y sacarosa como controles, respectivamente. Se alcanzaron valores similares de acumulación de PHA con mosto de cereal y glucosa (aproximadamente 60% P3HB/CDW). Sin embargo, con la sacarosa sintética se alcanzó una acumulación más baja (54% P3HB/CDW) que no fue posible igualar con el medio complejo de jugo de caña (49% P3HB/CDW). Las productividades obtenidas a escala de matraz con ambos medios complejos (0,049 y 0,044 g l^{-1} h^{-1} con mosto de cereal y jugo de caña, respectivamente) superaron a las obtenidas con los medios compuestos por los azúcares comerciales (0,033 y 0,025 g l^{-1} h^{-1} con glucosa y sacarosa, respectivamente). Sin embargo, el escalado a un reactor de 2 l incrementó la productividad hasta 0,254 g l^{-1} h^{-1}, en el caso del mosto de cereal.

A pesar de las ventajosas y atractivas características de los PHA, como su biodegradabilidad y biocompatibilidad, sus costes de producción, todavía no pueden competir con los de los polímeros de origen fósil. Por lo tanto, es de especial importancia

tanto el desarrollo de estrategias de fermentación como la búsqueda de fuentes de carbono de bajo coste. El maíz es el cereal más usado en la industria de la producción de bioetanol en Europa y USA. Este sustrato requiere un proceso de pretratamiento o acondicionamiento, para su posterior uso como fuente de carbono. Tras la molienda del cereal, se lleva a cabo la gelatinización del mosto a alta temperatura y en presencia de la enzima α-amilasa. Finalmente, antes de la fermentación, es necesario someter a la corriente de mosto a un último proceso hidrolítico en presencia de la enzima glucoamilasa, para liberar la mayor cantidad de azúcares simples y fácilmente metabolizables. Este último proceso puede hacerse simultáneamente junto con la fermentación (SSF) o en dos etapas diferentes (SHF). En el Capítulo 6, se adaptó este proceso SSF, ampliamente usado en la producción de bioetanol de primera generación, a la producción de PHA con la bacteria *H. boliviensis*. Esta estrategia de proceso se comparó con la sacarificación y fermentación en dos etapas, SHF. Además de resultar una metodología de proceso más económica, se obtuvo una mayor producción de P3HB con el proceso SSF. La aplicación del proceso SSF permitió una reducción del tiempo de fermentación del 47%, mientras que la producción de P3HB fue un 60% mayor que en el caso del SHF. En este capítulo, se demostró, por primera vez, la posibilidad de aplicar un proceso SSF para producir PHA a partir de una corriente real de mosto de cereal y su integración en una biorrefinería de etanol de primera generación.

El copolímero formado por monómeros de 3-hidroxibutirato y 3-hidroxivalerato, P(3HB-co-3HV), presenta mejores propiedades mecánicas que el polímero P3HB. El polímero conformado solo por unidades de 3HB presenta una gran cristalinidad, lo cual dificulta los procesos de transformación, sin embargo, la incorporación de una pequeña fracción de monómeros de 3HV mejora significativamente las propiedades termomecánicas del biopolímero, incrementando el número de posibles aplicaciones de estos materiales, así como su precio. Algunos sustratos como el ácido levulínico, propiónico o valérico, están descritos como precursores de monómeros de 3HV para algunos microorganismos. La gran flexibilidad de las biorrefinerías permite la obtención de cualquiera de estos precursores a partir de sustratos renovables o de corrientes residuales de diferentes procesos o de la misma biorrefinería. El ácido levulínico se obtiene tras un tratamiento con ácido y altas temperaturas de una corriente de azúcares. Esta corriente podría ser el mosto de cereal o el jugo de caña. Por otro lado, los residuos orgánicos derivados del proceso global, que generalmente se derivan a la planta de residuos, pueden ser transformados en ácidos grasos volátiles tras un proceso de acidogénesis con un cultivo mixto. La mezcla de ácidos grasos volátiles que se obtiene, suele estar formada por ácido acético, propiónico, butírico y/o valérico, en diferentes proporciones. En el Capítulo 7 se analizó la producción del co-polímero P(3HB-co-3HV) con la bacteria *H. boliviensis* a partir de ácido levulínico sintético y una mezcla de ácidos grasos volátiles sintéticos, con proporciones semejantes a las obtenidas tras una fermentación acidogénica. Varias características intrínsecas de este microorganismo, tales como su tolerancia a altas concentraciones de sal y a pH alcalinos, podrían ser beneficiosas para incrementar la tolerancia a estos ácidos, que pueden resultar inhibitorios en determinadas condiciones.

El ácido levulínico no actuó como precursor de 3HV en cultivos con *H. boliviensis*, a pesar de que se conoce que otros microorganismos realizan este proceso. Se evaluaron a escala de matraz diferentes mezclas de ácidos grasos volátiles, variando el porcentaje de cada uno de ellos, en base a estudios previos encontrados en bibliografía. La mezcla con

la que se alcanzó la máxima producción de PHA se utilizó para escalar el proceso a un biorreactor de 2 l. Así, se obtuvo una concentración máxima de 13 g l^{-1} de PHA, lo que equivale a una acumulación del 70% P(3HB-co-3HV)/CDW, con una fracción de 3HV de 8.5 mol %.

1

General Introduction

OUTLINE

1.1 The age of plastics: a brief history

1.2 Biopolymers

1.3 Polyhydroxyalkanoates

1.4 Towards the bioeconomy: Biorefinery concept

1.5 *Halomonas boliviensis*

1.6 Aims and scope

1.7 Outline

1.1 The Age of Plastics: a brief history

We live in a world made of plastic; this material is actually surrounding us everywhere we look. According to its transformation process, plastic can be used either to wrap a sandwich or to hold an astronaut during a spacewalk. The age of plastic started in 1869, with the celluloid invention by John Wesley Hyatt, and it lasts until nowadays. Plastic was invented to free us from the limitation of the natural materials and the scarcity of resources. Celluloid –obtained from the natural polymer, cellulose– was mainly applied in the manufacture of combs. Due to its ability to imitate the appearance of materials such as ivory or hawksbill, it gave a break to elephants, tortoises and corals. But, probably, the highest achievement of celluloid was the photographic film, considered one of the most important cultural legacies of plastics.

Bakelite was the first plastic made from synthetic compounds –formaldehyde and phenol– developed by Leo Baekeland in 1907. On the contrary to celluloid, bakelite has its own identity; it lacked the imitation gift, but it could be easily malleable and transformed into anything. During the 1920s and 1930s a huge quantity of new materials appeared all over the world such as polystyrene (PS), nylon or polyethylene (PE), all of them thermoplastics. This characteristic, based on the effect of temperature for moulding, and the invention of new processes such as injection moulding, allowed a faster and easier manufacturing of plastic products. After the WWII, the chemistry of the polymers left the lab and was introduced into the real life. By 1979, the plastics production already led steel production. It is obvious that plastic offers several advantages over the natural materials, but this is not enough explanation for its ubiquity. With the boom of the petrol industry, the necessity to find a use for the subproducts of the cracking such as ethylene gas, rapidly increased. As a solution for this request, PE was developed at the beginning of 1930s. The continuous flux of petrol not only supply fuel, but plastic, feeding a culture based on the consumerism of plastics objects, but also boosting the development of the society and its democratization.

Worldwide plastics production reached 322 Mt in 2015 (Figure 1.1). During the few past years there is a stable production in Europe, while it is still growing globally. In 2015, China was the biggest plastic producer, followed by Europe (27.8 and 18.5% of the total plastic produced, respectively). The plastics industry in Europe is one of the largest; there are 60,000 companies that generate 1.5 million of job positions (Plastics Europe – The Facts 2016).

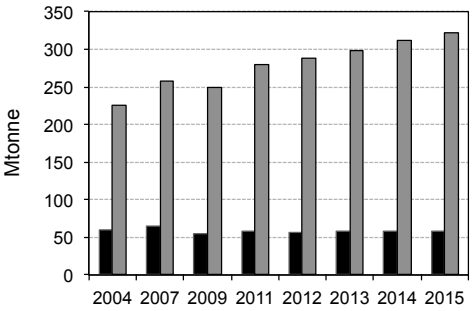

Figure 1.1: Worldwide (grey) and Europe (black) plastic production in million tonnes from 2004 to 2015.

However, several issues threaten the dependence on the fossil fuel resources as raw material, such as, the worldwide oil reserves-to-production ratio, geopolitical instabilities, greenhouse gas emissions, spills and wastes. These issues boost the research of new renewable resources and biotechnology processes to substitute the classic petrol based products.

Moreover, the generation of plastic waste, tightly linked with the huge worldwide plastic production, is becoming a dramatic issue. From the 59 Mt of plastics produced in Europe in 2014, 25.8 Mt of plastic waste was generated, and only 69.2% of the total plastic waste was recovered through recycling or used for energy production (Plastics Europe – The Facts 2015), with the remaining fraction posing a major environmental issue. A recent study estimated that 0.25 Mt of plastic is floating adrift in the oceans (Eriksen et al., 2014), thereby directly affecting marine fauna, as such debris is known to entangle or be ingested by marine life (Gregory, 2009). These types of materials should also be considered as hazardous wastes due to their pollutant sorption ability (Rochman et al., 2013). To overcome such issues, our consumer ethics and consumption rates must change, especially to reduce the generation of plastic waste. Moreover, conventional petroleum-based plastics must be substituted with environmentally friendly biopolymers in several applications. In fact, several countries from the European Union have already established policies against the consumption of petroleum-based packaging by the imposition of eco-taxes to plastic shopping bags. A recent European Directive (Directive (EU) 2015/720) requires governments to introduce a charge on plastic carrier bags by end 2018 or to take other measures to ensure a reduction in their consumption to 90 bags per person by the end of 2019 and to 40 bags per person by 2025. With this, European consumption of plastic bags should be reduced by 80% in the next 10 years.

1.2 BIOPOLYMERS

Biopolymers are defined as those materials that present plastic like properties and are biobased, biodegradable, or both (Figure 1.2) (European Bioplastics, 2016)., Nowadays, there is a bioplastic alternative for almost every conventional plastic material and its corresponding application. Some of the additional advantages that present the bioplastics in comparison with the fuel-based plastics are a reduced carbon footprint and additional waste management options such as composting. The bioplastic industry is a young, innovative sector with an enormous economic and ecological potential. According to the Institute for Bioplastics and Biocomposites, the biopolymers global production is predicted to grow from 4.2 Mt, in 2016, to approximately 6.1 Mt by 2021 (European Bioplastics, 2016).

Among the various types of biodegradable plastics, polyhydroxyalkanoate (PHA) is one of the most well known, being recognized as biobased and biodegradable, completely recyclable into organic waste and with no generation of toxic compounds during its degradation (Chanprateep, 2010), even in marine environments by ASTM standards. It is important to highlight this last feature since it is an important difference to other biobased polymers such as polylactic acid (PLA), which is compostable, but may remain in marine ambients for up to a thousand years (DiGregorio, 2009).

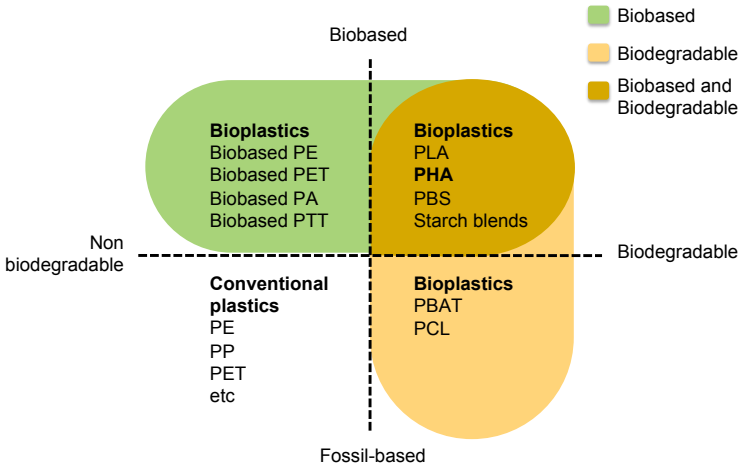

Figure 1.2: Bioplastic classification (adapted from the European Bioplastics Association). PE, polyethylene; PET, polyethylene terephthalate; PA, polyamide; PTT, polytrimethylene terephtalate; PP, polypropylene; PLA, polylactic acid; PHA, polyhydroxyalkanoate; PBS, polybutylene succinate; PBAT, polybutyrate adipate terephthalate; PCL, polycaprolactone.

1.3 Polyhydroxyalkanoates

Polyhydroxyalkanoates or PHA are homo- or heteropolyesters produced and intracellularly stored by numerous types of organisms. Most of the known PHA are polymers of 3-hydroxyacids possessing the general formula represented in Figure 1.3. The first PHA, poly(3-hydroxybutyrate) (P3HB), was discovered in *Bacillus megaterium,* by the French scientist Lemoigne (1926). Surprisingly, this material presented the structure and properties of a thermoplastic polyester.

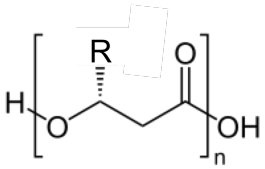

Figure 1.3: General formula of PHA.

P3HB has been found to be a ubiquitous component of the cellular membranes of plants and animals (Reusch et al., 1992). However, there are several microorganisms able to accumulate huge amounts of PHA as carbon reserve material in response to the excess of carbon source and the starvation of an essential nutrient, such as nitrogen or phosphorous. The accumulation is subjected to extensive regulation by biosynthesis genes (Anderson and Dawes, 1990). When the carbon source is exhausted, the stored material is depolymerised, and the degradation products can be used as carbon and energy.

There are more than 300 different microorganisms that are known to synthesize and accumulate PHA. The bacterium *Ralstonia eutropha* is one of the most studied, being a reference for the research of the biological aspects of PHA. There are likewise different types of PHA, depending on the chemical structure of the monomer (Figure 1.3). P3HB is the most widespread and best characterized type of PHA. It is considered a strong candidate as biopolymer since it presents very similar properties to synthetic polymers (Table 1.1). All the properties summarized in the table present similar values between both materials, with the exception of the Young's modulus, which converts P3HB in a material with higher stiffness.

Table 1.1: Properties of polypropylene and poly(3-hydroxybutyate) (adapted from Harding et al., 2007).

	Polypropylene	P3HB
Density (kg m^{-3})	900-910	1250
Melting point (°C)	176	45-180, P3HB=180
Tensile strength (MPa)	38	13-40
Elongation (%)	400	5-680
Young's modulus (MPa)	17000	350-1000
Glass-transition temperature (°C)	-10	15, P3HB=4
Service temperature (°C)		-30 to 120
Specific heat 20-80°C (kJ $kg^{-1}K^{-1}$)	1.9	
Thermal conductivity 20-150°C (kW $m^{-1}K^{-1}$)	0.42-0.61	

Several companies have been interested in the use of PHA for packaging, biomedical and agricultural applications, based on its properties. Since PHA are composed by natural non-toxic constituents and are considered inherently biocompatible, several medical applications and uses have been developed such as scaffolds or matrices in tissue engineering, wound dressing and drug delivery (Zinn et al., 2001).

PHA can be produced in large quantities from renewable resources by means of well-known fermentation processes and applying particular culture conditions (Figure 1.4). Downstream is a key step of the process. There are different downstream strategies to recover the PHA from the cell biomass (López-Abelairas et al., 2015). Usually, after the separation of the cells, chemicals or enzymatic cocktails are applied for its digestion, and halogenated agents are used to extract the PHA.

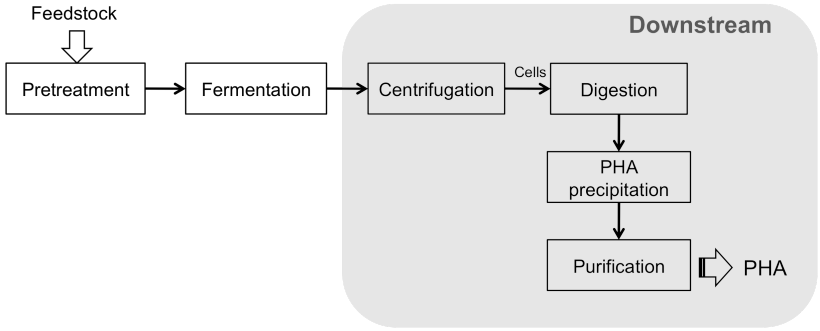

Figure 1.4: General scheme for PHA production process.

The first patent that described PHAs potential application as plastic material dated from 1962 (Baptist J.N., United States), but the industrial production of this material did not start until 1982, with the commercialization of Biopol™ by Imperial Chemical Industries Ltd. (ICI/Zeneca BioProducts, Bellingham, UK). In 1990, the German company Wella released a new shampoo bottle made of Biopol™. A summary of the current worldwide PHAs production plants is presented in Table 1.2. However, this is still an emerging industry, only the 2% of the global biopolymers production from 2016 (4.2 Mt) were PHA. So far, P3HB, poly(3-hydroxybutyrate-co-3-hydroxyvalerate) (P(3HB-co-3HV)), poly(3-hydroxybutyrate-co-4-hydroxybutyrate) (P(3HB-co-4HB)) and poly(3-hydroxybutyrate-co-3-hydroxyhexanoate) (P(3HB-co-HHx)), are being produced at large scale nowadays.

Table 1.2: Current PHAs production plants (adapted from Mozejko-Ciesielska and Kiewisz (2016).

Trade name	Manufacturer	Polymer type	Carbon source
Biomer	Biomer, Germany	P3HB, P(3HB-co-3HV)	sucrose
Biocycle	PHB Industrial S.A., Brazil	P3HB	sugarcane
Minerv-PHA	Bio-On, Italy	PHA	sugar beets
Kaneka PHBH	Kaneka Corporation, Japan	P(3HB-co-HHx)	fatty acids
Mirel	Metabolix, USA	P(3HB-co-4HB)	glucose
Enmat	Tianan Biologic Material Co., Ltd. Ningbo, China	P(3HB-co-3HV)	glucose + propionate
GreenBio	Tianjin GreenBio Materials, China	P(3HB-co-4HB)	glucose + 1,4-butanodiol
Jiangsu Nantian	Jiang Su Nan Tian, China	P3HB	glucose

In a recent study, the environmental analysis of plastic production processes was carried out by comparing the petroleum-based PP and the biological-based P3HB production processes using life cycle assessment (Harding et al., 2007). P3HB was superior to PP in all the life cycle categories; the energy requirements for P3HB production are significantly lower than those of petroleum-based plastics. However, the environmental benefits that could be obtained by the replacement of the conventional plastics by biopolymers may imply an important economic loss (Mozejko-Ciesielska and Kiewisz, 2016). The main parameters of the process that increase the final costs of PHA are the price of substrates used as carbon source, bacterial productivity and downstream process (Choi and Lee, 1997). However, a 20% of reduction in the overall production costs was achieved when PHA production was integrated into a sugarcane mill (Nonato et al., 2001).

1.4 Towards the Bioeconomy: Biorefinery concept

Climate change concerns, decreasing of fossil fuel resources and the rapid increase of the world population, triggered in 2012 the development of a strategy, by the European Commission, to shift the European economy towards a greater and more sustainable use of renewable resources to make the transition to a post-petroleum economy. The term "Bioeconomy" refers to an economy based on biological resources from the land and sea, as well as waste, as inputs for food and feed, chemicals, materials and energy production. It can be defined as a restorative and regenerative industry. The European bioeconomy aims to activate the potential of biobased products and generate new markets and industries while enhancing the sustainability of production and consumption, by the replacement of the petroleum-based refineries with biorefineries.

A biorefinery is a network of facilities that integrates biomass conversion processes and equipment to produce biofuels, energy and chemicals from biomass (Moncada et al., 2016). Depending on the raw materials and the technological processes, the biorefinery involves different platforms, such as carbohydrate, syngas or carbon-rich chains (organic acids or oils) (Agler et al., 2011; Moncada et al., 2016). The high flexibility of the biorefineries allows the incorporation and combination of process from different platforms (Figure 1.5). Raw materials are classified as first (1G), second (2G) and third (3G) generation feedstocks. 1G feedstocks include edible crops (e.g. edible vegetables oils,

sugarcane, wheat, maize); but these present social, economic and environmental issues. 2G feedstocks can overcome the challenges of 1G feedstocks (fuel *vs.* food dilemma) since these include e.g. wood, wood waste, non-food crops, waste cooking oil, forestry and agricultural residues. 3G feedstocks are mainly microalgae and presents remarkable advantages such as low-cost, eco-friendly and entirely renewable (Brennan and Owende, 2010). However, despite the high availability of renewable resources, the identification of the platform and the intermediate chemicals for its transformation into a substitute for a petrol industry product suppose a very difficult task. There is a wide spectrum of alternatives, and moreover, the technologies available are scarce and not well developed (Koutinas et al., 2014).

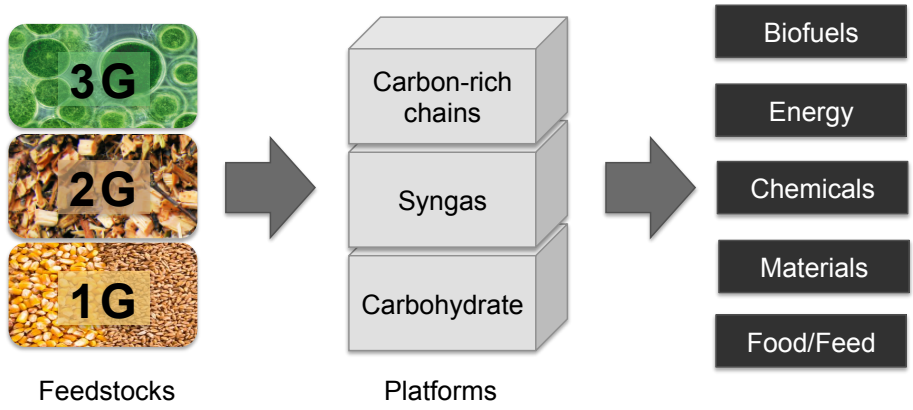

Figure 1.5: General scheme of a biorefinery.

Bioplastics may play a central role in the biorefineries of the future (Philp et al., 2013). In fact, the use of biodegradable and biobased plastics as substitutes for petroleum-based plastics might be part of the solution in the struggle with climate change and the decrease of fossil fuel reserves. As occurs in oil refineries, there is a significantly low profit margin with the fuel production in the biorefineries and it is highly subjected to market dynamics. However, the 7-8% of crude oil derived to chemicals production in the oil refineries yield the 25-35% of the annual profits. Biopolymers could act as an intermediate-volume product between high-volume fuels and low-volume chemicals in the case of the biorefineries.

1.5 *HALOMONAS BOLIVIENSIS*

The selection of the bacterium *Halomonas boliviensis* as the PHA-producer for the development of this Thesis was based on a previous study (López-Abelairas PhD Thesis, 2014), where a screening of different PHA-producer strains, such as *R. eutropha*, *Hydrogenogova pseudoflava*, *Pseudomonas putida* and *H. boliviensis* was done. Using glucose as substrate, *H. boliviensis* showed the best PHA accumulation and yield (70.3±1.3% and 145±4 mg PHA g^{-1} consumed glucose, respectively), while the most utilized bacteria for PHA production, *R. eutropha*, presented an accumulation of 55.0±0.2% and a yield of 131±6 mg PHA g^{-1} consumed glucose. The other two bacteria tested, *H. pseudoflava* and *P. putida* reached an accumulation of 10.3±0.4% and 1.6±0.6%,

respectively. It was also observed that *H. boliviensis* was the only bacterium able to grow and accumulate PHA using non-detoxified hydrolysates from steam exploded wheat straw.

H. boliviensis is a bacterium isolated from the hypersaline lake Laguna Colorada in Bolivia (Quillaguamán et al., 2004), able to accumulate PHA in high yields (50-80 wt.%). It is an aerobic, Gram-negative rod. It presents some characteristics of extremophile organisms, such as moderately halophile, alkalitolerant and psychrophilic. In Table 1.3 is summarized the range of key parameters in which is possible to detect bacterial growth and its optimal value. *H. boliviensis* is a heterotrophic bacterium, able to utilize different carbon sources i.e. glucose (Quillaguamán et al., 2008), sucrose (Quillaguamán et al., 2007), xylose (López-Abelairas PhD Thesis, 2014), volatile fatty acids (Quillaguamán et al., 2006) and hydrolysed starch (Quillaguamán et al., 2005).

Table 1.3: Growth characteristics of *H. boliviensis*, global growth range and optimal value.

Characteristic	Growth range	Optimum
Moderately halophilic	0 – 25% (w/v) NaCl	5% (w/v) NaCl
Alkalitolerance	pH 6 – 11	pH 7.5 – 8
Psychrophilic	0 – 45°C	25 – 30°C

Due to its high salt requirements for growth a quite narrower spectrum of microorganisms will be able to compete with this strain, minimizing sterilization requirements (Tan et al., 2011). Concomitantly, capital cost will be reduced, since a cheaper bioreactor material could be used (Yin et al., 2015), and the process would require lower energy consumption.

Moreover, this halophilic bacterium accumulates water-soluble organic compounds of low molecular weight, which are referred as compatible solutes or osmolytes, to maintain a low intracellular salt concentration (Quillaguamán et al., 2010; Van-Thuoc et al., 2010). Ectoine (1,4,5,6-tetrahydro-2-methyl-4-pyrimidinecarboxylic acid) and hydroxyectoine are the predominant compatible solutes, these can act as stabilizers for biological structures and allow the cells to adapt not only to salts, but also to heat, cold, desiccation or even freezing conditions (Pastor et al., 2010). These properties of stability and protection highlight ectoine applications in cosmetic and pharmaceutical industries. Ectoine is a low-volume product with a high value. According to the techno-economic and environmental analysis performed by López-Abelairas (PhD Thesis, 2014), the integration of ectoine together with the PHA production in a second-generation bioethanol plant, enables a reduction in prices of bioethanol and biopolymers.

Table 1.4: Summary of the main characteristics of *H. boliviensis* and its advantages or disadvantages.

Characteristic	Advantage	Disadvantage
Halophile	- Lower contamination risk - Cheaper materials for bioreactor construction - Lower sterilization requirements - PHA release by osmotic lysis	- High NaCl consumption
Ectoine production	- High-value by product	
Others	- Highest PHA accumulation - Detoxification ability - Growth and PHA formation in wide range of carbon sources (cheaper substrates, as well)	- Need of MSG as co-substrate

The main advantages and disadvantages of the application of *H. boliviensis* for PHA production are summarized in Table 1.4. A possible solution for the use of high amounts of NaCl during fermentation could be the separation and recycling of this stream by desalination with decanoic acid; as it was previously described by Bhattacharyya et al. (2014). The use of seawater would allow also a reduction in costs (Yue et al., 2014). Besides, its halophilic characteristic presents an intrinsic advantage for this strain regarding the PHA downstream process. By removing the medium and adding fresh water instead, the osmotic imbalance created will provoke an osmotic lysis of the cells allowing a better separation of the PHA granules (Rathi et al., 2012). Based on this feature, another *Halomonas* strain (*H. elongata*) has been used for the industrial production of ectoine, using a recovery process known as "bacterial milking" (Kunte et al., 2014). Applying this process, ectoine is currently produced on a scale of tons by the company Bitop AG (Witten, Germany) and commercialized for the formulation of several medical devices with applications in dermatology, allergy, cough and cold, airway diseases or dry epithelia.

In general, halophilic organisms are gaining much attention for industrial applications. Especially *Halomonas* spp., have been used for the production of several products with applications in various industrial fields, different than PHA or ectoine. There are growing interest in the production of alkaline enzymes (Setati, 2010), biosurfactants and emulsifiers (Satpute et al., 2010) by this type of organisms.

1.6 AIMS AND SCOPE

The general aim of the research described in this Thesis can be formulated as follows:

To increase the PHA productivity of the bacterium *Halomonas boliviensis* by the study of its biopolymer accumulation mechanisms, and to develop a biopolymer production process from first and second generation feedstocks that could allow its integration into a biorefinery.

Attention is focused on the comprehension of the special features and requirements of *H. boliviensis* either for biomass growth or for biopolymer accumulation, on the development of a faster methodology for PHA quantification, on the research of information about the mechanisms involved on PHA accumulation, and also on the integration of the PHA production into a biorefinery using 1G and 2G feedstocks as raw materials.

1.7 OUTLINE

This introduction briefly outlines the importance of plastics as driving-material for the development of the society and the importance of the plastics industry in the world. The reasons why petrol-plastics must be replaced by biopolymers are presented in detail, together with the special features and characteristics of the PHA.

The first part of this Thesis (Chapter 3 and 4) focuses on the description and study of the P3HB production by *H. boliviensis*. Chapter 3 presents a detailed description of the bacterium, a study of its nutrient requirements and how the type and grade of nutrient limitation influences the P3HB accumulation. In Chapter 4, a fast and straightforward method to quantify the P3HB production is developed, based on the flow cytometry technique.

The second part (Chapter 5 and 6) studies the P3HB production based on the carbohydrate platform, with the aim of integrating the biopolymer production into the current biofuel industries from sugars. First generation bioethanol streams, such as sugarcane juice and corn mash are used as carbon source for P3HB production in Chapter 5. A novel process based on the simultaneous saccharification of corn mash and fermentation for P3HB production is analysed in Chapter 6.

Finally, in Chapter 7, the biorefinery concept is upgraded form sugars to waste as carbon source for biopolymer production. Different substrates, which can be obtained from waste, were tested for PHA production, with the double advantage of reduce raw material costs and produce a co-polymer, P(3HB-co-3HV), that presents better properties and overall value than P3HB.

2

Materials and methods

The procedures for general bacterial growth and analytical methods used in this work are described in this chapter. First, bacterial growth requirements and general experimentation set-ups are detailed. The analytical methods applied for monitoring bacterial growth, products formation and substrates consumptions are also described.

The specific analytical methods and experimental set-up used in a single part of the work are detailed in the corresponding chapters.

OUTLINE

2.1 Bacterial Strain and Maintenance

Throughout this study, the Gram-negative, moderately halophilic bacterium *H. boliviensis* LC1 (ATCC® BAA-759™) was used. It was maintained at 4°C on solid HM medium (Quillaguamán et al. 2004), containing (per liter): NaCl, 45 g; MgSO4 4·7H2O, 0.25 g; CaCl2·2H2O, 0.09 g; KCl, 0.5 g; NaBr, 0.06 g; peptone, 5 g; yeast extract, 10 g; glucose, 1 g and granulated agar, 20 g. The pH of the medium was adjusted to 7.5 with 5 mol l^{-1} NaOH. Solid medium was sterilised by autoclave at 121°C during 20 min. The bacterium was spread onto a new agar plate before each experiment, working with fresh starting inoculum each time.

2.2 Culture Media

All the culture media were prepared in distilled water and sterilised by autoclave at 121°C during 20 min. Glucose, monosodium glutamate (MSG) and $MgSO_4 \cdot H_2O$ were autoclaved separately and added to the media afterwards in sterile conditions to avoid Maillard reactions and precipitations of salts. The pH of the media was adjusted to 7.5 with 5 mol l^{-1} NaOH. The compositions of the inoculum (IC), batch (BC) and fed-batch (FBC) culture media are depicted in Table 2.1. IC medium was used to prepare the seed culture for the experiments; BC medium was used at flask or bioreactor scale during batch growth, while, FBC medium was used at bioreactor scale during fed-batch growth.

Table 2.1: Composition of the inoculum, batch and fed-batch culture media (Quillaguamán et al. 2008).

	Concentration (g l^{-1})		
	Inoculation culture medium (IC)	Batch culture medium (BC)	Fed-batch culture medium (FBC)
Glucose*	10.0	20.0	700.0
NaCl	45.0	45.0	45.0
$MgSO_4 \cdot H_2O$	1.4	2.8	5.0
K_2HPO_4	0.55	2.2	–
NH_4Cl	2.3	4.0	–
$FeSO_4 \cdot 7H_2O$	0.005	0.005	0.125
MSG	3.0	20.0	–
Tris	15.0	–	–

*Carbon source would change in different experiments, it will be specified in each case.

2.3 Bacterial Growth

First, fresh agar plate spread with *H. boliviensis* was incubated at 30°C, for 24 h. The bacterium was transferred from agar plate to 25 ml of inoculation medium (Table 2.1). Flasks were incubated at 30°C for 20-24 h, after culture broth reached an OD of 2.5-2.8. An inoculation ratio of 10% in volume was maintained. Then, considering the working volume of the main experiment, the inoculation step in flasks was repeated increasing the volume in each step, until the final inoculation volume was reached. For the triplicates of experiments, the same seed culture was used.

2.3.1 Flask scale

The total and working volume of the flasks varied with the type of experiment. The cultures were incubated at 30°C with shaking at 200 rpm. Samples were withdrawn periodically during experimentation.

2.3.2 Bioreactor scale

Bioreactor experiments were performed in a 2 l Biostat® MD (B. Braun Biotech International) equipped with pH, dissolved oxygen, temperature and foam probes, using a working volume of 1.5 or 2 l (Figure 2.1). The temperature was maintained at 30°C by recirculating water from an external thermostat bath through the vessel jacket. Dissolved oxygen (pO_2) was monitored on-line as the percentage of the maximum oxygen saturation attained at the initial conditions of aeration, agitation and temperature. Previously to each fermentation, the pO_2 sensor (Mettler-Toledo OxyFerm) was calibrated using N_2 and air (0 and 100% pO_2, respectively). The pH was maintained in 7.5 by the automatic addition of 5 mol l^{-1} NaOH/HCl. The foam was controlled by the addition of antifoam A (Sigma) when it was necessary.

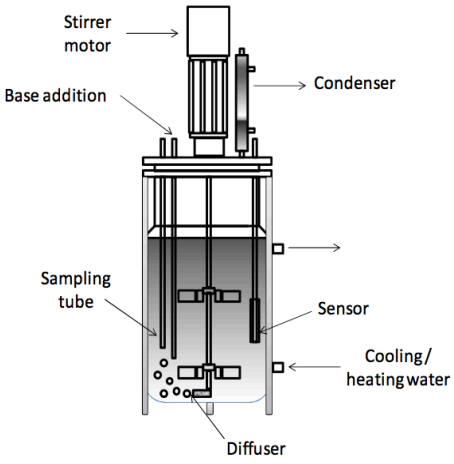

Figure 2.1: Bioreactor scheme (López-Abelairas PhD Thesis, 2014).

The bioreactor was operated in fed-batch mode. For the starting batch, the BC medium was used for bacterial growth (Table 2.1). Initial aeration and agitation rates were 1 l min^{-1} and 400 rpm, respectively, and these conditions were used to calibrate at 100% the pO_2 probe. For any of the experiments, air inflow rate and agitation speed were increased gradually when the dissolved oxygen decreased below 60%. The maximum air inflow rate and agitation attained were 5 l min^{-1} and 650 rpm, respectively. Glucose concentration was monitored during all fed-batch experiments by off-line analysis and maintained between 16 and 24 g l^{-1} by adding FBC medium (Table 2.1). Phosphate concentration was followed and maintained between 0.7 and 3.7 g l^{-1} of K_2HPO_4 to avoid limiting conditions of this nutrient.

2.4 ANALYTICAL METHODS

2.4.1 Biomass: CDW, RCM and OD

Cell dry weight (CDW) or total dry weight was determined from 10 ml cell suspension samples harvested by centrifugation at 9500 × *g* in a previously weighed tube, washed

twice with distilled water, and freeze-dried (Labconco FreeZone 1) for 24 h to a constant weight. The first supernatant was kept for further analysis.

Residual biomass or residual cell mass (RCM) was defined as the total dry weight minus PHA.

Optical density (OD) was determined from cell suspension samples. The sample was centrifuged at 9500 × *g* for 5 min. Then, the bacterial pellet was washed twice with distilled water. Final washed pellet was resuspended to the same original volume with distilled water. The absorbance of the sample was measured at a wavelength of 600 nm in a spectrophotometer (Shimadzu UV-1800, UV-Visible), but it was previously diluted to obtain an absorbance between 0.2 and 0.6. OD was expressed as the absorbance value multiplied by the dilution factor of the sample.

2.4.2 Polyhydroxyalkanoates

PHA content of cells, expressed as the percentage of PHA on the total CDW, was determined by a method adapted from Riis and Mai (1988) based on the propanolysis of PHA. Co-polymer P(3HB-co-3HV) (Sigma) with a P3HV content of 12 wt.% was used as external standard and 20 mg ml^{-1} of benzoic acid in 1-propanol was used as internal standard. Calibration curve for both PHA is shown in Figure 2.2.

Freeze-dried samples and PHA standard were weighed using an analytical balance into tubes with screw caps. 1.5 ml of HCl:1-propanol (1:4) solution and 1.5 ml of dichloroethane were added into the tubes and heated along with 50 µl of an internal standard for 2 h at 100°C. After cooling, 3 ml of distilled water was added to improve the liquid-liquid extraction. One millilitre of the organic phase (lower phase), enriched on the esters of the PHA, was filtered and analysed by gas chromatography (HP 6850 Series II GC).

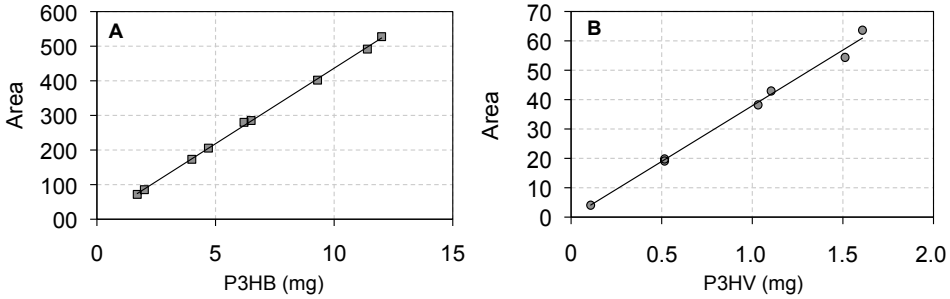

Figure 2.2: A. Calibration curve for P3HB by GC (A=43.64·P3HB (mg), R^2=0.9992). **B.** Calibration curve for P3HV by GC (A=37.907·P3HV (mg), R^2=0.993).

The GC was equipped with a FID detector and a HP-INNOWAX Agilent 19091N-133E column (30 m × 0.25 mm, 0.25 µm film thickness, Agilent Technologies, Santa Clara, USA). The carrier gas was helium at a flow rate of 1.0 ml min^{-1}. The injection temperature was 250°C, the detection temperature was 275°C and the initial temperature of the oven was set at 60°C, which was gradually increased to 230°C during analysis (10°C min^{-1} to reach 160°C and then 20°C min^{-1} to 230°C).

2.4.3 Ectoine

The compatible solute ectoine, the most common byproduct of *H. boliviensis* was quantified by HPLC following the method described by Van-Thuoc et al. (2010). The HPLC (HPLC XLC – DAD Jasco) was equipped with an Aminex HPX-C42 (300 x 7.8 mm Bio-Rad) column, and $CaCl_2$ 5 mM was used as mobile phase at a flow rate of 0.35 ml min^{-1}. An example of a calibration curve for this compound is shown in Figure 2.3.

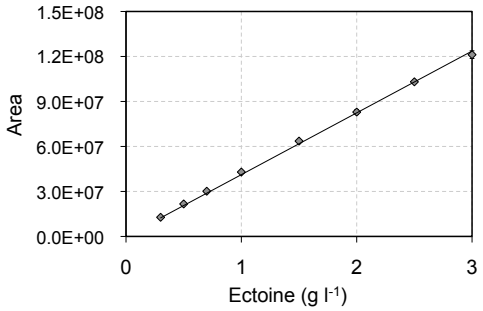

Figure 2.3: Calibration curve for ectoine by HPLC (A=4.12E^7·Ectoine (g l^{-1}), R^2=0.998).

2.4.4 Glutamate

MSG was quantified from sample supernatant using an enzymatic colorimetric method from Randox Laboratories (RX Series, Randox Laboratories Limited, United Kingdom). In this method, L-glutamate is first oxidised by L-glutamate oxidase to release H_2O_2. H_2O_2 further reacts with N-ethyl-N-(2-hydroxy-3-sulfo-propyl)-3 methylaniline (EHSPT) and 4-aminoantpyrine (4-AA) in the presence of peroxidase (POD) to generate quinine dye which is proportional to the amount of L-glutamate in samples.

A volume of 900 µl of reagent is mixed with 10 µl of sample or standard (1 g l^{-1} glutamate). After 20 min of incubation at room temperature (15-20°C), absorbance (A) was measured at 546 nm in a spectrophotometer (Shimadzu UV-1800, UV-Visible). Glutamate concentration was determined as followed:

$$\frac{(A)\,\text{Sample}}{(A)\,\text{Standard}} \cdot \text{Dilution} = \text{Glutamate}\left(g \cdot l^{-1}\right)$$

2.4.5 Glucose

Glucose was quantified by Trinder method, using a commercial enzymatic kit (GOD-PAP/Trinder, Spinreact, GI, Spain). This enzymatic method is based on the following chemical reactions (Trinder, 1969):

$$\text{Glucose} + O_2 + H_2O \xrightarrow{\text{GOD}} H_2O_2 + \text{Gluconic acid}$$

$$2H_2O_2 + \text{Phenol} + \text{Aminophenazone} \xrightarrow{\text{POD}} \text{Quinone} + H_2O$$

where GOD and POD are the enzymes glucose oxidase (EC 1.1.3.4) and peroxidase (EC 1.11.1.7), respectively.

One ml of reagent is mixed with 10 µl of sample or standard (1 g l^{-1} glucose). After 20 min of incubation at room temperature (15-20°C), absorbance (A) was measured at 505 nm in a spectrophotometer (Shimadzu UV-1800, UV-Visible). Glucose concentration was determined as followed:

$$\frac{(A)\,Sample}{(A)\,Standard} \cdot Dilution = Glucose\ (g \cdot l^{-1})$$

2.4.6 Dextrins

The concentration of the non-saccharified starch fraction (i.e. dextrins) was determined by measuring the glucose release after a sulphuric acid-catalyzed post-hydrolysis. A liquid sample from the supernatant was diluted 10-fold in a solution of H_2SO_4, reaching a final acid concentration of 4% (v/v) in a final volume of 10 ml. It was autoclaved at 121°C for 30 min in a sealed flask. Flasks were weighed before and after the thermal treatment to discard any possible losses via evaporation. After cooling down, the pH of the solutions was adjusted to 6 by adding NaOH 10 M. The amount of base added was considered as a dilution factor for the calculations of the released glucose. In order to check the extent of the saccharification, samples were analysed by HPLC using an Aminex HPX-87H column and an IR 1047 detector, at 60°C, using H_2SO_4 5 mM as the mobile phase with a flow rate of 0.6 ml min^{-1}.

This method enabled to quantify the fraction of dextrin that remained present after the acid post-hydrolysis, as well as to determine the amount of total glucose released. It was not possible, however, to quantify the length of the glucose polymers. The amount of hydrolyzed dextrins was determined by calculating the difference between the final glucose concentration after post-hydrolysis and the initial concentration. Dextrin concentration was expressed as starch, by multiplying glucose concentration by the anhydro conversion factor from glucose to starch 0.9 (i.e. 162/180).

2.4.7 Sucrose

Sucrose content was quantified by HPLC (1100 Agilent with an IR detector) analysis. Column Aminex C42 (300 x 7.8 mm Bio-Rad) was used, with water as mobile phase at a flow rate of 0.5 ml min^{-1}. With this method, sucrose and its monomers (glucose and fructose) can be measured. An example of a calibration curve for these compounds is shown in Figure 2.4.

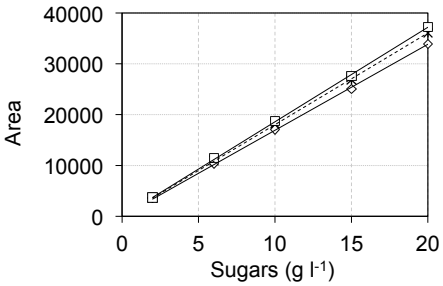

Figure 2.4: Calibration curve for fructose (white squares), sucrose (asterisk) and glucose (white rhombuses) by HPLC. (A=1859.5·Fructose (g l^{-1}), R^2=0.9997; A=1802.9·Sucrose (g l^{-1}), R^2=0.9998; A=1692.4·Glucose (g l^{-1}), R^2=0.9996).

2.4.8 Organic acids

The organic acids, such as acetic, propionic, butyric and valeric acid, were measured by an HPLC (1100 Agilent with an IR detector) using an Aminex HPX-87H column (BioRad), operated at 35°C with 10 mM H_2SO_4 as mobile phase at a flow rate of 0.4 ml min^{-1}. An example of a calibration curve for these compounds is shown in Figure 2.5.

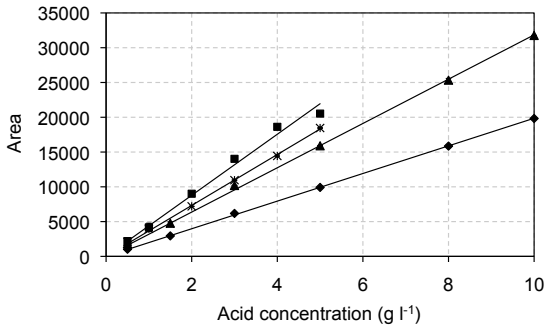

Figure 2.5: Calibration curve for acetic (rhombuses), valeric (squares), propionic (triangles) and butyric acid (asterisk) by HPLC. (A=1985.8·Acetic acid (g l^{-1}), R^2=0.9998; A=4389.5·Valeric acid (g l^{-1}), R^2=0.986; A=3184.7·Propionic acid (g l^{-1}), R^2=0.9993; A=3661.4·Butyric acid (g l^{-1}), R^2=0.999).

2.4.9 Ammonium nitrogen

Ammonium nitrogen (NH_4^+-N) was measured by a colorimetric method (4500-NH3 F) (APHA Standard Methods, 1998), based on the reaction of NH_3 with HClO and phenol, forming a strong blue compound (indophenol). The intensity of the blue colour is proportional to the ammonium concentration, which can be colorimetrically determined using a spectrophotometer at 635 nm.

Reagents preparation

- Solution A, Phenol-nitroprusiate: 15 g of phenol and 0.05 g of sodium nitroprusiate were added to 250 ml of buffer solution. The buffer solution was prepared by adding 30 g of $Na_3PO_4 \cdot 12H_2O$, 30 g $Na_3C_6H_5O_7 \cdot 2H_2O$ and 3 g EDTA per litre, adjusted to pH 12.

- Solution B, Hipoclorite: 15 ml of commercial bleach were mixed with 200 ml of NaOH 1 N and filled up to 500 ml with distilled water.

Determination procedure

The volume of sample was 2.5 ml (diluted if necessary to get a maximum concentration of 1 mg l^{-1}). 1.0 and 1.5 ml of solution A and B were added to the sample. After 45 min at room temperature, the concentration of NH_4^+-N was measured in a spectrophotometer (Shimadzu UV-1800, UV-Visible) at 635 nm. The quantification was done with a 6 points calibration curve in the range of 0-1 mg NH_4^+-N·l^{-1}, using NH_4Cl as

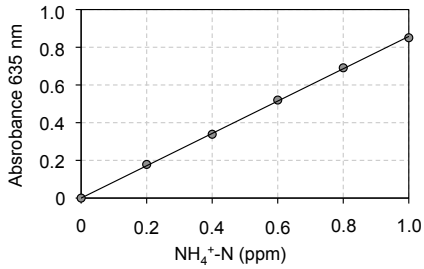

Figure 2.6: Calibration curve for ammonium nitrogen (Abs=0.857·NH_4^+-N (ppm), R^2=0.9996).

standard (Figure 2.6). A blank with reagents was also measured as a reference.

2.4.10 Orthophosphate phosphorus

Orthophosphate concentration (PO_4^{3-}-P) was analysed following the method 4500-P E (APHA Standard Methods, 1998). Ammonium molybdate and antimony potassium tartrate react with orthophosphate in an acid medium to form an antimony-phospho-molybdate complex. This compound is reduced by ascorbic acid into a blue-colored complex. The intensity of the blue colour is proportional to the orthophosphate concentration, which can be determined using a spectrophotometer at 880 nm.

Reagents preparation

- Solution A: Sulphuric acid 5 N.

- Solution B: Antimony potassium tartrate. 1.3715 g of $K(SbO)C_4H_4O_6 \cdot 0.5 \cdot H_2O$ was added to 500 ml of distilled water.

- Solution C: Ammonium molybdate. 20 g of $(NH_4)_6Mo_7O_{24} \cdot 4 \cdot H_2O$ was added to 500 ml of distilled water.

- Solution D: Ascorbic acid 0.01 M. 1.76 g of ascorbic acid was added to 100 ml of distilled water. This solution was stable for one week.

- Combined reagent: The above solutions were mixed in the following proportions to obtain 100 ml of the combined reagent: 50 ml of solution A, 5 ml of solution B, 15 ml of solution C and 30 ml of solution D. The mixture was mixed after the addition of each solution, following the mentioned order. This reagent was stable during 4 hours.

Determination procedure

The volume of the sample was 5 ml (diluted, if necessary, to a maximum concentration of 1 mg l^{-1}). One drop of phenolphthalein indicator solution, 0.5-1.0 g phenolphthalein in 1 l of ethanol at 80% concentration, was added to the sample. If a red colour was developed, some drops of solution A (H_2SO_4 5 N) were added until the colour disappeared. Then, 0.8 ml of the combined reagent was added and the mixture was vortexed. After at least 10 min but no more than 30 min, the intensity of blue colour was measured in a spectrophotometer (Shimadzu UV-1800, UV–Visible) at 880 nm. The quantification was done with a calibration curve in the range of 0 - 1 mg PO_4^{3-}-P·l^{-1} (Figure 2.7), prepared using a commercial standard solution of PO_4^{3-} (1000 mg PO_4^{3-}-P·l^{-1}; CertiPUR, Merck). For the calibration points, the combined reagent was added following the procedure previously indicated.

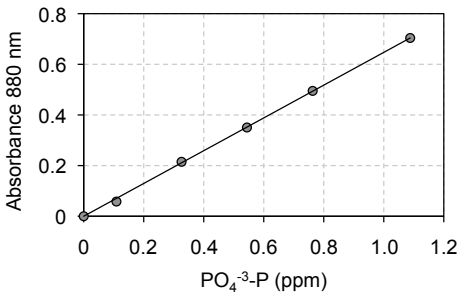

Figure 2.7: Calibration curve for orthophosphate phosphorous. (Abs=0.647·PO_4^{3-}-P (ppm), R^2=0.9995).

The absorbance of the samples and a blank sample was measured, and phosphorus concentration of the samples calculated using the corresponding calibration curve.

2.4.11 Total organic carbon and total nitrogen

The total organic carbon (TOC) and total nitrogen (TN) of the liquid supernatant were determined following the method 5310-B (APHA Standard Methods, 1998) using an automatic analyser (Shimadzu TOC-L_{CSN}).

2.5 CALCULATIONS

The physiological parameters, such as biomass and product yields ($Y_{X/S}$, $Y_{R/S}$ and $Y_{P/S}$), as well as the PHA productivity (Q_P), were calculated according to the following equations:

$$Y_{X/S} = \frac{\Delta X}{\Delta S} \quad \left[g \cdot g^{-1}\right]$$

$$Y_{R/S} = \frac{\Delta R}{\Delta S} \quad \left[g \cdot g^{-1}\right]$$

$$Y_{P/S} = \frac{\Delta P}{\Delta S} \quad \left[g \cdot g^{-1}\right]$$

$$Q_P = \frac{P_t - P_0}{t} \quad \left[g \cdot l^{-1} \cdot h^{-1}\right]$$

where X is the total cell dried weight (CDW); S is the consumed substrate; R is the residual cell mass (RCM); P is the PHA concentration and t is the fermentation time in hours. Q_P is the average productivity for each point of the experiment over the period from the start of the experiment to time t.

2.6 STATISTICAL ANALYSIS

The statistical analysis was conducted with the software R (version 3.2.0, R Core Team, 2015). A one-way analysis of variance (ANOVA) was carried out to determine if the values obtained were significantly different. Then, if the ANOVA confirmed the difference between the mean values, a post hoc analysis (Tukey's HSD) was applied to determine between which values the difference was significant, considering a level of significance of 0.05.

3

Effect of nitrogen and/or oxygen concentration on P3HB accumulation

The behaviour of *H. boliviensis* during growth in fed-batch culture under different kind of nutrient restrictions was examined. The metabolic switch between growth and accumulation phase is determined by the limitation in one or more essential nutrient for bacterial growth. The aim of this study was to test the effect of applying limitations of an essential nutrient, such as nitrogen, and the influence of different O_2 concentrations on P3HB production during the accumulation phase. Single limitations of nitrogen and oxygen provoke P3HB accumulations of 45 and 37% (g g^{-1}), respectively, while N-limitation with low O_2 supply causes the highest P3HB accumulation of 73%. The characterization of the P3HB production with the strain *H. boliviensis* would allow to optimise the process and to enrich the knowledge about the P3HB production from strains different than *R. eutropha*.

OUTLINE

3.1 INTRODUCTION

Nutrient limitation is one of the most powerful tools to force microbial cultures to perform in a defined way. It is well known that nutrients availability highly influences cell composition and metabolism (Herbert, 1961). As a matter of fact, nutrients constraint is usually applied to induce or optimise the formation of microbial products. For this reason, the study of limitations in such cultures is of high pertinence to biotechnology. Polyhydroxyalkanoates (PHA) are a good example of a microbial product whose synthesis is usually induced by a nutrient limitation.

Bacterial PHAs are polyesters produced as energy and carbon storage material, in the form of intracellular granules, when the carbon source is in excess, and another nutrient is limiting. Several types of nutrients deficiency are used to induce PHA production, i.e. nitrogen (Kim et al., 1994), phosphorous (Ryu et al. 1997), sulphur, magnesium (Witholt and Lageveen, 1992) or oxygen (Ward et al. 1977, Nath et al. 2008).

PHA microbial producers can be classified into three different types, based on their PHA production kinetics (Lopar et al. 2013): i) Strains that present clear separation between growth and accumulation phase, whose PHA production is promoted by imbalanced nutritional conditions; ii) strains that accumulate PHA under balanced nutritional conditions, but their PHA production is improved when a limitation in an essential nutrient is reached; and iii) strains that reach high PHA accumulations even without any limitation of an essential nutrient. The most studied PHA producer *R. eutropha* belongs to the second group; it accumulates PHA even under balanced conditions.

Poly(3-hydroxybutyrate) (P3HB), the most common type of PHA obtained from glucose, is generally synthesised in a three-step reaction, starting from acetyl-CoA (Figure 3.1). First, two molecules of acetyl-CoA are condensed by 3-ketothiolase (phaA) enzyme, forming a molecule of acetoacetyl-CoA. The product of the condensation is stereoselectively reduced by NADPH-dependent acetoacetyl-CoA reductase (phaB) to (R)-3-hydroxybutyryl-CoA. Finally, P3HB synthase (phaC) is the responsible of the P3HB polymerisation. Acetyl-CoA is a key molecule in bacterial metabolism. It is produced from pyruvate after the glycolysis pathway and it can be involved in the production of energy and growth through the TCA cycle, besides the P3HB pathway.

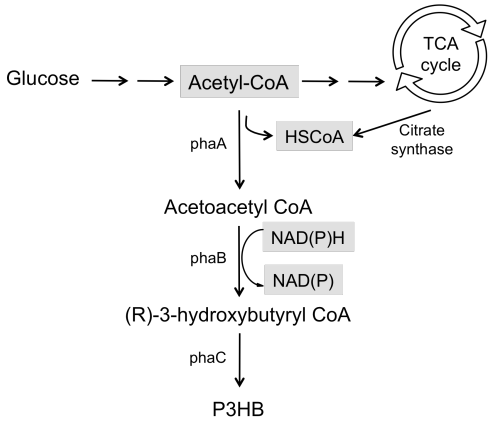

Figure 3.1: P3HB synthesis pathway (adapted from Kessler and Witholt, 2001). Critical metabolites, involved on P3HB pathway regulation, are highlighted in grey.

Not much is known about the regulation of PHA metabolism (Kessler and Witholt, 2001) at the transcription level. Regarding the regulation at enzymatic level, it is well

known that intracellular concentration of acetyl-CoA and free coenzymeA perform the main role in the PHA synthesis (Haywood et al., 1988). As well, a high intracellular concentration of NAD(P)H and a high ratio of NAD(P)H/NAD(P) enhance polymer accumulation (Lee et al., 1995).

Moreover, in *H. boliviensis*, ectoine and PHA are co-produced during the same fermentation process (Guzmán et al., 2009). Quillaguamán et al. (2008) reported the need of supplementing the medium of *H. boliviensis* with a complex nitrogen source to increase the PHA volumetric productivity. Different types of amino acids were tested and glutamine showed the best results. Nevertheless, glutamine was replaced by monosodium glutamate (MSG) in further experiments without a loss in PHA accumulation. MSG presents better aqueous solubility than glutamine and a drastic reduction in medium costs. However, the role of MSG in PHA accumulation, ectoine production or bacterial growth it is not clear.

The objective of this study was to determine how the type and severity of the limitation affect P3HB accumulation in *H. boliviensis*, and based on this knowledge to implement the optimal operational strategy to obtain the highest polymer accumulation with this strain.

3.2 MATERIALS AND METHODS

3.2.1 Experimental set-up for the study of ectoine production and the role of MSG

A flask volume of 500 ml with 200 ml of BC medium was used, testing two different MSG concentrations: 0 and 2%. Each point was carried out in triplicate. Cultures were incubated at 30°C and 200 rpm in an orbital shaker.

Bioreactor to study ectoine production was operated in fed-batch mode as described in Chapter 2. Dissolved oxygen was controlled and maintained by modifying the agitation speed and the airflow; from 25 h onwards these two variables were settled at their maximum value (650 rpm and 5 l min^{-1}, respectively). Glucose, ammonium chloride and potassium phosphate were maintained in no limiting conditions.

3.2.2 Ectoine and MSG quantification

Both, extracellular and intracellular ectoine concentrations were determined. For extracellular ectoine measurement, cells were separated from the culture media by centrifugation or serial filtration. Centrifugation was performed at 9500 x *g* for 5 min at room temperature, and then the liquid fraction was filtered through a 0.2 μm pore size membrane for HPLC analysis. Serial filtration of the culture broth was carried out through different pore size membranes i.e. 50, 5 and finally 0.2 μm. For intracellular ectoine analysis, cells were collected by the centrifugation of 3 ml culture broth (9500 x *g* for 5 min), resuspended in 1 ml distilled water and incubated at 25°C with shaking at 200 rpm for 30 min for ectoine release. The suspension was centrifuged at 9500 x *g* for 5 min and the supernatant filtered through a 0.2 μm pore size membrane for HPLC analysis.

Ectoine and MSG concentrations were quantified by HPLC and enzymatic colorimetric assay, respectively, as described in Chapter 2.

3.2.3 Nutrient limitation experiments at flask scale

An inoculum/culture volume ratio of 10% (v/v) was used in flask experiments with a vessel volume of 500 ml. BC medium was used, however, ammonium chloride concentration was reduced to 1 g l^{-1}, only in the case of the nitrogen limitation experiment. Four different culture volumes were used (50, 75, 150 and 300 ml) in order to test different oxygen mass transfer coefficients (k_La). The pH was initially adjusted at 7.5, and the culture media and salts were sterilised separately by autoclave. Cultures were carried out in triplicate in an orbital incubator at 30°C with a rotatory shaking of 250 rpm.

3.2.4 Oxygen transfer coefficient (k_La)

For the estimation of the k_La coefficient at flask scale, the correlation obtained by Liu et al. (2006) was used (Equation 3.1):

$$k_La = 0.141 \cdot N^{0.88} \cdot \left(V_L / V_0\right)^{-0.80} \qquad (R^2 = 0.997) \qquad (3.1)$$

where, N is the shaker speed (min^{-1}), V_L the liquid volume in the flask, V_0 the flask volume and k_La is expressed in h^{-1}. The constants were derived by linear regression of the data with the following equation: $\ln k_La = \ln k + a \ln N + b \ln (V_L/V_0)$. The close-to-unity R^2 value (the coefficient of determination) is indicative of a close fit of the experimental data to the regression model.

At bioreactor scale, k_La was determined in the absence of microorganisms in the liquid media. The dynamic gassing-out method proposed by van't Riet (1979) was used. Oxygen is displaced from the liquid phase by sparging nitrogen until the oxygen concentration is zero. Then, air is supplied again and the increase in oxygen concentration is measured in time. Dissolved oxygen was measured as the percentage of air saturation (pO_2).

3.2.5 Nutrient limitation experiments at bioreactor scale

Fed-batch cultivations were performed in a 2 l Biostat® MD, as described in Chapter 2, using a working volume of 1.5 l. Culture media was the same used at flask scale, only ammonium chloride concentration varied between experiments, 4 g l^{-1} was used for both N-limitation experiments, while, 6 g l^{-1} was used for O_2-limitation. Only in this last case, ammonium chloride concentration was monitored and maintained at 6 (± 2) g l^{-1} by adding a feed solution, composed by (per litre): 45 g of NaCl, 122 g of NH_4Cl and 270 g of K_2HPO_4. For carrying out off-line analysis, 10 ml samples were taken by triplicate from the bioreactor. Glucose concentration was monitored during all fed-batch experiments by off-line analysis and maintained at 20 (± 4) g l^{-1} by adding FBC medium.

3.2.6 Oxygen control

Aeration strategies varied between the different types of experiments. Initial aeration and agitation rates were 1 l min^{-1} and 400 rpm, respectively. These initial conditions were used to calibrate at 100% the pO_2 probe. For any of the experiments, air inflow rate and agitation speed were increased gradually when the dissolved oxygen decreased below 60%. The maximum air inflow rate and agitation attained were 5 l min^{-1} and 650 rpm,

respectively, which correspond to a k_La of 168 h^{-1}. In the case of O_2-limitation experiment, these maximum conditions were not enough to maintain a detectable dissolved oxygen signal, reaching an oxygen limitation state. To avoid the O_2-limitation state in the N-limitation experiment, pure O_2 was fed into the reactor instead of air, at an inflow rate of approximately 0.3 l min^{-1}. A particular operational case was the N-limitation experiment with low O_2 supply. To synchronise the limitation by nitrogen and the low oxygen supply, pure O_2 was fed into the bioreactor between 14 and 24 h. Afterwards, the airflow was restored at the previous conditions (5 l min^{-1}).

3.2.7 *In silico* analysis

The Basic Local Alignment Search Tool (BLAST) is a sequence comparison tool that approximates an alignment thus giving an optimal measure of similarity within the sequences. BLASTP 2.2.32+ software (Altschul et al., 1997; Altschul et al., 2005) was used to align the protein sequences of the genes forming the *phaCAB* operon from *R. eutropha* H16 strain with *H. boliviensis* genome (GenBank accession number: AGQZ00000000) in order to identify similar gene sequences in the halophilic bacteria genome. The Expectation value (E-value) cut-off was set to $1{\cdot}E^{-4}$ to minimise the chance of random occurrence of hits. The homologous proteins that presented more than 40% identity and 85% query coverage were subjected to further analysis to identify its genomic context.

3.2.8 Statistical analysis

Fermentation-to-fermentation reproducibility at bioreactor scale was determined by comparing the area under the curve (AUC) of glucose consumption and biomass concentration (RCM) of three independent fed-batch cultivations (two carried out under N-limitation conditions and one under N-limitation conditions with low O_2 supply). Since the three fermentations were conducted following the same experimental protocol and the profiles differences are expected to appear after the limiting N/C ratio is reached (~24 h), the parameters were calculated during a period from 0 to 24 h. First, the experimental biomass concentration and glucose consumption were fitted to exponential or polynomial equations, obtaining correlation coefficients (R^2) higher than 0.95, in all cases. Then, using these correlations, the values of glucose consumption and RCM were calculated every two hours, from 0 to 24 h. With this data, the AUC, its standard deviation and confidence interval at 95% level were calculated using the R package PK (Jaki and Wolfsegger, 2011).

A one-way analysis of variance (ANOVA) and post-hoc analysis (Tukey's HSD) were carried out as described in Chapter 2.

3.3 RESULTS AND DISCUSSION

3.3.1 Ectoine production by *H. boliviensis* and the role of MSG

H. boliviensis growth was tested with and without MSG at flask scale. The fermentation broth at 60 h of fermentation was collected, and the concentrations of extracellular and intracellular ectoine were determined. The results showed that this bacterium not only accumulates ectoine inside cells, but also excretes it into the medium, either with or without MSG (Table 3.1). No significant differences were detected in the measurement of the

excreted ectoine by the separation of the liquid broth either by centrifugation or filtration, with (p = 0.1878) or without (p = 0.4308) MSG.

Table 3.1: Ectoine production from *H. boliviensis* using two different growth media.

BC Medium	Intracellular ectoine (mg l^{-1})*	Extracellular ectoine (mg l^{-1})*	
		Centrifugation	Filtration
With MSG	500.9±99.0	1037.8±26.7	1194.6±169.1
Without MSG	9.5±1.9	367.3±81.7	421.7±70.1

*The data represent the average±SD from three independent experiments.

Intracellular and extracellular ectoine production with MSG was 500.9 and 1037.8 mg l^{-1}, respectively. Lower ectoine concentration was detected when MSG was not added to the medium (9.5 and 367.3 mg l^{-1}, intracellular and extracellular, respectively). The absence of MSG in the culture medium provokes a reduction in ectoine production of 74%. The distribution of the total ectoine, between the interior and exterior of the cells was represented in Figure 3.2. In both cases, the highest ectoine concentration was detected outside the cells rather than inside.

Protective role of ectoine as osmolyte define it as an intracellular product. In fact, for large-scale ectoine production *Halomonas elongata* is being used applying a process called bacterial milking in which ectoine is released by a hypoosmotic shock (Sauer and Galinski, 1998). Nevertheless, ectoine was found in the culture broth of *H. boliviensis* despite the fact that extracellular osmolarity was constant. This behaviour was previously described with the bacterium *Halomonas salina* DSM 5928 (Zhang et al., 2009; Lang et al., 2011; Chen et al., 2014).

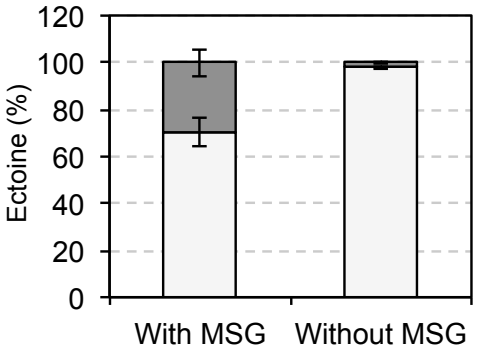

Figure 3.2: Ectoine distribution inside (grey) and outside (white) cells.

The absence of MSG in the culture medium affected not only ectoine production but also bacterial growth (RCM). As shown in Table 3.2, both parameters were clearly influenced by MSG. Higher P3HB accumulation was obtained when no MSG was added (40.8 and 50% with and without MSG, respectively). However, due to the low biomass reached, P3HB concentration without MSG was considerably lower than with MSG. Total ectoine produced was also substantially higher when MSG was added to the medium, as well as the ratio ectoine/RCM (mg of ectoine per g of biomass).

Table 3.2: Main fermentation parameters for *H. boliviensis* after 60 h of growth on different media. Each value represents the average±SD from three independent experiments.

	With MSG	Without MSG
CDW (g l^{-1})	6.2±0.1	3.4±0.1
P3HB (%)	40.8±2.6	50.0±0.4
P3HB (g l^{-1})	2.5±0.2	1.7±0.03
RCM (g l^{-1})	3.7±0.1	1.7±0.03
MSG consumed (%)	60.0	–
Total ectoine (mg l^{-1})	1607.2±155.5	431.2±70.2
Ectoine/RCM (mg g^{-1})	434.4	256.8

The beneficial effect of glutamate on bacterial growth and ectoine production was observed as well by other researchers with different strains (Onraedt et al., 2005; Zhang et al., 2009). This protective mechanism could be explained by considering glutamate as a carbon source for the production of ectoine (Onraedt et al., 2005). Glutamate is easily transformed into aspartate by transamination, which is an ectoine precursor. The combination of both metabolic routes enabled the reduction of ectoine synthesis to the reaction:

4 Glutamate → 1 Ectoine + 2 α-ketoglutarate + 4 CO_2 + 2 NH_3

From this reaction balance, a theoretical maximal production yield of 0.21 g ectoine g^{-1} MSG can be deduced (Onraedt et al., 2005).

Since bacterial growth was significantly lower in the absence of glutamate, it could be hypothesised that ectoine pathway from glucose is energetically more expensive for the bacteria, then a smaller amount of ectoine is produced, and the energy shortage hindered bacterial division.

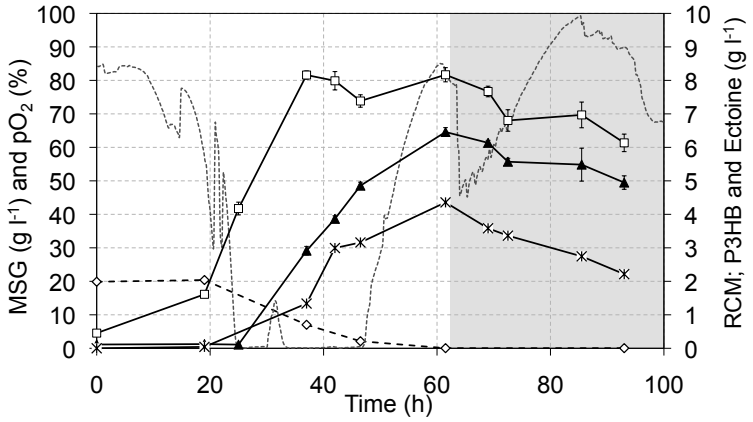

Figure 3.3: Time course of RCM (white squares), P3HB (black triangles), ectoine (asterisks), MSG (white diamonds with dashed line) and dissolved oxygen (dashed line) during fermentation. The grey area marks the fermentation decay.

In order to obtain a complete ectoine production profile, fed-batch fermentation was performed in a 2 l bioreactor (Figure 3.3). A concentration of 20 g l^{-1} MSG was added at

the beginning, and it was completely metabolised at 60 h. No ectoine was detected in the culture medium before 20 h; then its concentration started to increase while the maximum ectoine production (4.4 g l^{-1}) was reached at 60 h, yielding a ratio of 0.22 g ectoine g^{-1} MSG, which corresponds to the maximal theoretical yield previously mentioned. Ectoine concentration was measured from the supernatant obtained after centrifugation of the sample. Although during exponential growth (19-37 h) either agitation or air inflow rate were settled at their maximum value, oxygen consumption was very fast, and dissolved oxygen decreased enormously. At 47 h, coinciding with MSG depletion and the arrestment of biomass growth, the dissolved oxygen level increased to the original level. After MSG exhaustion, biomass, ectoine and P3HB concentrations started to decrease despite the main medium components i.e. glucose, ammonium and phosphorous, were not in limitation conditions (data not shown).

Maximal P3HB concentration was reached at the same time than maximal ectoine concentration, being possible a downstream separation of both products at their maximal levels. However, the main drive force of this study is the optimization of the P3HB production rather than ectoine. MSG was added throughout the development of this Thesis to avoid growth-limiting conditions.

3.3.2 Nutrient limitation experiments at flask scale

Different oxygen transfer rates were tested at flask scale to study the influence of oxygen in *H. boliviensis* growth (Figure 3.4). Maintaining the volume of the flask, four different culture volumes were used to obtain different oxygen mass transfer coefficients (k_La). A lower volume of culture (with a higher transfer area to volume ratio) will allow a better oxygen transfer and therefore a higher k_La value (Figure 3.4A). In Figure 3.4B, it is shown that the higher k_La value is, the higher the OD of the culture broth. Then, culture volume is inversely proportional to the oxygen transfer rate, and to the bacterial growth. In this previous experiment, it was detected a clear influence of the aeration on bacterial growth. A lower culture volume improves the oxygen mass transfer, and then, a higher OD was obtained (Figure 3.4B). It could be concluded that among all the conditions tested, the highest culture volume corresponded to the experiment with the highest oxygen deprivation.

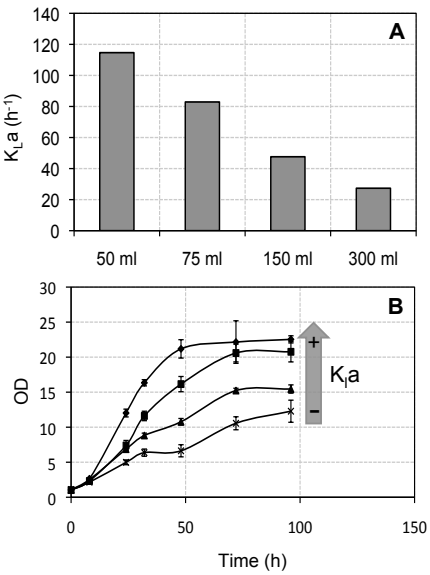

Figure 3.4: A. Estimated K_La values for the experiment at flask scale, varying the working volume. **B.** Influence of the culture volume on the bacterial growth measured by the OD at flask scale. Volumes of 50 ml (black diamonds), 75 ml (black squares), 150 ml (black triangles) and 300 ml (crosses) were tested.

Applying this last condition another experiment was carried out adding a nitrogen limitation. Two additional flask experiments were conducted to determine the influence of N-limitation at the lowest k_La used in the

previous experiment, trying to simulate low O_2 supply with and without N-limitation. The comparison of these experiments is shown in Table 3.3. P3HB accumulation was significantly higher when N-limitation was combined with low O_2 supply, 67.8 ± 1.8% against 50.3 ± 3.0% (p = 0.001). As observed in Table 4.1, under the same restriction in oxygen supply the application of a nitrogen limitation improves the P3HB accumulation significantly. These results suggested the need for a more robust and complete set of experiments to clarify the importance of oxygen and nitrogen concentrations in obtaining higher P3HB accumulations. For this reason, subsequent experiments were carried out at bioreactor scale, which allow a better control of the processes.

Table 3.3: Comparison of the results of two experiments with the same (low) k_La value, with or without N limitation at flask scale.

	Without N limitation	With N limitation
P3HB (%)	50.3±3.0	67.8±1.8
CDW (g l^{-1})	4.6±0.3	5.1±0.3
P3HB (g l^{-1})	2.3±0.2	3.5±0.3
RCM (g l^{-1})	2.3±0.3	1.7±0.1

3.3.3 The influence of different nitrogen and oxygen concentrations on P3HB production

The study of the single (N or O_2) limitations and the effect of oxygen concentration were carried out at bioreactor scale. Figure 4.3 shows the time courses of the concentrations of total cell weight, residual biomass, P3HB, ammonia, monosodium glutamate and the dissolved oxygen percentage in the culture broth. During fermentations, phosphorous and glucose concentrations were also followed and maintained at 2.2(±1.5) g l^{-1} of K_2HPO_4 and 20(±4) g l^{-1} of glucose (data no shown) to avoid limiting conditions of these nutrients.

The standard error of the area under the curve (AUC) of glucose consumption and biomass concentration, calculated during the growth period (from 0 to 24 h) of three independent bioreactor fermentations, were 3.80 and 2.17%, respectively. This analysis indicates that fermentation-to-fermentation variability at bioreactor scale is low and similar to that obtained during the flask experiments (5.34 and 1.14%, respectively). AUC is a parameter commonly used in pharmacokinetic studies for comparing concentration-time responses. AUC has also been used for determining the reproducibility of ABE fermentations at bioreactor scale (Gonzalez-Peñas et al., 2015) and for evaluating the relative abilities of commercial wine yeast strains to utilise glucose and fructose (Liccioli et al., 2011).

Nitrogen limitation fed-batch culture of *H. boliviensis* was first carried out, and the results are shown in Figure 3.5A. During the first 24 h, CDW and RCM values were the same; no P3HB accumulation was detected. Nitrogen and MSG exhaustion were noted between 24 and 36 h of cultivation, when the N/C ratio was 0.04 and 0.02, respectively. P3HB started to accumulate significantly at that moment, while cell growth gradually slowed down. Maximum P3HB and CDW concentrations of 15 and 33 g l^{-1}, respectively, were reached after 60 h of fermentation.

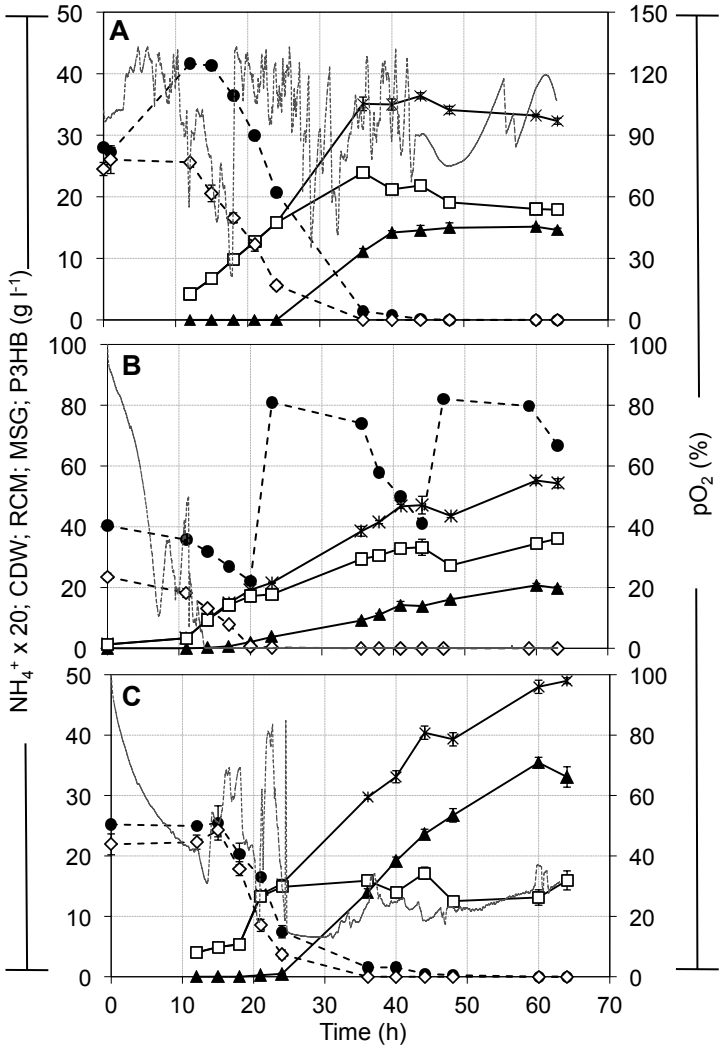

Figure 3.5: Time course of dissolved oxygen (dashed line); ammonium concentration (black rounds with dashed line); CDW (black crosses); RCM (white squares); MSG (white diamonds with dashed line) and P3HB (black triangles) during fermentations under (A) nitrogen limitation; (B) oxygen limitation and (C) nitrogen limitation with low oxygen supply.

Similar accumulation content was obtained with the single limitation by oxygen, as it is shown in Figure 3.5B. Nitrogen was added to the media to avoid its limitation; therefore the N/C ratio was maintained between 0.10 and 0.36 during the process. MSG was exhausted at 20 h. After applying the maximum agitation rate (650 rpm) and the maximum aeration flow (5 l min^{-1}), the oxygen concentration was below the detection limit from 13 h until the end of the fermentation. At this moment the P3HB accumulation started, reaching the maximal P3HB concentration and CDW of 20 and 55 g l^{-1}, respectively, at 60 h of fermentation. However, the residual biomass growth did not stop, and there was a gradual increase during limitation conditions.

The N-limitation with low O_2 supply fed-batch culture reported the highest P3HB accumulation (35 g l^{-1}) and CDW concentration (48 g l^{-1}) at the same fermentation time (60 h), as it is shown in Figure 3.5C. The initially added nitrogen was exhausted after 24 h of fermentation, together with the MSG, yielding a N/C ratio of 0.02 as in the N-limitation fed-batch. Dissolved oxygen was lower than the 20% at that moment as well, even though the maximum agitation speed and aeration flow were used. Both nutrient constraints converged in time, triggering the P3HB accumulation, while residual biomass growth was again stopped.

Figure 3.6 shows the changes in P3HB content and productivity with time. P3HB value was similar (45.7-37.6%) in both single limitations (Figure 3.6AB), while the N-limited culture with low O_2 supply reported the highest P3HB accumulation (73.0%). The maximum productivity for the three limitation conditions was reached at the same fermentation time (40 h). No statistical differences were detected for the maximum productivity achieved with both single limitations, 0.93±0.04 and 1.02±0.15 g l^{-1} h^{-1}, for N- and O_2-limitation, respectively (p = 0.552). However, the maximum productivity reached in the N-limited culture with low O_2 supply 1.32±0.08 g l^{-1} h^{-1} (Figure 3.6C) was the highest ($0.007 < p < 0.025$).

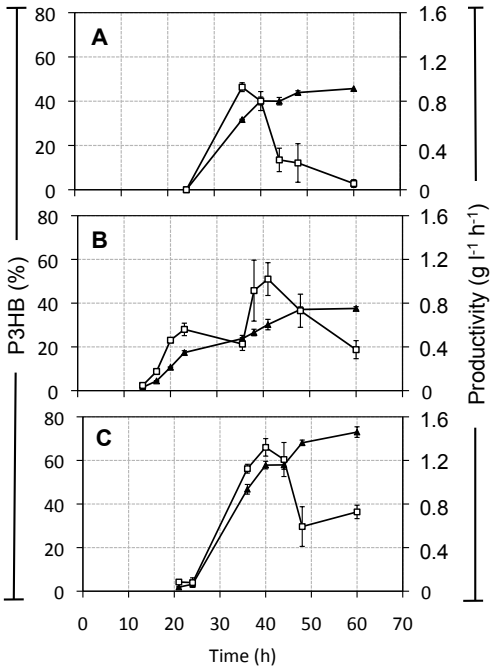

Figure 3.6: P3HB accumulation (black triangles) and P3HB productivity (white squares) during **(A)** nitrogen limitation; **(B)** oxygen limitation and **(C)** nitrogen limitation with low oxygen supply.

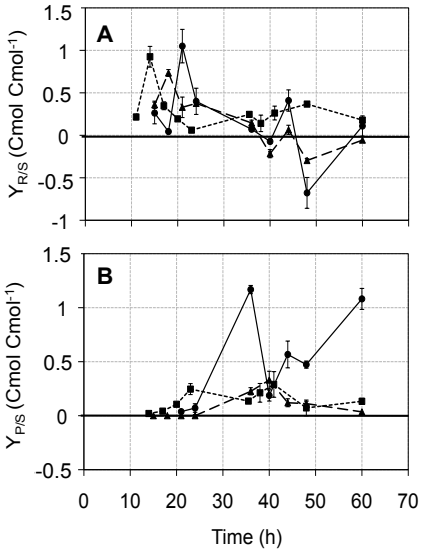

Figure 3.7: Different production yields: **(A)** residual biomass; and **(B)** P3HB, on consumed glucose during fermentations with nitrogen limitation (black triangles), oxygen limitation (black squares) and nitrogen limitation with low oxygen supply (black rounds).

Figure 3.7 shows the time courses of residual biomass ($Y_{R/S}$) and P3HB ($Y_{P/S}$) yields from glucose. Biomass yield was higher during the first 24 h of fermentation in all the cases (Figure 3.7A). Nevertheless, P3HB yield from glucose presented an the opposite trend, after the first 24 h the yield increased, being highest in the case of the N-limitation with low O_2 feeding (Figure 3.7B). The negative yields are due to a slight decrease of biomass concentration at the end of the fermentation.

Glucose consumption during fermentations is represented in Figure 3.8A. The highest glucose consumption was obtained under O_2-limitation and the lowest during the N-limited culture with low O_2 supply. There was a difference of 91 g l^{-1} glucose between the highest and the lowest consumption rates. In Figure 3.8B the distribution of the main products obtained from the carbon source for each fermentation condition is represented. Carbon uptake for biomass was similar in both cases of N-limitation with high or low O_2 supply (around 15%). However, in the O_2-limitation the carbon used for biomass was slightly higher (20%). The carbon source employed in P3HB production for both single limitations was around 13%. Nevertheless, 37% of the consumed carbon was transformed into P3HB in the case of the N-limitation with low O_2 supply. Single limitations presented a similar profile, where 60-65% of the carbon was mainly utilised for CO_2 production, while double nutrient constraint employed 41% of the consumed carbon for the same purpose.

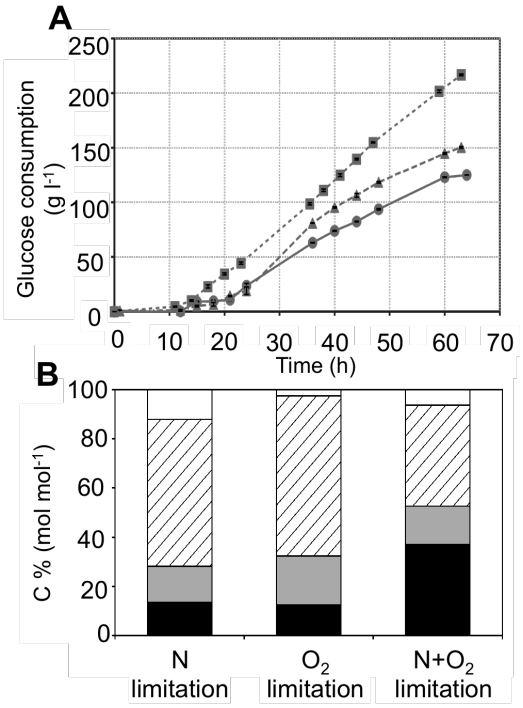

Figure 3.8: A. Glucose consumption during fermentations with nitrogen limitation (black triangles), oxygen limitation (black squares) and nitrogen limitation with low oxygen supply (black rounds). **B.** Global carbon balance, percentage of the carbon source distributed in P3HB (black), RCM (grey), estimated CO_2 (hatched) and other byproducts (white).

At bioreactor scale under different nutrient concentrations, the same growth and P3HB production patterns were observed during the phase of balanced growth culture. During the first 24 h of operation, glucose was mainly used for residual biomass synthesis before nitrogen and/or oxygen were exhausted and no P3HB was produced (Figure 3.5). This pattern can also be observed in Figure 3.7A, where the yields of biomass ($Y_{R/S}$) presented the same and the highest values during the first 24 h of culture in any of the fermentations. This behaviour contrast with that of *R. eutropha*, which can accumulate P3HB even under balanced nutrient media. On the contrary, *H. boliviensis* metabolism under balanced growth conditions seems to be driven mainly towards the carbohydrate catabolic pathway. After the glycolysis step, acetyl-CoA is fed into the TCA cycle and the resultant CoA inhibits acetyl-CoA acyltransferase (phaA), blocking then the P3HB pathway. The cells utilised the available carbon source for biomass and energy production at the beginning of the batch culture due to the balanced nutrient composition. Nevertheless, when nitrogen and/or oxygen started to decrease provoking an imbalance in the culture media, the P3HB production took place. This phenomenon can be observed in the fermentation profiles in Figure 3.5, but also in the production yields ($Y_{P/S}$), represented in Figure 3.7B, which started to increase after 24 h of fermentation.

In the late 1980s, it was reported the presence of the *phaCAB* operon in *R. eutropha* (Schubert et al., 1988; Slater et al., 1998; Peoples and Sinskey, 1989). This operon harbours three genes (*phaC*, *phaA* and *phaB*) encoding the enzymes involved in P3HB biosynthesis, where the *phaC1* gene is constitutively expressed (Haywood et al., 1989).

According to our experimental results the P3HB production in *H. boliviensis* does not seem to be constitutively expressed. Since the *phaC1* gene from *R. eutropha* forms part of the operon, an *in silico* analysis was conducted to search for the same operon structure in *H. boliviensis* (Table 3.4). This kind of gene construction was not found in *H. boliviensis*; however, it is worth to notice that the copies of the *phaA*, *phaB* and *phaC* genes of *H. boliviensis* were found randomly distributed into its genome. This allows us to speculate that the absence of the *phaCAB* operon could be an explanation of the lack of P3HB production under balanced nutrient medium. Albeit it would not be possible to asseverate that the presence of *phaCAB* operon is the only reason for the constitutive expression. For a more detailed discussion, a deeper study of the promoters involved in the PHA synthesis of *H. boliviensis* should be done.

Table 3.4: *In silico* analysis of the relevant genes for P3HB metabolism in *H. boliviensis*.

Query gene locus (*R. eutropha* H16)	Query cover (%)	E-value	Identity (%)	Locus (*H. boliviensis*)	Product	Genomic context	
						Upstream	Downstream
PHA synthases (*phaC*)							
H16_A1437 (*phaC1*)	88	$7{\cdot}e^{-153}$	44	KUC_2319	Poly(3-hydroxyalkanoate) synthetase	AhpF	
H16_A2003 (*phaC2*)	94	$9{\cdot}e^{-175}$	48	KUC_3350	Poly-beta-hydroxybutyrate polymerase		*LpqC*
	94	$2{\cdot}e^{-148}$	42	KUC_3102	Poly-beta-hydroxybutyrate polymerase	ECH	
β-Ketoacyl-CoA thiolases (*phaA*)							
H16_A1438 (*phaA*)	99	0.0	70	KUC_0835	Acetyl-CoA acetyltransferase	AD	Transporter
	99	$1{\cdot}e^{-113}$	47	KUC_2179	Acetyl-CoA acetyltransferase	*TetR*	MAC
	99	$1{\cdot}e^{-100}$	44	KUC_1527	β-ketoadipyl-CoA thilolase	HCD	
	99	$2{\cdot}e^{-89}$	42	KUC_2157	3-ketoacyl-CoA thiolase	HD	*fadB*
H16_A1445 (*bktB*)	99	$1{\cdot}e^{-143}$	57	KUC_2165	3-ketoacyl-CoA thiolase	LCFACL	*TatD*
	99	$1{\cdot}e^{-89}$	50	KUC_2195	Acetyl-CoA acetyltransferase	AT	*sigZ*
β-Ketoacyl-CoA reductases (*phaB*)							
H16_A1439 (*phaB1*)	98	$1{\cdot}e^{-78}$	54	KUC_0794	3-ketoacyl-ACP reductase		
	99	$1{\cdot}e^{-63}$	43	KUC_3832	3-ketoacyl-ACP reductase	MCT	ACP
H16_A2460 (*abmB*)	96	$6{\cdot}e^{-42}$	41	KUC_1852	Short-chain dehydrogenase		XP

ACP = Acyl carrier protein; AD = Aspartate decarboxylase; AT = Arsenic transporter; ECH = bifunctional Enoyl-CoA hydratase/phosphate acetyltransferase; HCD = 3-hydroxyacyl-CoA dehydrogenase; HD = histone deacetylase; LCFACL = Long-chain fatty-acid-CoA ligase; MAC = Methyl-accepting chemotaxis; MCT = Malonyl CoA-ACP transacylase; XP = xylose repressor; Blank = Region not identified.

According to Kessler and Witholt (2001) the regulation of PHA metabolism can take place at different levels; i) activation of the genes involved in the expression (*phaA*, *phaB* and *phaC*) due to specific environmental signals, such as nutrient starvation; ii) activation of the expression genes by specific cell components or metabolic intermediates; iii) inhibition of metabolic enzymes or competing pathways; or iv) a combination of those. Nitrogen forms part of the proteins, DNA and other cell components, therefore is an essential nutrient for biomass growth. Nitrogen exhaustion will inhibit bacterial growth since the machinery needed for the bacterial division will not be built, but trigger the P3HB synthesis as it was mentioned above. In the absence of a nitrogen source, the intracellular pyruvate concentration is quite higher than under optimum growth conditions. As a consequence, the concentration of acetyl-CoA will be high, but the concentration of free CoASH will be low; then acetyl-CoA acyltransferase (phaA) will not be inhibited, and acetoacetyl-CoA synthesis will take place (Oeding and Schlegel, 1973). As it can be observed in Figure 3.5A, after nitrogen exhaustion, biomass growth was stopped and P3HB accumulation took place for 16 h more. After 40 h of fermentation, both, accumulation and growth were arrested.

MSG was followed during all the cultivations since it could act as a nitrogen source. MSG was depleted together with the ammonium, or at 20 h in the case of the O_2 limitation experiment, causing no interference with the nitrogen limitation conditions. Since nitrogen is easy to control, it is usually chosen as limiting nutrient to trigger P3HB formation (Kim et al., 1994). In fact, in some cases, P3HB accumulation promoted due to the nitrogen exhaustion is even higher than using oxygen limitation (Du et al., 2000).

According to the metabolic response to oxygen deprivation studied for other bacterial strains (Quillaguamán et al., 2008), O_2 limitation increases the NADH/NAD ratio and high concentrations of NADH inhibits citrate synthase and isocitrate dehydrogenase, blocking the TCA cycle. The accumulation of acetyl-CoA triggers the P3HB synthesis, during which the P3HB assumes the role of an alternative electron acceptor. In the single O_2-limitation experiment, P3HB accumulation took place after the O_2 exhaustion (Figure 3.5B). There are many studies focused on the role of the oxygen concentration in PHA synthesis from different microorganisms. In some cases leading to enhancements in P3HB production, such as in *Pseudomonas putida* (Kim et al., 1997) or *Methylobacterium* (Nath et al., 2008), but it also could have a negative influence like in the case of *Bacillus mycoides* (Borah et al., 2002). It has also been reported that another *Halomonas* strain (*H. campisalis*) needs oxygen during the growth phase and oxygen limitation to enhance PHA accumulation within cells (Kshirsagar et al., 2012). In fact, the accumulation increased from 41 to 56% of PHA in that study. In this work under single limitations provoked either by nitrogen or oxygen the P3HB accumulation was significantly different ($p < 0.001$), slightly higher in the case of N-limitation, 45.7±0.8%, while 37.6±0.8% under O_2-limitation (Figure 3.6). Only when a nitrogen limitation is combined with low O_2 supply, the P3HB accumulation increased to 73.0±2.4%, almost twice the accumulation obtained with the single limitations. These results demonstrate that the simultaneous limitation by nitrogen and a light restriction of oxygen is more effective than any of the limitations separately for this strain. Oxygen starvation regulates PHA metabolism by the inhibition of the TCA cycle, which is the most important competing pathway for P3HB route and, on the other hand, the nutrient limitation has as well a role in the regulation of the PHA metabolism by the

activation of P3HB gene expression. Then, it seems that both kinds of regulation mechanisms have an additive effect towards the PHA accumulation with *H. boliviensis*.

It is worth to notice that during O_2 limitation and light O_2 restriction, the same aeration and agitation was used; nevertheless, it was only observed a clear pO_2 limitation in the former case. An explanation of this could be that during single O_2 limitation, since the nitrogen is available, the biomass –RCM– is continuously growing, reaching a value of 36.1±0.5 g l^{-1}. Meanwhile, with the N-limitation under low O_2 supply, biomass growth was arrested after the nitrogen exhaustion in a value around 17.9–19.1 g l^{-1} and, consequently, half of the biomass consumed less oxygen. Despite the fact that the dissolved oxygen during the N-limitation was around 20%, the effect of the low oxygen available is not negligible, since it was reached a 73.0±2.4% of P3HB accumulation while during single N-limitation, when oxygen was always near saturation, only 45.7±0.8% of P3HB was obtained.

Regarding the efficiency of the process according to the carbon source consumed and employed in P3HB accumulation, the N-limitation with low O_2 supply process was, as well, the most efficient one. The global amount of carbon source (glucose) consumed was the lowest (125 g l^{-1}) among all the processes. Moreover, and in line with the previous results, the N-limitation with low O_2 supply culture presents the highest amount of consumed carbon used for P3HB production (37%).

3.4 Conclusions

Ectoine production by *H. boliviensis,* under the conditions tested in this study, was found to be mainly extracellular secreted, despite, this is usually described as an intracellular product. The supplementation of the growth medium with MSG enhances the total ectoine production and yield (ectoine/RCM), but it also improves biomass production and P3HB concentration.

On the other hand, P3HB production by *H. boliviensis* presents a high dependence on the type and degree of nutrient limitation. Bacterial cultivation under balanced nutrient medium did not drive to P3HB accumulation. The results obtained in this study demonstrate that the simultaneous limitation by nitrogen and a light restriction of oxygen is more efficient than a single limitation by nitrogen or oxygen, separately, for this strain.

4

Application of flow cytometry for monitoring the production of P3HB

A flow cytometry (FC) protocol was implemented to measure poly(3-hydroxybutyrate) content in *H. boliviensis*, to have a faster and easier control of the process. The halophilic bacterium was stained with BODIPY 493/503 and analyzed using FC. Bacterial polymer accumulation induced by two different nutrient limitations during the operation of a 2 l bioreactor was studied using traditional gas chromatography (GC) analysis and FC.

The application of this rapid and straightforward method is useful to obtain complex and precise information about PHA accumulation that could be used for the monitoring, control and optimization of the production of PHA. A clear correlation between the PHA concentration determined by GC and the fluorescence signal obtained from stained bacteria by using FC was observed. Additionally, the heterogeneity of bacterial population as a function of PHA content was measured.

.

OUTLINE

4.1 Introduction

Analytical methods for PHA detection and determination include gravimetry, turbidimetry, optical, fluorescence, or electron microscopic techniques, UV, Raman, and infrared spectrometry, genetic methods (Southern blot hybridization, PCR, fluorescence-labeled in situ hybridization), ^{1}H and ^{13}C NMR, and advanced gas and liquid chromatographic approaches (Koller and Rodríguez-Contreras, 2015). Nevertheless, most of these methods are laborious and time-consuming. From an industrial point of view, one of the key aspects of microbial process control and optimization relies on the possibility of making measurements of cell viability, biomass growth and product formation in real-time conditions (Díaz et al., 2010). For that reason, the application of a faster technique such as flow cytometry (FC), which allows an easier sample preparation for PHA quantification and even a fully automatic analysis (Kacmar et al., 2005), is required.

FC technology started in the 20-30's when the ancestors of modern flow cytometers were built for analysis of flowing colloidal suspensions and for detection, counting and sizing of particles in aerosols, such as mine dust. The first flow cytometric application in microbiology was done by Gucker et al. (1947), for the detection of bacterial cells in aerosols. The driving force of FC development was its clinical use. From the 70's onwards, commercial flow cytometers have been produced (Shapiro, 1995). At that moment FC has been used mainly in blood and cancer cells identification. And since monoclonal antibodies became available in the 80's, FC has been applied for antigen detection, with especial importance in prediction the course of HIV infection. The application of this technique to biotechnology process has been done for the last 30 years, and nowadays it is a common technique that can be easily applied for several purposes.

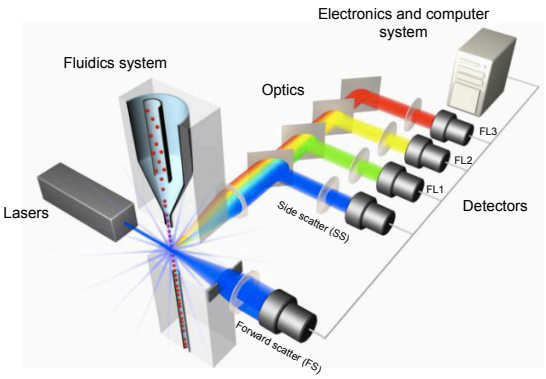

Figure 4.1: Scheme of a typical flow cytometer. Source: Thermo Fisher Scientific.

FC is a technique used for the characterization of cell populations at single cell level. It is a multiparametric technique due to its capacity of measuring physical and chemical/biological characteristics of microorganisms at single cell level. A laser beam illuminates cells (or other particles) and the intensity of the generated optical signals is measured as scattering or fluorescence signals (Figure 4.1).

Forward and side scattering (FS and SS, respectively) are correlated with structural parameters like size or granulometry, which allows e.g., the study of morphological changes (Gónzalez-Peñas et al., 2015) or the monitorization of the plasmid loss in recombinant strains (Lu-Chau et al., 2001). Several parameters such as DNA, RNA, specific proteins, lipids, etc. and functions or states like viability or membrane

potential (Tracy et al., 2010) can be measured as well with FC by using dyes that allow to stain cells selectively and measure the fluorescence signal.

As it was previously tested for *R. eutropha*, intracellular PHA accumulation modifies the bacterial size and internal granulometry, and these changes can be easily measured by FC (Srienc et al., 1984) and by different analytical techniques, such as scanning electron microscopy (Cavalheiro et al., 2013). Using a Coulter counter, Pedrós-Alió et al. (1985) determined that the cell volume of *R. eutropha* increased from 1.2 to 3.8 g m^{-3}, which was directly related to a P3HB content increase from 0 up to 1.7 pg $cell^{-1}$. However, changes in cell size and granulometry, measured by FC, can be attributed as well to cell modifications different to PHA accumulation. For this reason, the use of fluorescent dyes, which stains specifically the PHA, is a more reliable procedure to get a direct correlation of flow cytometric signals to the amount of accumulated PHA (Kacmar et al., 2005). We found no previous studies about the characterization of a bacterium from the genus *Halomonas* with flow cytometry, despite the rising interest of halophilic bacteria for industrial biotechnology.

In this study, we have established a correlation between the PHA accumulation in *H. boliviensis* measured by GC and flow cytometry. FC also allowed the study of parameters such as the percentage of PHA-containing cells, cell size and the dynamic evolution of the heterogeneity of bacterial population.

4.2 MATERIALS AND METHODS

4.2.1 Bacterial cultivation

In this study, bioreactor experiments were carried out in order to obtain PHA accumulation under two different nutrient limitations: nitrogen-limiting (NL) conditions and low O_2 supply in addition to nitrogen starvation (NL-O_2). Each sample was measured by GC and FC with and without staining.

Experiments under N-limiting (NL) and N-limiting with low O_2 supply (NL-O_2) conditions were carried out as described by Chapter 3.

4.2.2 Biomass quantification

CDW and RCM were determined gravimetrically as described in Chapter 2. In this case, the standard deviation (SD) of RCM carried out by triplicate was in the range of 0.7 to 9.9%, with a typical value of 3.8%. OD was also determined as described in Chapter 2.

4.2.3 PHA quantification by GC

The protocol for PHA quantification by GC was described in Chapter 2. In this case, the standard deviation of PHA content determined by triplicate was in the range of 0.6 to 16.1%, with a typical value of 4.1%.

4.2.4 Staining bacteria for cytometric PHA analysis

Staining protocol was based on the previous work of Kacmar et al. (2005) with some modifications for this strain. First, cells were made permeable to the stain by incubation in

50% (v/v) ethanol for 20 min. Next, cells were pelleted and resuspended in 1 ml of phosphate buffered saline (PBS) at room temperature in a 1.5 ml Eppendorf tube. The sample was diluted in PBS before staining. Cells were stained with 30 μl BODIPY 493/503 (Molecular Probes, Invitrogen) with a concentration of 100 μg ml^{-1} dissolved in 1% (v/v) DMSO. After 5 min of incubation with the stain, bacteria were pelleted and resuspended in PBS at 4°C and placed on ice and in the dark before analysis.

4.2.5 Flow cytometry

A Beckman Coulter FC500 (Inc. Brea, CA, USA) flow cytometer (CACTI, University of Vigo, Vigo, Spain) with a 20 mW Argon laser and a wavelength of 488 nm was utilized to measure the single cell fluorescence intensity after staining. BODIPY 493/503 fluorescence was measured using a 525 nm band-pass filter (FL1). At least 30,000 cells were measured in each sample, and the flow rate was set at medium speed. Signals were recorded using logarithmic amplification and the data was stored as list mode data files (LMD) for subsequent analysis. These LMD files store data according to the FSC 2.0 standard (Dean et al., 1990). Data were analysed with the software WEASEL FC v3.0.2. (Walter and Elisa Hall Institute, Melbourne, Australia). Mean signal values of fluorescence, side scatter and forward scatter are shown in arbitrary units, which scale goes from 0 to 1024. The percentages of cells containing and not containing PHA (PHA^+ and PHA^-, respectively) were calculated from dot plot graphs of FL1 *vs.* FS. The limits of the region of PHA^-, which corresponds with the cell autofluorescence, were determined by measuring the fluorescence signal (FL1) from non-stained cells, but previously permeabilized with ethanol and diluted with PBS.

4.2.6 Microscope images

A JEOL JEM-1011 (JEOL Ltd., Akishima Japan) transmission electron microscope (TEM) was used to evaluate the morphological differences between different accumulation states. For that purpose, cells were taken from samples stored for flow cytometric analysis, fixed with glutaraldehyde, embedded, and sectioned using an ultramicrotome.

4.2.7 *In silico* analysis

BLASTP 2.2.32+ software (Altschul et al., 1997; Altschul et al., 2005) was used to align the protein sequences of the genes *phaM* and *phaF/phaI* from *R. eutropha* and *Pseudomonas putida* strains, respectively, with *H. boliviensis* genome (GenBank accession number: AGQZ00000000) to identify similar gene sequences in the halophilic bacteria genome. The Basic Local Alignment Search Tool (BLAST) is a sequence comparison tool that approximates an alignment thus giving an optimal measure of similarity within the sequences. The Expectation value (E-value) cut-off is usually set to $1 \cdot e^{-4}$ to minimize the chance of random occurrence of hits. Moreover, only gene matches with identity and query coverage values higher than 40% and 85%, respectively, were considered as similar sequences.

4.2.8 Statistical analysis

Profiles of the experimental values were compared with the values obtained using the equations derived from flow cytometry and optical density data to determine the accuracy of the model. The area under the curve (AUC) of triplicate results of CDW, P3HB percentage, P3HB concentration and productivity (Q_P) were calculated with the software R version 3.2.0 (R Core Team, 2015) using the package PK (Jaki and Wolfsegger, 2011). The *auc* function of the PK package was used to determine the confident intervals (CI) of triplicate results considering a complete sampling design at a level of significance (α) of 0.05. Then, the output of the previously calculated *auc* function was compared with the AUC of the values predicted by the model using the *test* function of the same package. This comparison permitted to determine if there were significant differences between the fermentation profiles based on experimental and predicted values.

4.3 RESULTS AND DISCUSSION

4.3.1 Forward and side scatter signals

H. boliviensis presented a relation between P3HB accumulation and FS/SS signals, as can be observed in Figure 4.2. In a sample with a small P3HB accumulation (7% w/w P3HB/CDW, measured by GC), most of the bacterial population was gathered in a unique region (R0), which presented a mean value of the signal of 52.5 and 6.7 for FS and SS, respectively (Figure 4.2 A). As observed with the increase of P3HB accumulation in the FS *vs.* SS dot plot (Figure 4.2 B), a fraction of the cell population (R1) was displaced from the original state (R0) by the increase in FS and SS signals. These cell populations were also observed by TEM (Figure 4.2 CD), where the white content of cells represent the P3HB inclusions. TEM images also made possible to detect some qualitative morphological differences between both cultivation states. However, it is necessary to have into account that TEM analysis may present several interferences due to the sample preparation (e.g. cells orientation for cutting, cutting angle, infiltration with the epoxy resin) that can affect the shape of granules (Mravec et al., 2016).

One could expect that once P3HB accumulation is trigger by a nutrient limitation, all the cells would start the accumulation process as described for *R. eutropha* (Kacmar et al., 2005). However, it is worth to notice that the cell population of *H. boliviensis* did not change homogeneously. A high cell population in region R0 (71.4%), *a priori* without P3HB, was observed when the total P3HB content measured by GC was the highest (Figure 4.2 B). A similar heterogeneity in P3HB content can be found in TEM photographs of *H. boliviensis* obtained by Quillaguamán et al. (2006) from samples harvested at the point of maximum P3HB accumulation.

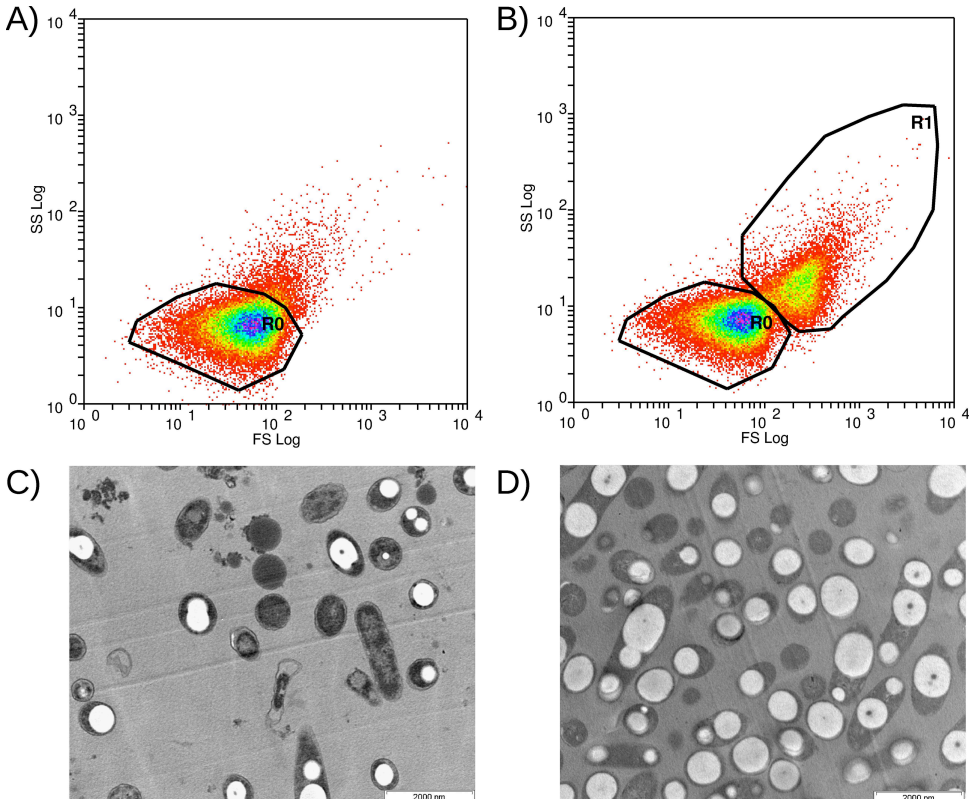

Figure 4.2: Forward and side scattering signals measured by flow cytometry for different P3HB accumulation states of *H. boliviensis*: (A) 7% and (B) 67.5% w/w P3HB/CDW. And TEM photographs of the bacteria observed at the same accumulation states: (C) 7% and (D) 67.5% w/w P3HB/CDW. Samples at 7 and 67.5% w/w P3HB/CDW were taken at 24 and 64 h of growth, respectively, during fermentation with nitrogen limitation and low oxygen supply.

The bacterial population (Figure 4.2 B) surrounded by region R1, which only represents the 27.7% of the total population measured by FC, showed the highest size and most complex granulometry. The mean value of the FS signal for the cell population from region R1 was 275.5, while the same parameter from region R0 was 55.6. These differences between bacterial populations may indicate that the cells that belong to the region R1 (PHA^+) contribute to PHA accumulation. However, the limits of the regions -R0 and R1- in the dot plot diagram is not very clear; then this signal can not be used to obtain a robust correlation between the PHA accumulation and the morphological changes.

4.3.2 PHA staining: fluorescence signal

A more sensitive method, based on the use of a specific dye, was applied to monitor PHA accumulation. BODIPY 493/503 was the lipophilic dye chosen, due to its more specific staining compared with Nile red (Kacmar et al., 2005; Lee et al., 2013). The same sample from Figure 4.2 B (67.5% w/w P3HB/CDW, by GC) was stained and measured with FC. The resultant signals of fluorescence (FL1) *vs.* FS were plotted in Figure

4.3 B. Here, two different cell regions were separated even easily than in Figure 4.2 B. The bacterial region called R3 represents the 29.2% of cells. These cells contain PHA (PHA^+ cells) since this region presented the highest mean values of FS (265.3) and FL1 signals (234.2). Meanwhile, the most populated region, R2, was composed of cells that do not contain PHA (PHA^- cells) and presented the lowest mean values of FS (52.3) and FL1 signals (7.2). Both, FL1 and FS signals, were separately drawn in the histograms of Figures 4.3 A and 4.3 C, in which the gray area shows the PHA^+ cells from region R3. Only the bacterial population that presented the highest size and granulometry (FS and SS) was stained with BODIPY 493/503. This means that 29.2% of the bacterial population accumulated 67.5% w/w P3HB/CDW (i.e. 33 g l^{-1} P3HB). Considering that the biomass concentration (RCM) was 16 g l^{-1} at that moment, 4.7 g l^{-1} of bacterial biomass (i.e. 29.2% of 16 g l^{-1}) contained 87.5% w/w P3HB/CDW, while the other 11.3 g l^{-1} of biomass contained no P3HB. Thus, the fraction of bacteria that did not accumulate P3HB would have the potential to increase the total P3HB production. It also explains why the maximum P3HB content obtained during the two fermentations was not higher than 70%. This information about the distribution of bacterial cells in two sub-populations (PHA^+ and PHA^-) could not be possible to obtain without applying flow cytometry.

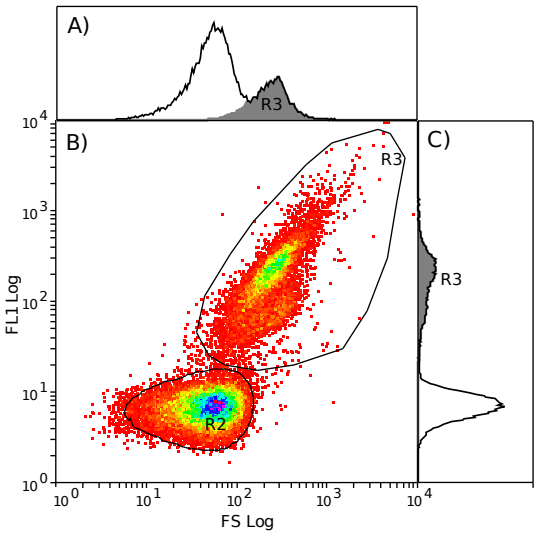

Figure 4.3: Different FC signals obtained from *H. boliviensis* culture with 67.5% w/w P3HB/CDW: **(A)** fluorescence histogram; **(B)** fluorescence versus forward scatter dot plot and **(C)** forward scatter histogram. The sample was taken at 64 h of growth, during fermentation with nitrogen limitation and low oxygen supply.

4.3.3 Correlation between FC data and the parameters determined experimentally

The mean value of the fluorescence signal from the region of PHA-containing cells of a stained sample ($FL1_{PHA^+}$), in fluorescence arbitrary units (au) per cell, minus the FL1 mean signal of the same non-stained sample ($FL1_0$), which is the intrinsic fluorescence of the cells, can be directly correlated with the quantity of BODIPY attached to each cell, which gives an estimation of the PHA content per cell (Equation 1). Concomitantly, this latter parameter (BODIPY/cell) is directly proportional to the P3HB concentration per residual cell mass concentration (P3HB/RCM) obtained from GC and gravimetric analysis, respectively.

$$P3HB/RCM \;\alpha\; BODIPY/cell \;\alpha\; FL1_{PHA^+} - FL1_0 \qquad \text{Equation 1}$$

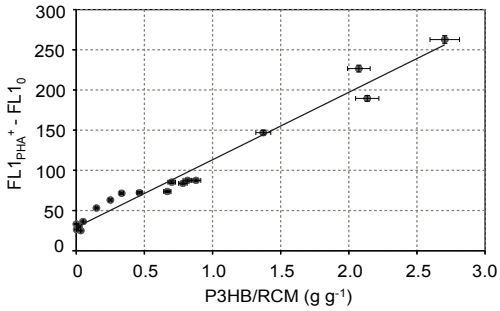

Figure 4.4: Calibration curve for *H. boliviensis* cells stained with BODIPY 493/503. The mean value of the fluorescence signal for the population PHB^+ minus its intrinsic fluorescence obtained by FC is represented *versus* the mass of P3HB per mass of cells determined by gas chromatography and gravimetrically, respectively. The regression line obtained is: $FL1_{PHA}^{+} - FL1_0 = 83.94 \cdot P3HB/RCM + 29.21$; with a correlation factor (R^2) of 0.975.

When the values of fluorescence signal were plotted against the P3HB/RCM ratio the curve presented in Figure 4.4 was obtained. A linear correlation with a R^2 value of 0.975 was obtained by applying a least square method (Equation 2). This calibration curve was plotted with values of P3HB in the range of 0 to 68.1% obtained from the two different types of fermentations (NL and NL-O_2). The intercept of the equation (29.21) represents the background fluorescence of non-specific BODIPY binds, i.e. lipids from membranes or other lipidic storage materials. The ratio P3HB/RCM that it is possible to obtain by FC using this calibration curve could give us an idea of how the P3HB accumulation is evolving during the fermentation. However, this parameter is not as common or useful as the P3HB percentage or concentration for monitoring P3HB production and for comparing results.

$$FL1_{PHA}^{+} - FL1_0 = 83.94 \cdot (P3HB/RCM) + 29.21 \qquad \text{Equation 2}$$

The percentage of PHA is obtained directly by GC analysis, however, to calculate an absolute value of PHA concentration, the total CDW is also required. An indirect and fast method for obtaining a value directly proportional to CDW from a culture sample is the determination of the optical density (OD). However, some deviations from a linear trend have been observed when using samples of PHA-producing bacteria. For example, Kedia et al. (2013) found that bacterial cells of *R. eutropha* changed their optical properties and density while accumulating PHA. In this study, we have found two different correlations between OD and CDW (Figure 4.5). The first calibration curve was obtained for the exponential growth phase of *H. boliviensis* (18-24h), which corresponds with the correlation shown in Equation 3. The correlation changed during the PHA accumulation, to that presented in Equation 4.

$$CDW_{growth} = 1.3297 \cdot OD + 0.7294 \qquad \text{Equation 3}$$

$$CDW_{accumulation} = 0.2007 \cdot OD + 9.4985 \qquad \text{Equation 4}$$

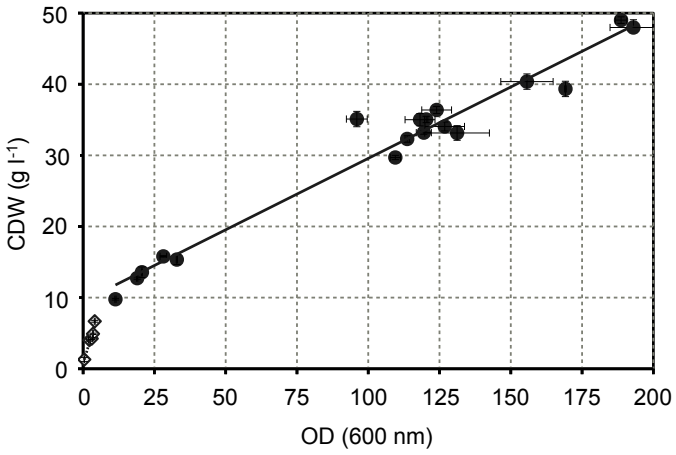

Figure 4.5: Calibration curves for biomass growth measured gravimetrically (CDW) or by the optical density (OD) of the sample. Biomass modification due to bacterial division (white rhombuses) presented a different correlation than biomass modification by PHA accumulation (black circles). The respective regression lines and correlations factors obtained were: $CDW_{growth} = 1.3297 \cdot OD + 0.7294$; $R^2 = 0.943$ and $CDW_{accumulation} = 0.2007 \cdot OD + 9.4985$; $R^2 = 0.965$.

The CDW concentration, which is the sum of RCM and PHA concentrations, was calculated by substituting the variable OD by the experimental value in Equation 4. On the other hand, the ratio PHA/RCM (x) was obtained from FC data as shown in Equation 1. By combining these two parameters, the percentage of PHA can be calculated, as expressed in Equation 5.

$$x = PHA/(CDW - PHA) \rightarrow PHA\ (\%) = x \cdot 100/(1 + x) \qquad \text{Equation 5}$$

Samples from different experiments were measured in triplicate, and the typical standard deviation of $\%PHA^+$, FL1 and FS values were 3.96, 1.92 and 0.97%, respectively.

The results obtained applying the analytical methods during both fermentations and the calculated values obtained by FC are presented together in Figure 4.6. As can be observed, the values of PHA percentage and the concentration obtained from the FC and OD data applying the proposed equations correlate well with the experimental results obtained using GC and gravimetric analysis (Figure 4.6A and 4.6B). The accuracy of the model prediction to experimental data during the two fermentations was also determined by comparing the area under the curve (AUC) of P3HB (%), P3HB productivity (Q_P), CDW and P3HB concentration. The AUC is commonly used in pharmacokinetic studies for comparing concentration-time profiles, and it has been also used for determining the reproducibility of ABE fermentations at bioreactor scale (Gónzalez-Peñas et al., 2015). As shown in Table 4.1, there were not significant differences between the profiles obtained using the experimental and the predicted values. Only in the case of RCM in the NL fermentation, the difference was slightly significant ($p = 0.0386$). It is worth to notice that this latter parameter was calculated using only optical density, and not FC data.

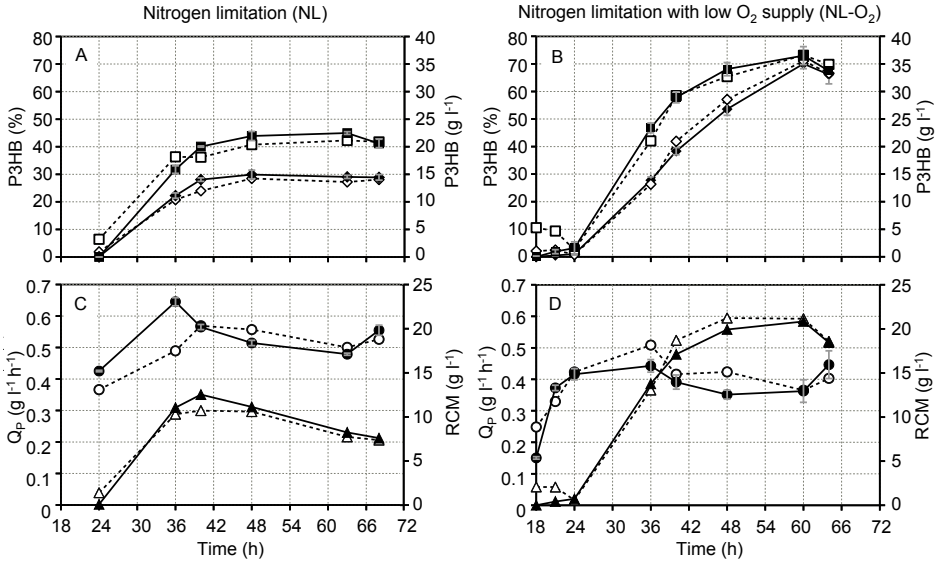

Figure 4.6: Validation of the FC correlations (dotted line and white symbols) with the experimental data (solid line and black symbols) obtained from bioreactor fermentations at two different conditions: nitrogen limitation (A and C) and nitrogen limitation with low oxygen supply (B and D). The parameters represented are P3HB percentage (square), P3HB concentration (rhombuses), RCM concentration (circle) and P3HB productivity (triangle).

The combination of both correlations (FC and OD) allowed us to calculate the residual cell mass concentration and the P3HB productivity (Figure 4.6C and 4.6D). The optimal harvesting time, defined as the time of highest P3HB productivity, can be readily determined using the information provided by FC. For the NL and NL-O_2 fermentations, this point occurred at 40 and 60 h respectively, reaching maximal P3HB productivities of 0.351 and 0.584 g l^{-1} h^{-1}.

Table 4.1: Area under the curve (AUC) and CI of the experimental values of RCM, P3HB and Q_P, obtained in the fermentations NL and NL-O_2, and its comparison against the AUC of the corresponding values predicted by the model.

NL	AUC of experimental values		Test against the value predicted by the model	
Parameter	Mean ± SE	95% CI	AUC_{mod}	*p*-value
RCM (g l^{-1})	861.61 ± 7.09	831.11 – 892.11	826.59	0.0386*
P3HB (g l^{-1})	525.92 ± 10.69	479.92 – 571.92	495.34	0.1035
P3HB (%)	1551.37 ± 22.92	1452.74 – 1649.99	1541.98	0.7218
Q (g l^{-1} h^{-1})	10.95 ± 0.23	9.97 – 11.93	10.42	0.1452

NL-O_2	AUC of experimental values		Test against the value predicted by the model	
Parameter	Mean±SE	95% CI	AUC_{mod}	*p*-value
RCM (g l^{-1})	630.72±19.31	547.65 – 713.78	680.70	0.1224
P3HB (g l^{-1})	844.82±17.73	768.53 – 921.11	875.68	0.2240
P3HB (%)	2150.81±41.44	1972.50 – 2329.12	2128.90	0.6498
Q (g l^{-1} h^{-1})	17.44±0.38	15.80 – 19.08	18.19	0.1902

* Differences are significant for values of $p < 0.05$

Applying the proposed method that uses FC and the determination of optical density, the time of the analysis can be reduced from about 17.5 h to 1 h. A summary of the different steps of both methods and their corresponding times are presented in Table 4.2. Other advantages of FC are: i) its small standard deviation (SD), ii) it is an environmentally-friendly protocol since it does not use organic solvents, iii) smaller sample volume is required, and iv) the information obtained from samples taken more frequently can be used to implement precise segregated mathematical models of PHA production, which could later be used in process optimization. In the past, the cost of flow cytometers represented a disadvantage for its application in bioprocess monitoring. However, recent technical advances in standard flow cytometry instrumentation have made it possible to perform such experiments using small and comparatively cheap devices, in standard research laboratories (Arnoldini et al., 2013).

Table 4.2: Summary of the time expended for FC and GC protocols, considering the same starting point for both analyses, which is the washed pellet.

Flow cytometry (FC)	Time
1. Cell fixation in 50% EtOH	20 min
2. Centrifugation	5 min
3. Pellet dilution in PBS + BODIPY staining	5 min
4. FC measurement	5 min
Total FC time	*35 min*
Gas chromatography (GC)	
1. Freeze the pellet	120 min
2. Freeze-dry	720 min
3. Sample preparation (pellet homogenization + weight + reactive addition)	15 min
4. Oven	120 min
5. Cooling	5 min
6. Final sample treatment	5 min
7. GC analysis	20 min
Total GC time	*1005 min*

4.3.4 Population heterogeneity

PHA synthesis requires the coordinated reactions of several enzymes, and it is highly sensitive to the culture environment (York et al., 2001). In some cases, individual cells respond differently to their environment and accumulate PHA at different levels. Consequently, PHA-producing and non-producing cells can coexist in the same bioreactor (Lee et al., 2013), giving rise to a heterogeneous cell population. Since this heterogeneity can only be detected by flow cytometry, and not using conventional methods, the studies describing the appearance of heterogeneous PHA-producing cells populations are scarce. In general, more studies have reported the presence of homogeneous cultures of PHA-producing cells (Kacmar et al., 2005; Obruca et al., 2013), while heterogeneous populations have been described less frequently, and most of the times when using recombinant PHA-producing bacteria or mutant strains (Lee et al., 2013; Prieto et al., 2016).

Focusing on those studies of recombinant or mutant strains, it has been observed that when the gene *phaM* from *R. eutropha* is deleted the PHA granules of the mutant strain (Δ*phaM*) become very large, while cells accumulate only a very few number of granules (≤2) and the distribution of granules to daughter cells is impaired (Wahl et al., 2012). The protein PhaM is a novel type of PHA granule-associated protein that has phasing properties but also can bind to DNA (Pfeiffer et al., 2011). In *Pseudomonas putida,* the gene *phaF* and *phaI* were reported to have a similar function to that of *phaM* (Prieto et al., 2016). Both genes express proteins that have been shown to be involved in the organization of the granules into a needle array along the long axis of the cell, and to organize granule sharing during cell division (Prieto et al., 2016).

To elucidate if the absence of such protein is responsible for *H. boliviensis* heterogeneity, we carried out an *in silico* analysis to determine if a gene homologous to *phaM*, *phaF* or *phaI* was present in its genome. As observed in Table 4.3, we could not find any gene in *H. boliviensis* significantly similar to those. Prieto et al. (2016), have found that the lack of PhaF results in a different phenotype; the PHA granules in the mutant strain *P. putida* ΔF KT40F remained accumulated in one of the cell poles. An additional effect of the deletion of the gene *phaF* in *P. putida* was the observation of cell heterogeneity during PHA production and the impaired distribution of PHA to daughter cells.

Table 4.3: *In silico* analysis of the genes involved in the organization of the PHA granules.

Bacterium/Gene	Query cover (%)	E-value	Identity (%)	Locus (*H. boliviensis*)	Product
R. eutropha/*phaM*	15	3.3	33	KUC_0149	Transporter
P. putida/*phaI*	No significant similarity found				
P. putida/*phaF*	No significant similarity found				

Despite that no similar gene to *phaM*, *phaF* or *phaI* was found in *H. boliviensis* genome, it is not possible to asseverate that no other gene structure in this bacterium encodes a protein with a similar role. However, all the features of the mutant strains, in which those genes were deleted, were observed in the fermentations presented in this study.

The formation of a small number of big granules and its orientation along the longitudinal axis of the cells is noted in the TEM photographs of Figure 4.2 (C-D). The percentage of PHA^+ cells increased when PHA accumulation increased as well. However, it diminished in both fermentations after 36 h of culture, and this could reflect the impaired distribution of cells (Figure 4.7). After the cell division of a PHA-containing cell, PHA remained in one of the two daughter cells (PHA^+), while the other cell contained no PHA (PHA^-). During the experiment at nitrogen-limiting conditions, from 36 h onwards PHA concentration was maintained constant, as well as the mean fluorescence value of the PHA^+ population, however, the percentage of PHA^+ cells decreased, indicating that after dividing, the percentage of PHA^- cells increased. In the experiment NL-O_2, after the 36 h peak, the percentage of PHA^+ cells also decreased, but contrary to that observed in fermentation NL, PHA accumulation still increased as indicates the fluorescence signal.

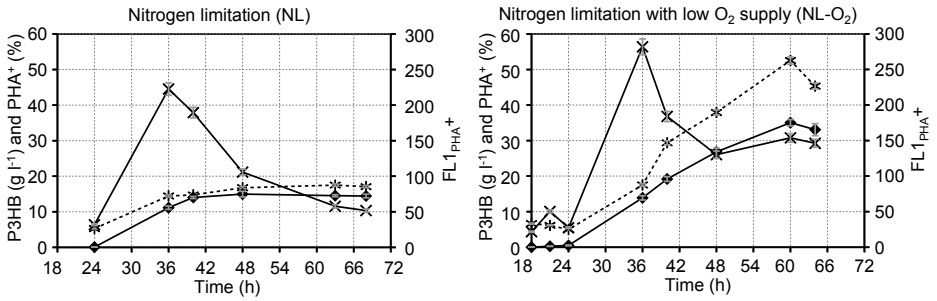

Figure 4.7: Mean value of fluorescence from PHA^+ cells region (asterisk and dotted line), percentage of PHA^+ cells (crosses), RCM (white circles) and P3HB concentration measured by GC (rhombuses) for bioreactor fermentations at two different conditions: nitrogen limitation and nitrogen limitation with low oxygen supply.

4.4 CONCLUSIONS

Flow cytometry is a useful technique to measure PHA production of a process that was design to be applied in a biorefinery. Its two main advantages for monitoring the production of PHA are that FC is significantly faster than conventional methods (i.e. GC and gravimetric analysis) and that it provides population dynamic performance and multiparametric information at the cellular level that cannot be obtained measuring global parameters from culture samples. Besides the savings in time, FC provides additional information about PHA accumulation that cannot be obtained by typical GC analysis. It was possible to distinguish two different populations during the PHA accumulation by the halophilic bacterium *H. boliviensis*. The application of FC permits to determine in a short time the point of maximal PHA productivity that is a critical parameter in PHA production.

5

First generation bioethanol streams as carbon source for P3HB production

Corn and sugarcane are the main raw materials used for 1G bioethanol in USA, Brazil and EU. To improve PHA competitiveness against petroleum-based plastics, the search of a readily available and low-cost material is necessary.

The main objective of this work was to study the feasibility of the bacteria *H. boliviensis* for producing PHA using the main carbon sources –cereals and sugarcane– also used in the bioethanol production. The use of these process streams would enable to integrate the production of bioethanol and PHA following a biorefinery approach.

PHA accumulation by *H. boliviensis* was studied using corn syrup, sugarcane juice and two synthetic media composed of glucose and sucrose as controls, respectively. After 48 hours of growth, a similar PHA accumulation was found with corn syrup and the glucose control (60.7 and 60.0% P3HB/CDW, respectively). A lower accumulation was detected with sugarcane juice and the sucrose control (48.8 and 54.2% P3HB/CDW, respectively). Complex medium showed better productivities than synthetic medium in both cases. Similar productivities were reached after 72 h of cultivation at flask scale with corn syrup and sugarcane juice (0.049 and 0.044 g l^{-1} h^{-1}, respectively). However, the scale up of the cultivation to a 2 l bioreactor yielded a productivity with corn juice of 0.254 g l^{-1} h^{-1} after 64 h. This study could be considered a previous step for a future bioplastics production integrated into the bioethanol industry.

OUTLINE

5.1 Introduction

Conventional first-generation biofuels are mainly produced from starch, oil or sugar crops, such as cereals (i.e. wheat, corn), sugar cane, palm, rapeseed and beets. According to the International Energy Statistics (U.S. Department of Energy), USA, Brazil and EU are the highest bioethanol producers in the world. The primary feedstock for ethanol in the United States is currently corn (U.S. Department of Energy). Sugarcane is almost the exclusive feedstock for bioethanol production in Brazil (Global Agricultural Information Network). According to the stats from the European Renewable Ethanol Association (ePURE), the share of corn as a feedstock to produce ethanol has grown over the past years in the EU. Since 2013, corn has replaced wheat as the dominant raw material. In 2014, 42% of all feedstock used for bioethanol was corn. Corn and sugarcane are the most used feedstocks for bioethanol production in the world. Thus, these two substrates show the highest potential for PHA production in a biorefinery.

A summary of the main steps for bioethanol production from starch crops is shown in Figure 5.1 (Pena PhD Thesis, 2009). The conversion of starch to ethanol includes a liquefaction step, carried out through a thermal and enzymatic treatment with α-amylase to make the starch soluble. Then, during the simultaneous saccharification and fermentation (SSF) starch is completely hydrolysed to glucose by glucoamylase, while glucose is simultaneously transformed into ethanol, usually by the yeast *Saccharomyces cerevisiae*. Ethanol is obtained through distillation and a solid residue called stillage is also produced. Distiller's dried grains with solubles (DDGS) is obtained by the removal of water (centrifugation and drying) from stillage and its main application is as animal feed.

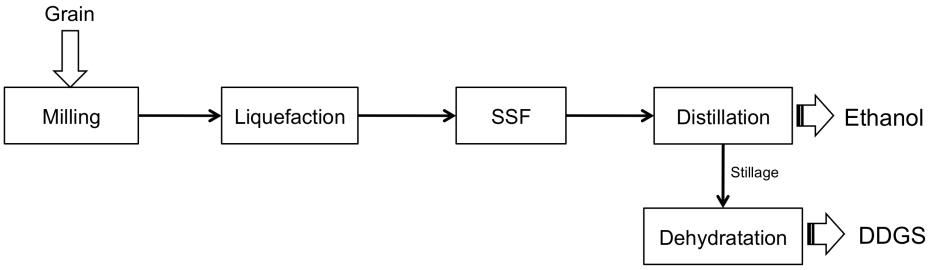

Figure 5.1: Process scheme for bioethanol production from grain.

Sugarcane mills in Brazil are large agroindustries that produce sugars, ethanol and other by-products. A summary of the main process units for bioethanol production from sugarcane is shown in Figure 5.2 (Ensinas et al., 2007; Quintero et al., 2008). Two different fractions are obtained during sugarcane milling (i.e. juice and bagasse). The incineration of bagasse provides all the energy necessary for the process. Sugarcane juice is transferred to a clarification process, where pH is adjusted, some impurities are removed and the filter cake is generated. The filter cake is commercialised as a component of animal feed or for composting. Juice for sugar production is concentrated in a multiple-effect evaporator. Part of the juice for ethanol production is concentrated in a five-effect evaporation system to reach the concentration necessary for the fermentation. After fermentation, ethanol is obtained by distillation.

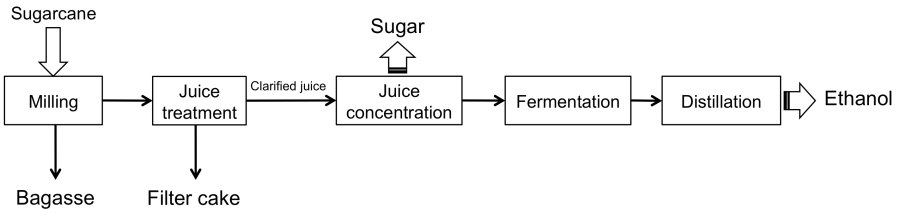

Figure 5.2: Process scheme for bioethanol production from sugarcane.

As reported in previous studies, *H. boliviensis* is able to grow and accumulate PHA using commercial starch (Quillaguamán et al., 2005; Rivera-Terceros et al., 2015) and sucrose (Quillaguamán et al., 2007) as the carbon source. Complex substrates such as wheat bran hydrolysate and potato residues were tested as well with this bacterium (Van-Thuoc et al., 2008). However, the use of process streams from 1G biorefineries (1G bioethanol feedstocks) to obtain P3HB with this strain has not been previously studied.

In this chapter, both complex carbon sources, corn syrup and sugarcane juice, were deeply characterized and adapted for *H. boliviensis* growth and PHA production at flask and bioreactor scale.

5.2 MATERIALS AND METHODS

5.2.1 Substrates characterization

Total solids and ashes were determined gravimetrically. A portion of the sample was weighed in a dry crucible, previously weighed. The sample was dried until constant weight in an oven at 105±5°C. The difference in weight between the dried crucible with the sample and the empty crucible is the total solid content of the sample. Ashes or inorganic solids were determined by the calcination of the previously dried sample in an oven at 550°C for 2 h. The difference in weight between the calcinated sample and the empty crucible is the ash content.

Sugar content, ammonium nitrogen, orthophosphate phosphorus, total organic carbon and total nitrogen were measured as described in Chapter 2.

The cations sodium (Na^+), potassium (K^+), magnesium (Mg^{2+}), calcium (Ca^{2+}) and the anions chloride (Cl^-), nitrite (NO_2^-), bromide (Br^-), nitrate (NO_3^-) and sulphate (SO_4^-) were determined by ion chromatography (IC) with an Advanced Compact IC System (861, Metrohm) equipped with a CO_2 suppressor (MCS 853, Metrohm) and a sample processor (AG 838, Metrohm). Cations were determined with a Metrosep C3 column (250 × 4.0 mm, Metrohm) and 3.5 mM nitric acid was used as mobile phase. Anions were measured with a Metrosep A column (250 × 4.0 mm, Metrohm) and 3.2 mM Na_2CO_3 + 1.0 mM $NaHCO_3$ was used as mobile phase. The flow rate used in both columns was 0.7 ml min^{-1}. The injection volume of the sample was 20 µl and data collection was done with the Processor software IC net 2.3. The calibration ranges for the different inorganic ions are shown in Table 5.1. Dilution of the samples was done to obtain a value in these ranges.

Table 5.1: Calibration ranges for the different inorganic ions in mg l^{-1}.

Cation	Low value	High value	Anion	Low value	High value
Na^+	1.5	150	Cl^-	1	100
K^+	0.5	50	NO_2^-	0.05	5
Mg^{2+}	0.5	50	Br^-	0.2	20
Ca^{2+}	0.5	50	NO_3^-	0.5	50
			SO_4^-	1.5	150

5.2.2 Substrate pretreatment

Corn kernel mash, after the liquefaction step, was obtained from Bioetanol Galicia SA (Teixeiro, A Coruña, Spain) and stored at -20°C until use. The major steps followed for cereal mash conditioning are summarised in Figure 5.3. The thawed mash was centrifuged at 2370 × g for 10 min before fermentation to prevent the high solid content (29.6% wt/wt) of the cereal mash from interfering with PHA downstream separation and biomass quantification. Solids removed can be directed to the DDGS production stream before fermentation instead of after, as occurs during bioethanol process. Centrifuged cereal mash, hereafter called cereal juice, was saccharified before fermentation using 146 mg l^{-1} of a glucoamylase commercial solution (Spirizyme, Novozymes A/S, Denmark) for 72 h at 50°C, with a rotary shaking of 200 rpm. The enzyme is obtained from *Aspergillus niger*. The commercial solution presents a density of 1.13 g ml^{-1} and an activity of 100 U l^{-1}, where one unit of glucoamylase (U) is defined as the amount of enzyme that releases 1 g l^{-1} of glucose in1 h at 35°C and pH 4.5. After this step, a stream called corn syrup, with a glucose content of 271±37 g l^{-1} was obtained. This value is the mean concentration (± standard deviation) obtained after carrying out three times the saccharification of the cereal juice.

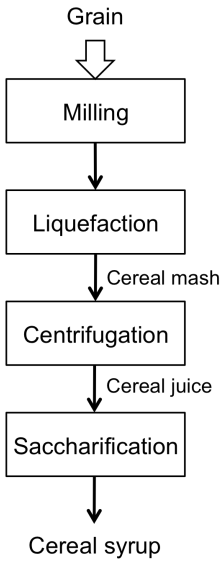

Figure 5.3: Main steps in corn pretreatment.

Sugarcane juice after the concentration step was obtained from Abengoa Bioenergy SA (São João da Boa Vista, Brazil) and was stored at -20°C until use. The thawed juice is ready to use since no pretreatment step is required.

5.2.3 Flask scale fermentations

Complex carbon sources, corn and sugarcane juices, were tested at flask scale and compared to the corresponding synthetic sugar (i.e. glucose and sucrose). Inoculation procedure was described in Chapter 2. For the different experiments, the synthetic sugar of the IC medium was replaced by the complex carbon sources. Then, four different inocula were prepared for the four carbon sources tested. The BC medium was used for the flask scale experiments, containing 30 g l^{-1} of either carbon source tested.

In order to trigger PHA accumulation, N-limitation with low O_2 supply was simulated by reducing the ammonium content in the medium (0.8 g l^{-1} of NH_4Cl) and by increasing the working volume. Fermentations were carried out in 1 l Erlenmeyer flasks with a working volume of 500 ml.

Applying the correlation obtained by Liu et al. (2006) for the estimation of the K_La coefficient (described in Chapter 4), a value of 26 h^{-1} was achieved with this flask configuration. This value is in the range of the lowest K_La coefficient tested in Chapter 4 (27 h^{-1}).

5.2.4 Bioreactor scale fermentations

Scale-up cultivation was performed in a 2 l bioreactor using a working volume of 1.5 l, as described in Chapter 2. Corn syrup and sugarcane juice were used as carbon source in two different experiments. The fed-batch operation was carried out applying N-limiting conditions with low O_2 supply as described in Chapter 4. During the growth phase, BC medium with either corn syrup or sugarcane juice as carbon source was used until nitrogen exhaustion. The accumulation phase took place under N-limitation with low O_2 supply and glucose in the FBC medium was replaced by the complex substrates.

5.3 RESULTS AND DISCUSSION

5.3.1 Characterization of the 1G feedstocks

Before fermentations, both complex substrates were characterised in terms of their water content, the main carbohydrate composition and concentration, and also the quantification of the main anions and cations (Table 5.2).

After the centrifugation of cereal mash, the total content of solids and ashes of the cereal juice decreased to 24.2±0.08% and 0.41±0.01%, respectively. Hydrolysis of cereal juice at the optimal conditions for glucoamylase (50°C and pH 6.1) modified sugars concentrations in cereal syrup, by increasing glucose concentration to 271±37 g l^{-1} and reducing dextrins to 4.3±1.1 g l^{-1}.

The ammonium content in both substrates could be considered insignificant compared with the initial ammonium concentration of the medium (1046.7 mg l^{-1} $N\text{-}NH_4^+$). Corn syrup presents a high concentration of orthophosphate phosphorus and potassium (equivalent to 2.5 g l^{-1} K_2HPO_4), useful to avoid the external supply of phosphate and to prevent limitation by phosphorus during the fermentation. On the other hand, other elements such as sodium (Na^+), calcium (Ca^{2+}), magnesium (Mg^{2+}), chlorine (Cl^-) and bromine (Br^-) were found in small amounts.

Sugarcane juice presents a very low concentration of orthophosphate phosphorus. However, the concentration of either magnesium or sulphate was very high (equivalent to 4.2 g l^{-1} $MgSO_4{\cdot}H_2O$). Then, during the feeding phase of the bioreactor with FC medium the addition of synthetic magnesium sulphate was avoided. High amounts of chlorine, potassium and calcium were also detected in sugarcane juice.

Table 5.2: Characterization of cereal mash and sugarcane juice.

	Cereal mash	Sugarcane juice
Total Solids (%)	30.3±0.07	52.6±0.3
Ashes (%)	0.55±0.01	2.3±0.02
Glucose (g l^{-1})	5.7±0.5	14.7±0.2
Dextrins (g l^{-1})	219.9±5.6	–
Sucrose (g l^{-1})	–	690.9±86.1
Fructose (g l^{-1})	–	17.7±4.8
N_{TOTAL} (mg l^{-1})	456.1±38.6	1782
N-NH_4^+ (mg l^{-1})	55.4±5.9	34.3±1.4
NO_3^- (mg l^{-1})	13.9	139.9
NO_2^- (mg l^{-1})	ND	27.4
P-PO_4^{3-} (mg l^{-1})	453.5±18.8	66.2±3.1
SO_4^{2-} (mg l^{-1})	ND	3876.9
Cl^- (mg l^{-1})	164.9	6619.6
Br^- (mg l^{-1})	1.9	ND
Na^+ (mg l^{-1})	30.4	41.3
K^+ (mg l^{-1})	1138.1	11,880.1
Mg^{2+} (mg l^{-1})	230.6	733.3
Ca^{2+} (mg l^{-1})	10.9	1411.3

ND: Not detected; –: not measured.

Both substrates were diluted in the fermentation media to reach the desired carbon source concentration; thus the inorganic anions were diluted as well. All other components of the fermentation media were added as described in Chapter 2.

5.3.2 Preliminary study at flask scale

A comparison between the fermentation profiles with the complex carbon source and the respectively synthetic substrate was first carried out at flask scale. P3HB accumulation started almost immediately either with corn syrup or synthetic glucose. However, in the case of glucose, a sharp increase was detected during the first 24 hours (Figure 5.4). No differences were noticed between the maximum P3HB reached with corn syrup (70.8±2.9%) and glucose (70.3±1.8%) (p = 0.486).

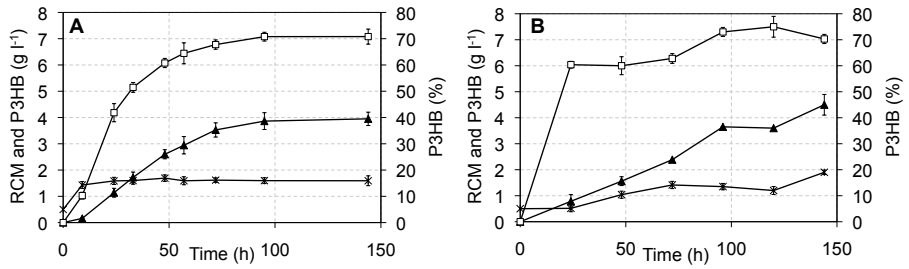

Figure 5.4: P3HB accumulation (white squares), RCM (black crosses) and P3HB concentration (black triangles) during flask scale fermentation using corn syrup (A) and glucose (B) as carbon sources.

With corn syrup, biomass increased at the beginning of the process and from 24 h onwards it was maintained almost constant in 1.6±0.18 g l^{-1}. The growth on glucose progressively increased at a very slow rate, reaching a final concentration of 1.9±0.17 g l^{-1}. N-limiting conditions and low oxygen supply, due to the small K_La coefficient used, did not favour bacterial growth. Regarding final P3HB concentration, a slightly significant difference between feeding with corn juice (3.9±0.2 g l^{-1}) and glucose (4.5±0.4 g l^{-1}) was observed ($p = 0.035$).

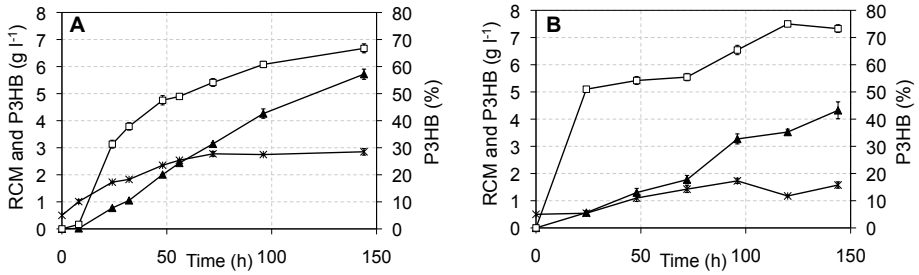

Figure 5.5: P3HB accumulation (white squares), RCM (black crosses) and P3HB concentration (black triangles) during flask scale fermentation using sugarcane juice **(A)** and sucrose **(B)** as carbon sources.

In the case of sugarcane juice and sucrose, P3HB accumulation also started immediately (Figure 5.5). P3HB accumulation on sucrose was higher than on sugarcane juice ($p < 0.05$), reaching final values of 73.3±1.3 and 66.7±1.7%, respectively. However the highest P3HB concentration was obtained with sugarcane juice (5.7±0.2 and 4.3±0.3 g l^{-1}, for sugarcane and sucrose, respectively) ($p < 0.05$), due to the differences in biomass growth. In fact, despite the use of the same limiting conditions with both substrates, biomass growth was higher in the case of sugarcane juice (2.8±0.1 g l^{-1}) than with sucrose (1.6±0.1 g l^{-1}) ($p < 0.05$).

Sucrose concentration was monitored during flask scale fermentation, together with its hydrolytic products, fructose and glucose. Fructose was detected in the culture broth (Figure 5.6), suggesting an extracellular hydrolysis of sucrose. Glucose seems to be a preferred substrate rather than fructose since free glucose was not detected during the experiment.

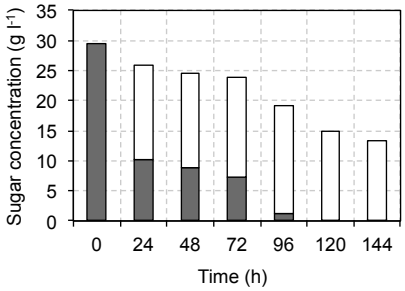

Figure 5.6: Sucrose (grey bar) and fructose (white bar) consumption profile in flask scale.

Three main sucrose-utilizing pathways have been described for bacteria: sucrose phosphotransferase (PTS) system, sucrose permease system and β-fructofuranosidase system (Reid and Abratt, 2005). The latter pathway needs less ATP than the other two and presents an external sucrose hydrolysis, while the other systems –PTS and sucrose permease– are based on the intracellular utilisation of sucrose. According to the experimental results obtained, the β-fructofuranosidase seems to be the pathway that *H. boliviensis* utilised for sucrose consumption.

Table 5.3: Main fermentation parameters obtained with both complex and synthetic carbon sources at 72h of fermentation at flask scale

	Corn syrup	Glucose	Sugarcane	Sucrose
RCM (g l^{-1})	1.6±0.2	1.9±0.2	2.8±0.1	1.6±0.1
P3HB (%)	70.8±2.9	70.3±2.3	66.7±1.7	73.3±1.5
P3HB (g l^{-1})	3.9±0.2	4.5±0.4	5.7±0.2	4.3±0.3
Productivity (g $l^{-1}h^{-1}$)	0.049	0.033	0.044	0.025

The main results obtained at flask scale experiments with both complex and synthetic carbon sources are summarised in Table 5.3. Statistical analysis was conducted to compare the results obtained with the four carbon sources (Table 5.4). Significant differences were detected among the final P3HB accumulation, P3HB concentration, and biomass growth obtained with the different substrates ($p < 0.001$). Post-hoc analysis showed that P3HB accumulation with sugarcane juice was slightly lower than the value obtained with any of the other substrates ($p < 0.05$). The highest P3HB concentration was also achieved with sugarcane juice (5.7±0.2 g l^{-1}, $p < 0.001$). Finally, the maximum biomass concentration was also reached with sugarcane juice (2.8±0.1 g l^{-1}, $p < 0.001$), while the second highest value was obtained with glucose (1.9±0.17 g l^{-1}, $p < 0.001$). Synthetic sucrose and corn juice reported the same and lowest biomass concentrations (1.6±0.1 and 1.6±0.2 g l^{-1}, respectively, $p = 0.997$).

The highest P3HB productivities were reached with both complex carbon sources (Table 5.3) rather than with the synthetic ones. Despite the experiments were not focused on biomass growth optimization, a possible explanation of the high values obtained with sugarcane juice could be the beneficial effects of sucrose on protecting cells from oxidative, heat and acids stresses, which have been previously documented by several researchers (Kilimann et al., 2006; Prestrelski et al., 1993).

Table 5.4: Statistical analysis of the effect of the four carbon sources, i.e. corn syrup (CS), glucose (G), sugarcane (SC) and sucrose (S) on PHB accumulation and bacterial growth.

	Carbon source	*p*
P3HB (%)		
ANOVA	CS, G, SC, S	< 0.001
Tukey's HSD	CS-G, S-CS, G-S	0.105<*p*<0.835
	SC-CS, SC-G, SC-S	<0.05
P3HB (g l^{-1})		
ANOVA	CS, G, SC, S	< 0.001
Tukey's HSD	CS-S, G-S	0.133<*p*<0.707
	CS-G, SC-CS, G-SC, S-SC	< 0.001
RCM (g l^{-1})		
ANOVA	CS, G, SC, S	< 0.001
Tukey's HSD	CS-S	0.997
	CS-G, CS-SC, SC-G, S-G, SC-S	< 0.001

This study demonstrates that complex substrates obtained from 1G biorefineries such as corn mash and sugarcane juice are readily metabolised by *H. boliviensis*, reporting similar P3HB accumulation and biomass growth than the respectively synthetic carbohydrates. However, among all the tests, the highest P3HB concentration was obtained with sugarcane juice.

5.3.3 Biorefinery integration and bioreactor scale fermentations

The proposed scheme for the integration of the P3HB production into a bioethanol plant from cereals is depicted in the process diagram of Figure 5.7. Both processes share milling and liquefaction steps. A fraction of the cereal mash after liquefaction was diverted into the P3HB production route. Centrifugation of the cereal mash is needed as the first step to avoid interferences of the bigger solids in the downstream process. Solids retained during centrifugation were diverted to DDGS dehydration unit, while the liquid fraction was hydrolysed with glucoamylase. Once, most of the starch was converted into glucose, the fermentation process took place. After biomass separation, P3HB was extracted and purified, while ectoine was recovered from the liquid culture media. As was described in Chapter 4, ectoine production, at bench top bioreactor scale using synthetic glucose as carbon source and MSG as nutritional supplement, reached 4 g l^{-1}, and it was mainly found in the extracellular broth. Moreover, as was previously described by López-Abelairas (PhD Thesis, 2014), the inclusion of the ectoine production into a biorefinery scheme, which includes as well PHA and ethanol production, enhances the competitiveness of the plant.

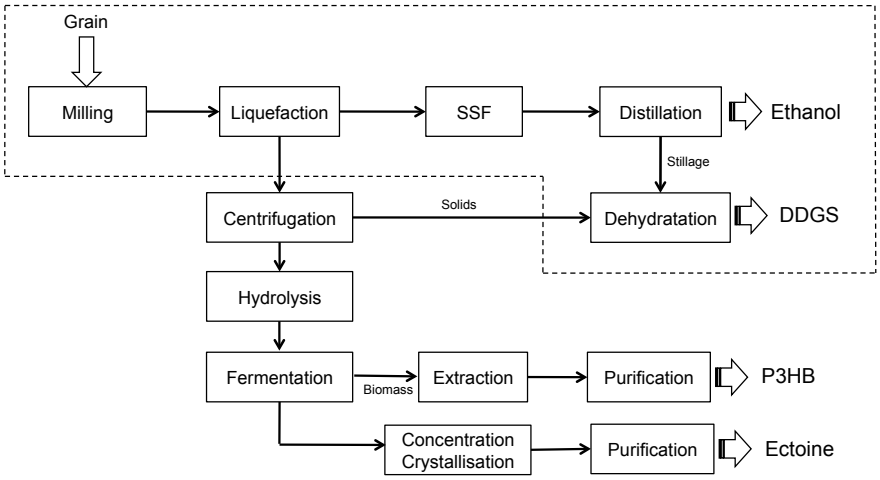

Figure 5.7: Process diagram with the main operational units of the proposed biorefinery from cereals. Bioethanol process is represented inside the dotted line.

The same integration procedure was followed for the sugarcane bioethanol plant (Figure 5.8). In contrast with the previous scheme, less operational units are needed for P3HB production in this case. After its concentration, a fraction of the sugarcane juice was diverted to the P3HB process without any previous treatment step. The recovery process for P3HB and ectoine are the same as in the case of the cereal biorefinery.

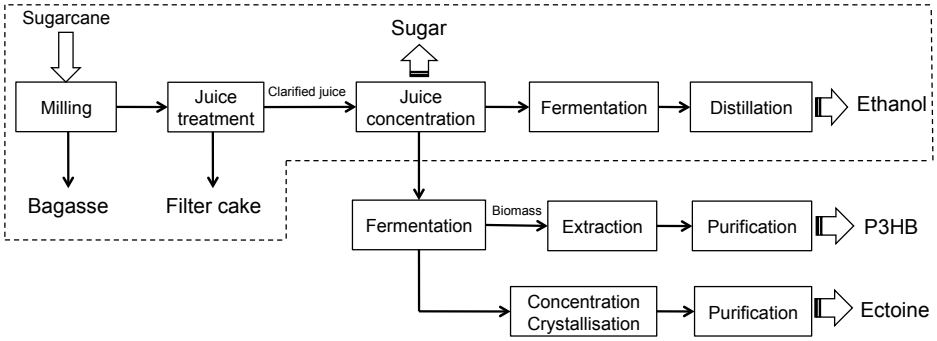

Figure 5.8: Process diagram with the main operational units of the proposed biorefinery from sugarcane. Bioethanol process is represented inside the dotted line.

Fermentation steps of both processes were scaled up from the preliminary tests at flask scale to a 2 l bioreactor. Bioreactor operation allows a more robust control of the key variables involved in the fermentation, such as dissolved oxygen and pH. Fed-batch experiment at bioreactor scale was tested using either corn syrup or sugarcane juice as the carbon source. The main results for corn syrup are presented in Figure 5.9. The MSG and the ammonium source were depleted at 24 h and between 24 and 37 h, respectively. Between 24 and 37 h biomass reached its maximum (16.7±0.4 g l^{-1}) and P3HB accumulation started, reaching a final and stable concentration of 16 g l^{-1} from 60 h onwards. A final P3HB accumulation of 57.7±2.1% was obtained.

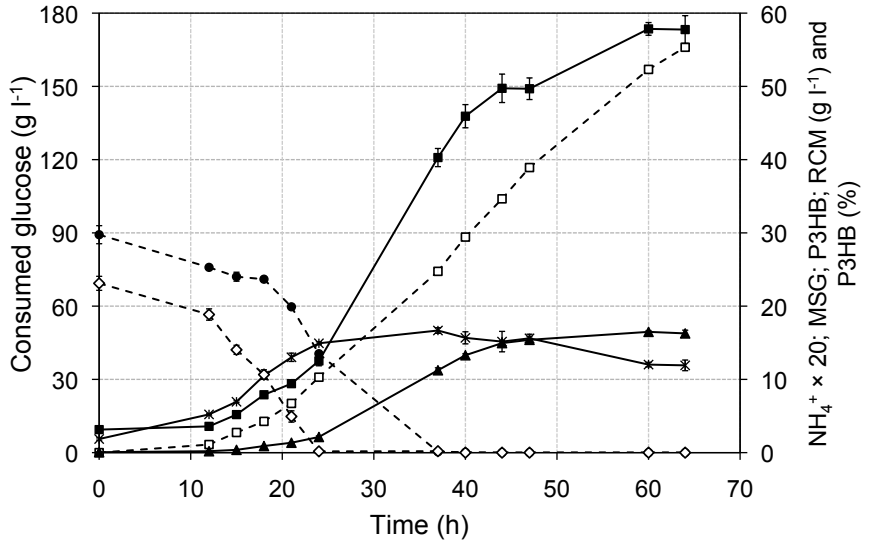

Figure 5.9: Fed-batch fermentation profile of *H. boliviensis* at bioreactor scale using corn syrup as carbon source. Glucose consumption (white squares), ammonium concentration (black circles), MSG concentration (white rhombuses), P3HB accumulation percentage (black squares), P3HB concentration (black triangles) and residual biomass concentration (crosses) are represented.

In a previous study of *H. boliviensis* on synthetic starch as the carbon source (Quillaguamán et al., 2005), a slightly lower P3HB accumulation percentage was reached

(49%). However, the most remarkable difference was that bacterial growth obtained in that research, working with similar conditions at bioreactor scale, was significantly lower (0.8 g l^{-1}) than the value obtained in this study (16.3 g l^{-1}). Probably, these differences were due to a reduced hydrolysis of the starch, since they only applied a maltooligosaccharide forming amylase.

In our previous experiments with *H. boliviensis* using synthetic glucose as substrate and applying a fed-batch operation with N-limitation and low O_2 supply (Chapter 4), 73% of P3HB and a biomass growth of 13 g l^{-1} were obtained. Corn syrup fermentation under the same operational parameters, enhanced biomass growth to 16.7±0.4 g l^{-1}. However, P3HB accumulation was lower (57.7%). The improvement of biomass growth with corn syrup could be attributed to the complex composition of the substrate. Minority compounds of corn syrup, not measured in this study (e.g. vitamins, amino acids, etc), could exert a positive effect on bacterial division.

The results of sugarcane juice fermentation are depicted in Figure 5.10. MSG was depleted at 24 h and its consumption profile was similar to that obtained with corn syrup. However, ammonium consumption was slower and its depletion was not detected until 47 - 60 h. The maximum values of biomass were reached between 37 and 47 h (18.5±0.5 and 19.4±0.1 g l^{-1}). Afterwards, a decrease in biomass concentration was observed (11.2±0.9 g l^{-1} at 88 h). Despite similar biomass concentrations were reached and the same N-limitation with low O_2 supply conditions were used with both complex substrates at bioreactor scale, P3HB accumulation was very small with sugarcane juice. A maximum P3HB accumulation of 15.0±0.5 % was obtained at 68 h.

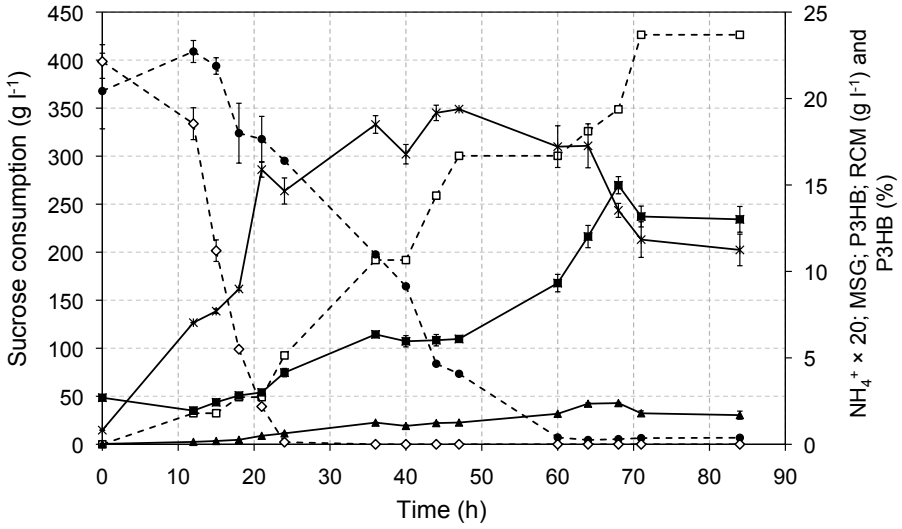

Figure 5.10: Fed-batch fermentation profile of *H. boliviensis* at bioreactor scale using sugarcane juice as carbon source. Glucose consumption (white squares), ammonium concentration (black circles), MSG concentration (white rhombuses), P3HB accumulation percentage (black squares), P3HB concentration (black triangles) and residual biomass concentration (crosses) are represented.

In this study, biomass and P3HB concentration was lower than those previously obtained with *H. boliviensis* at bioreactor scale using synthetic sucrose as the carbon source

(Quillaguamán et al., 2007). The final P3HB accumulation and total CDW reached were 54% and 14 g l^{-1}, respectively, thus, a final P3HB concentration of 7.7 g l^{-1} was obtained by Quillaguamán et al. (2007). With sugarcane juice, a final P3HB accumulation and concentration of 15% and 2.3 g l^{-1}, respectivel, were reached in this study at bioreactor scale. These results contrast to those obtained with the same substrate at flask scale, where 66.7% of P3HB was accumulated.

Total sucrose consumption during the fed-batch operation was 426 g l^{-1}, which was supplemented by adding a huge amount of sugarcane juice (1.35 l) into the bioreactor. Therefore, fluid properties of the culture broth varied considerably and the concentration of compounds such as anions and cations from sugarcane juice highly increased (i.e. sulphate, magnesium, chlorine, potassium and calcium), probably causing an imbalance of the culture medium. This issue could be an explanation for the low P3HB productivity reached with sugarcane juice at bioreactor scale.

Table 5.5: Main fermentation parameters obtained with both complex sources at 64 h of fermentation at bioreactor scale.

	Corn syrup	Sugarcane
RCM (g l^{-1})	11.9±0.7	17.3±1.3
P3HB (%)	57.7±2.1	12.1±0.6
P3HB (g l^{-1})	16.3±0.4	2.3±0.04
$Y_{RCM/S}$ (g g^{-1})	0.061	0.051
$Y_{P3HB/S}$ (g g^{-1})	0.097	0.007
Productivity (g $l^{-1}h^{-1}$)	0.254	0.037

A great difference between the consumption of the different substrates was detected. Corn syrup and sugarcane fermentations consumed 166 g l^{-1} of glucose and 426 g l^{-1} of sucrose, respectively. The total amount of corn syrup and sugar cane fed into the bioreactor were 983 and 1353 ml respectively. Despite the fact that sugars consumption with sugarcane juice was 2.6-fold higher than with corn syrup, its final biomass concentration was only 1.4-fold higher. Moreover, biomass and P3HB yields obtained with sugarcane juice were 16.4 and 92.7%, respectively, lower than those reached with corn syrup (Table 5.5). The low P3HB accumulation with sugarcane juice is reflected as well in production yield and global productivity, which suggests that a significant fraction of the C-source was converted in a product different than P3HB.

5.4 Conclusions

Complex substrates used for 1G bioethanol production, such as sugarcane juice and corn syrup can be applied directly as the carbon source by *H. boliviensis* for growth and PHB production. These complex substrates present a great abundance of sugars and different minerals. At flask scale, a similar successful performance was observed with both substrates. However, when the process was scaled-up to a 2 l bioreactor and the operation mode was changed to fed-batch PHB production with corn syrup was much higher than with sugarcane juice. Besides, although PHB accumulation using corn syrup was slightly reduced

after scaling up the PHB production from flask to the bioreactor (from 60.7 to 57.7%, respectively), the PHB concentration and productivity were increased four-fold.

6

Production of P3HB by simultaneous saccharification and fermentation of cereal mash

The production of P3HB by the halophilic bacterium *H. boliviensis*, using cereal mash as the carbon source, was carried out in this study. Simultaneous saccharification and fermentation (SSF) methodology, commonly used in first generation (1G) biorefineries, was applied in order to evaluate the integration of P3HB production in a bioethanol plant. Separate hydrolysis and fermentation (SHF) was compared to the SSF process based on the results of overall mass balance and productivities. The highest P3HB production (26 g l^{-1}) was obtained by applying the SSF configuration, which was 60% higher than the value reached with the SHF mode. Moreover, the application of the SSF mode permitted a 47% reduction in the overall processing time. This study demonstrates, for the first time, the feasibility of applying an SSF process for producing P3HB from a real cereal mash and its integration within a 1G ethanol biorefinery.

OUTLINE

6.1 Introduction

Despite the attractive advantages of bioplastics, such as biodegradability and biocompatibility, PHA production costs still cannot compete with those of petroleum-based plastics (Koning et al., 1997). The costs of PHA production are mainly determined by the price of the carbon source used in the fermentation process and the downstream step (Choi and Lee, 1997). Therefore, the development of fermentation strategies and the search for cheap carbon sources are of special importance.

Agricultural residues were studied as cheap carbon sources for PHA production by Van-Thuoc et al. (2008). However, in that study, wheat bran and potato residues gave a low final P3HB concentration, of only 4 g l^{-1}. Cereal crops, which are rich on starch and are also relatively cheap carbon sources, have not yet been used with *H. boliviensis* to produce P3HB. Only synthetic starch hydrolysate has been tested with this bacterium (Quillaguamán et al., 2005) and, in comparison with Van-Thuoc et al. (2008), the P3HB content was not improved. Koutinas et al. (2007) obtained better results (51 g l^{-1} of P3HB) when they studied the production of PHA from wheat by applying a two-step process for hydrolysis and fermentation using *Ralstonia eutropha*.

Of the various cereals used in the European bioethanol industry, corn kernel is the most used (European Renewable Ethanol Association) and was therefore chosen to study the PHA production with *H. boliviensis*. During the bioethanol process, after the milling of the grain and the gelatinization of the cereal mash at high temperature, a two-step hydrolysis process is applied. First, a thermostable α-amylase is added during the liquefaction step at 70-80°C for quick and random hydrolysis of the α-1,4 bonds. This step greatly reduces the size of the starch polymer. Secondly, glucoamylase converts the liquefied starch into glucose. Hydrolysis with glucoamylase can either be performed together with fermentation in a single-step process known as simultaneous saccharification and fermentation (SSF), or in a two-step process called separate hydrolysis and fermentation (SHF).

The main advantage of SHF is that each step can be performed using the optimal conditions for the enzyme or the microorganism, while with SSF, a compromise must be found. However, a major drawback of SHF is the end-product inhibition of glucoamylase by glucose. SSF was first performed by Takagi et al. (1977) and was shown to be superior to SHF in several cases (Söderström et al., 2005; Öhgren et al., 2007; Dahman and Ugwu, 2014). The advantages of the SSF process stem from the continuous and slow production of glucose. This reduces both the risk of microbial contamination and the initial osmotic stress due to the low glucose concentration at the beginning of the fermentation, and is generally more energy-efficient (Bothast and Schlicher, 2005).

In addition to ethanol, various bioproducts, such as butanol (Davidov et al., 2010), monosodium glutamate, latic and succinic acids (Bergsma et al., 2012; Gullón et al., 2007), were obtained using the SSF technique. Dahman and Ugwu (2014) evaluated the production of P3HB from wheat straw by *Ralstonia eutropha* by applying the SHF and SSF process. However, the application of an SSF process to produce PHA from corn mash and its integration in a first generation biorefinery scheme has not been previously evaluated.

The aim of this study is to evaluate the feasibility of PHA production from corn mash by *H. boliviensis* using an SSF process and the integration of the biopolymer production within a 1G-biorefinery platform.

6.2 MATERIALS AND METHODS

6.2.1 SSF and SHF experiments

SHF and SSF cultivations were performed in a Biostat® MD bioreactor, described in Chapter 2. The initial aeration and agitation rates were 1 l min^{-1} and 400 rpm, respectively. For all the experiments, the airflow rate and agitation speed were increased gradually when the dissolved oxygen fell below 60%. The maximum airflow rate and agitation speed attained were 5 l min^{-1} and 650 rpm, respectively. The phosphate concentration was monitored and maintained in the range of 0.7-3.7 g l^{-1} K_2HPO_4 to avoid limiting concentrations of this nutrient.

Corn kernel mash was pretreated as it was described in Chapter 5 (epigraph 5.2.2). In the case of the SHF experiment, the stream called corn syrup, with a glucose concentration of 271±37 g l^{-1}, was used. Two inoculation stages were needed for inoculum preparation. First, a *H. boliviensis* culture from an agar plate was inoculated into 20 ml of seed medium in a 100-ml flask and, after 18 h of incubation at 30°C, this pre-inoculum was transferred into 200 ml of seed medium in a 1-l flask. The latter seed culture was incubated at 30°C for 22 h with rotary shaking at 200 rpm Seed medium and the initial medium for the bioreactor were formulated as IC and BC medium (Chapter 2), respectively, but commercial glucose was replaced by glucose from corn syrup in both cases. The glucose concentration was monitored during the fed-batch experiments through off-line analysis and maintained in the range of 16-24 g l^{-1} by adding a feeding solution based on corn syrup (100% v/v) and all the components of the FBC medium, with the exception of the glucose.

In the case of the SSF experiment, the same two-stage inoculum preparation was performed. After the first pre-inoculum, the bacterial culture was grown in Erlenmeyer flasks with 100 ml of seed medium. This seed medium was composed of 50% v/v corn juice and 50% v/v water, the same amount of all the salts added to the IC medium used in the SHF process, and 146 mg of glucoamylase per l of corn juice. Seed culture was incubated at 30°C for 22 h with a rotary shaking at 200 rpm.

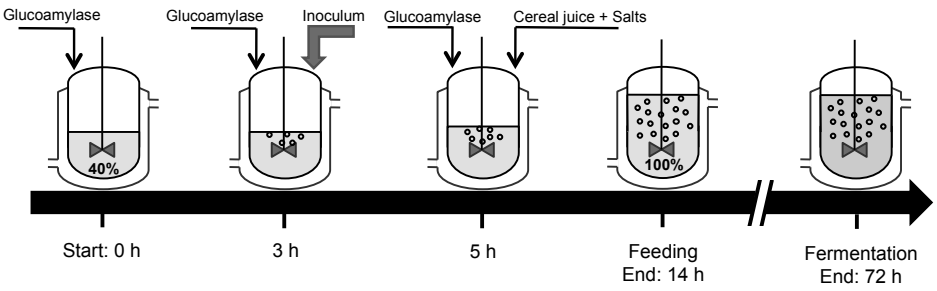

Figure 6.1: Description of the SSF process.

Implementation of SSF for PHA production was based on the common process used for bioethanol production, as described by Pena (2009). Thus, 80% of the working bioreactor volume was composed of cereal juice, the rest was composed of inoculum (5%), glucoamylase enzyme solution (5%) and salt solution required for *H. boliviensis* growth (10%). The bioreactor filling sequence (Figure 6.1) and the overall saccharification and fermentation time (72 h) were adapted from the standard bioethanol process. The minimum volume of 700 ml of corn juice (35% of the total working volume), necessary to cover the probes, was filled into the bioreactor, which was then sterilized in an autoclave at 121°C for 20 min. The concentrated solution of medium salts (100 ml) was autoclaved separately and added into the bioreactor afterwards (40% of the final volume). The final salts concentration in the bioreactor after the total filling was that of BC medium (Chapter 2). The process started with the addition of glucoamylase, which was diluted in 100 ml of water. The enzyme was progressively added into the bioreactor at a constant rate, until the end of the filling step (14 h). During the first 3 h of hydrolysis, the pH of the corn juice was not modified, agitation was set at 400 rpm, the temperature was fixed at 30°C and no air was supplied. At 3 h, the pH was adjusted to 7.5, the airflow was fixed at 1 l min^{-1} and the pO_2 sensor was calibrated. Then, inoculum was pumped into the bioreactor in a single pulse. At 5 h, the filling of the bioreactor was started by the addition of the remaining corn juice (900 ml) and the concentrated solution of salts (100 ml) to complete the final volume of 2 l. The filling process and glucoamylase addition took a total of 14 h. From this point forward, fermentation continued without any addition of medium.

6.2.2 Mass balance

A mass balance was performed around the whole conversion process for each of the different scenarios tested, SHF and SSF. The calculation base used was 100 g of corn juice in dry weight. Error bars in the figures represent the standard deviation of the sample. In the tables, as well as in the text, the presented values represent the mean ± standard deviation (SD).

Glucose consumption during the SSF process was calculated as the difference between the initial concentration of glucose equivalents (by the conversion of starch concentration into glucose with the anhydro conversion factor, measuring the dextrins content as described in Chapter 2) and the final non-consumed glucose or starch.

6.3 Results and Discussion

The biorefinery scheme that sums up the process described in this study is shown in Figure 6.2. A fraction of the liquefied cereal mash stream was diverted into the PHA route. After centrifugation of the cereal mash, two different process scenarios were proposed for the PHA integration into a first generation bioethanol plant. Scenario 1 involves PHA production by separate hydrolysis and fermentation (SHF), with these two processes being carried out in different vessels, while scenario 2 involves PHA production in a single vessel by simultaneous saccharification and fermentation (SSF).

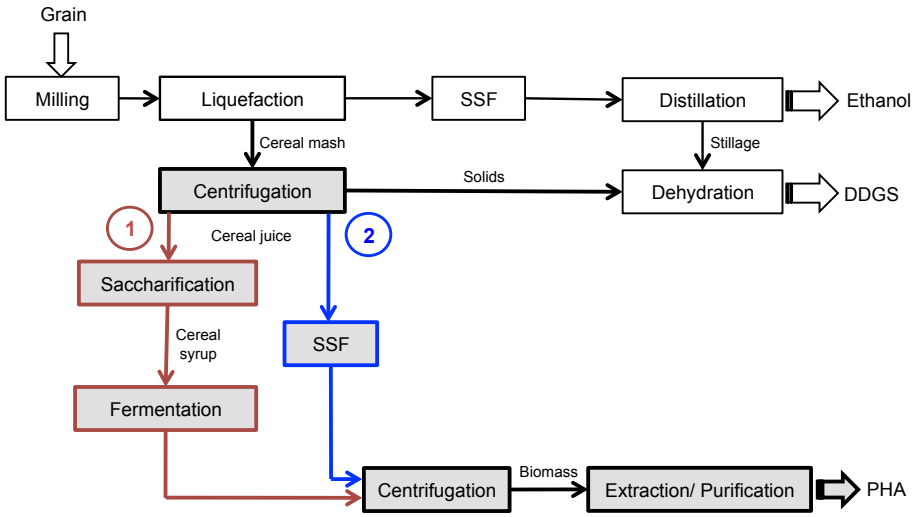

Figure 6.2: Process diagram with the main operational units of the two proposed biorefinery scenarios. The bioethanol process is represented with the black line. The red line (1) represents scenario 1 based on the SHF process and the blue line (2) corresponds to the SSF process of scenario 2.

The application of the SHF process allows the use of optimal hydrolysis conditions for the enzyme (50°C and pH 6.1) in the hydrolysis step, while optimal conditions for the microorganism (30°C and pH 7.5) are used in the SSF process. Then, the cereal juice hydrolysis was carried out at different pH (6.1 and 7.5) and temperatures (30 and 50°C) in order to check the saccharification efficiency of glucoamylase. The glucose obtained after saccharification at optimal enzyme conditions was 271±37 g l^{-1}. At 30°C, glucose saccharification decreased considerably to 94±4 g l^{-1}, using the same glucoamylase dose. The lowest glucose yield (61±3 g l^{-1}) was obtained at 30°C, pH 7.5 and with the presence of medium salts. These latter conditions are typically used for PHA fermentation by *H. boliviensis* (Quillaguamán et al., 2008). The strategy tested to increase the sugar release under such unfavourable conditions was to increase the concentration of glucoamylase during SSF. Thus, the standard dose was raised 10-fold and both SSF conditions were tested. Saccharification was also tested before and after the centrifugation stage, used to remove the suspended solids, and no differences were detected in glucose release (data not shown).

The SHF experiment involved the operation of a fed-batch bioreactor using corn syrup, saccharified using the optimal conditions for the enzyme (50°C and pH 6.1), as the carbon source. The main results are presented in Figure 6.3. The ammonium source was depleted between 24 and 37 h. PHA accumulation started at 24 h, reaching a final and stable concentration of 16 g l^{-1} from 44 h onwards. The total amount of corn syrup fed into the bioreactor was 983 ml and the total glucose consumed was 166 g l^{-1}.

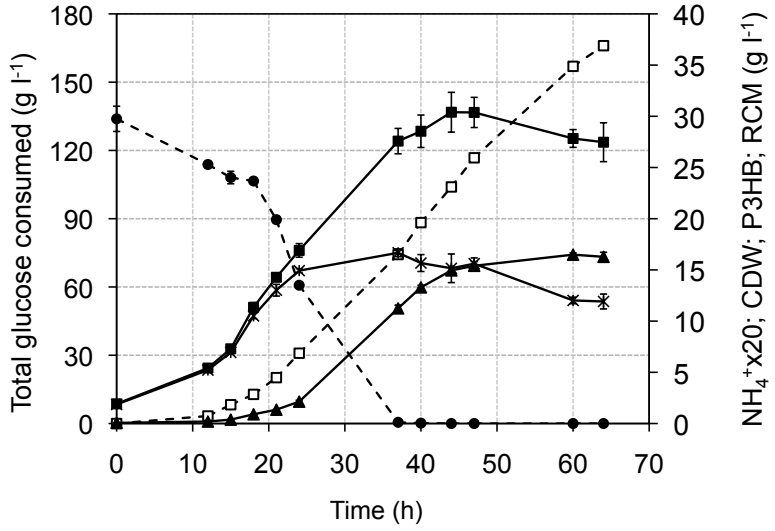

Figure 6.3: Fed-batch fermentation of the SHF process using corn syrup. Glucose consumption (white squares), ammonium concentration (black circles), total cell dry weight concentration (black squares), P3HB concentration (black triangles) and residual biomass concentration (crosses) are represented.

In a previous study with *H. boliviensis*, using synthetic starch as the carbon source and applying a SHF configuration, Quillaguamán et al. (2005) obtained 45% of P3HB with a CDW of 1.5 g l^{-1}, representing a P3HB production of 0.68 g l^{-1}. In the present study, the P3HB production in the SHF process reached 16.5 g l^{-1}, 23-fold higher. This substantial difference could be due to an inefficient hydrolysis of the starch in the work of Quillaguamán et al. (2005), since they used an α-amylase, which only forms maltooligosaccharides. Chen et al. (2006) obtained 20 g l^{-1} of PHA using the extremely halophilic Archaeon *Haloferax mediterranei* in a medium composed of enzymatic extruded corn starch and yeast extract, which is closer to our result. However, the application of this extremely halophilic microorganism implies the use of 20-23% (w/v) of salt and yeast extract as nitrogen source, increasing the production costs considerably.

Two different glucoamylase doses were tested, the standard dose of 146 mg l^{-1} (D) and 10 times the standard dose (10·D). The results obtained applying the SSF mode with the 10·D dose (SSF-10·D) are presented in Figure 6.4A. The glucose concentration increased considerably in the first 3 h, reaching more than 80 g l^{-1} and remained between 60 and 100 g l^{-1} during the whole process. Between 28 and 32 h, the ammonium source was exhausted. At that point, P3HB started to increase and the residual biomass remained almost constant, fluctuating between 21 and 25 g l^{-1} until the end of the process. P3HB production reached its maximum value (26 g l^{-1}) at 72 h. A glucose concentration of 60 g l^{-1} remained unconsumed at the end of the fermentation.

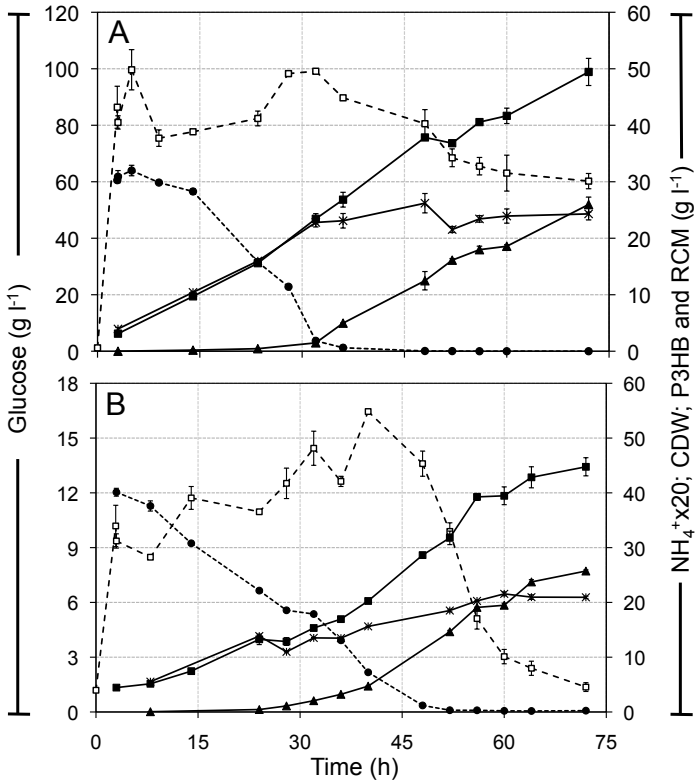

Figure 6.4: Results from the SSF process using **A**, the high glucoamylase dose (10·D) and **B**, the standard glucoamylase dose (D). Concentration of released glucose (white squares), ammonia (black circle), total cell dry weight (black squares), P3HB (black triangles), and residual biomass (crosses) are represented in both cases.

The standard dose of glucoamylase was also tested in SSF operation (SSF-D). As shown in Figure 6.4B, the glucose concentration remained between 8 and 16 g l^{-1} during the first 48 h, decreased afterwards to 2-5 g l^{-1}, and at the end of the fermentation was 1.4 g l^{-1}. The efficiency of corn juice hydrolysis was significantly lower than with the 10·D dose, since the maximum glucose concentrations measured were 16.5 and 100 g l^{-1} for SSF-D and SSF-10·D, respectively. The ammonium source was exhausted between 40 and 48 h, and P3HB started to accumulate at 30 h. Residual biomass increased slightly until 60 h, reaching a final concentration of 21.5 g l^{-1}. The maximal concentration of P3HB (25.7 g l^{-1}) was obtained at 72 h. The main difference between the SSF processes with the two glucoamylase doses was the glucose concentration reached in the supernatant (20 and 100 g l^{-1} for SSF-D and SSF-10·D, respectively). Despite this fact, P3HB production was not affected, since no differences were found in P3HB concentrations for both configurations (25.7±0.14 and 25.9±1.3 g l^{-1} of P3HB for D and 10·D, respectively) (p = 0.675). However, they were considerably higher than those obtained applying the SHF process (16.3±0.4 g L^{-1}). P3HB was previously produced in SSF and SHF configurations solely from wheat straw, using *R. eutropha* (Dahman and Ugwu, 2014). In that study, a higher P3HB

concentration was obtained when operating in SSF mode than in SHF (10 and 7 g l^{-1}, respectively).

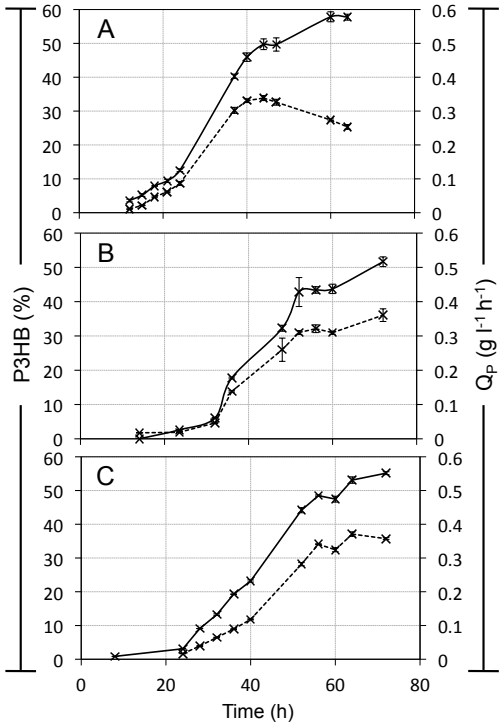

Figure 6.5: Evolution of P3HB accumulation (solid line) and P3HB productivity (dotted line) during **A**, fed-batch fermentation of SSF; **B**, SSF with the high glucoamylase dose (10·D); and **C**, SSF with the standard glucoamylase dose (D).

It is noteworthy that the progressive filling of the bioreactor (Figure 6.1) allowed a reduction in the inoculum size to half the volume used during SHF, and this has a direct impact on the decrease of operational costs on an industrial scale (Stanbury et al., 1995). Besides, SSF also enhanced RCM production, reaching 21 and 24 g l^{-1} using the D and 10·D glucoamylase doses, respectively, whereas only 12 g l^{-1} was obtained in SHF process. It is probable that a gradual release of sugars, in the case of the SSF process, enhanced biomass growth.

The profiles of the productivity (Q_P) and the percentage of P3HB accumulated during the three different processes are represented in Figure 6.5. There were significant differences among the final P3HB contents; the highest value was obtained with the SHF mode (57.7±2.1%), closely followed by the SSF-10·D and SSF-D processes (51.6±1.1% and 54.9±0.6%, respectively; $p < 0.01$). There was no significant difference between the maximal P3HB productivities obtained with either SSF operation mode (0.36±0.02 at 72 h and 0.37±0.006 g l^{-1} h^{-1} at 64 h, for 10·D and D, respectively; $p > 0.026$). A lower maximal productivity (0.34±0.007 g l^{-1} h^{-1}; $p = 0.35$) was obtained with the SHF mode at 44 h. Despite this value being reached in a shorter time with SHF than with SSF, the P3HB concentration obtained at the time of maximal productivity in SHF mode (15.0±0.3 g l^{-1}) was substantially lower than in SSF mode (23.7±0.4 and 26.0±1.3 g l^{-1} for D and 10·D, respectively).

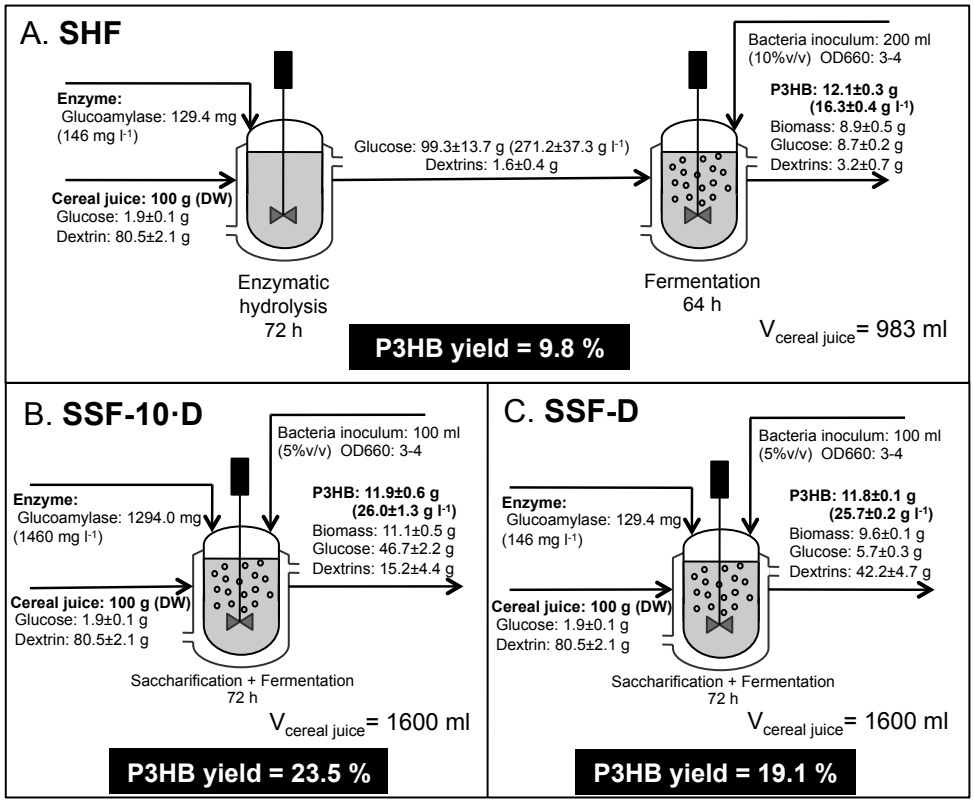

Figure 6.6: Mass balance analysis for: A, fed-batch fermentation of SHF; B, SSF with the high (10·D) glucoamylase dose; and C, SSF with the standard (D) glucoamylase dose.

Mass balance calculations were performed in order to evaluate and compare the corn juice conversion process under the different scenarios (Figure 6.6). The overall time used in the SHF process was 136 h (Figure 6.6A), while this value was reduced to 72 h when the SSF mode was evaluated applying either dose of glucoamylase (Figures 6.6B and 6.6C). The saccharification step was very efficient in SHF, since 99±14 g of glucose per 100 g of cereal juice (in dry weight) was obtained (Figure 6.6A). The cereal juice hydrolysis under the optimal conditions for enzymatic hydrolysis (50°C and pH 6.1) allowed a more efficient exploitation of cereal syrup. Thus, a lower volume of cereal juice was used and the non-consumed sugars at the end of the fermentation were the lowest in SHF, since the feed rate of cereal syrup during the fed-batch phase was controlled based on the glucose consumption. Unconsumed carbon source was the highest in the case of the SSF-10·D process. Depending on the dose of glucoamylase applied, a higher final concentration of dextrins or glucose was detected (Figures 6.6B and 6.6C). The final concentrations of unconsumed glucose for SSF-D and SSF-10·D were 1.7 and 60 g l^{-1}, respectively, while in the case of dextrin, the final concentrations reached were 92.3 and 33.2 g l^{-1}, respectively. The main disadvantage of the SSF process was the non-consumed carbon source that remained at the end of the process.

The biomass yields, expressed as grams of biomass per gram of corn juice, were 8.9±0.5, 9.6±0.1 and 11.1±0.5 (g/100 gDW) for the SHF, SSF-D and SSF-10·D processes, respectively. Approximately the same P3HB yield, expressed as grams of P3HB per gram of corn juice (11.8-12.1 g/100 gDW), was obtained with the three configurations tested. However, the P3HB yield, expressed as grams of P3HB produced per gram of consumed glucose, was quite different among all the configurations tested; 9.8, 19.1 and 23.5% were obtained for SHF, SSF-D and SSF-10·D, respectively.

6.4 Conclusions

This study compared the two most studied operational protocols for starch fermentation (SSF and SHF) in order to find the most suitable operation for PHA production integrated into a 1G-biorefinery. The main disadvantages of the SHF process are the higher inoculum size, the use of two processing units, and a longer process time. These drawbacks were overcome by applying the SSF configuration, which permitted a reduction of the inoculum volume, a shortening of the process time and the use of a single reaction vessel. However, a higher amount of corn syrup remained unconsumed after SSF when compared with the SHF mode. Despite the poor hydrolytic efficiency of the SSF-D mode, the greatest yield and total concentration of P3HB were obtained with this process configuration. In fact, P3HB yields in the cases of the SSF-D experiment (19.1 %) and the SSF-10·D experiment (23.5 %) were considerably higher than with the SHF (9.8 %) configuration. For an optimal exploitation of corn syrup, a compromise between the amount of corn juice and the glucoamylase dose utilized must be found.

7

Co-polymer P(3HB-co-3HV) production in a biorefinery

Co-polymer P(3HB-co-3HV) presents better properties and overall value than P3HB. Its production depends on the substrate fed to the microorganism and its metabolism. Taking profit of the processing flexibility of a biorefinery two different substrates, levulinic acid (LA) and volatile fatty acids (VFA), were tested to produce the co-polymer. LA is known as 3-hydroxyvalerate (3HV) precursor for other microorganisms, and it is easy to obtain from a sugar-rich stream. Different VFA mixtures can be obtained by an anaerobic acidogenesis process of complex waste generated in the biorefinery. Some of the VFA obtained, such as propionic or valeric acid, are known as 3HV precursors as well.

In this study, the behaviour of the bacterium *Halomonas boliviensis* on LA and different VFA mixtures was tested, as well as the effect of using these substrates as carbon and energy source for PHA production at flask scale. The substrate that yielded the highest PHA accumulation was used to scale-up the process. At bioreactor scale, a total amount of 13 g l^{-1} of PHA was obtained, which was formed by 70% of the copolymer P(3HB-co-3HV) with a 3HV fraction of 8.5 mol %.

OUTLINE

7.1 Introduction

The co-polymer P(3HB-co-3HV), consisting of 3-hydroxybutyrate (3HB) and 3-hydroxyvalerate (3HV) monomers, shows better mechanical properties in comparison to the homopolymer P3HB. P3HB shows a very high degree of crystallinity, which results in stiffness and brittleness properties. Additionally, the melting temperature of P3HB is close to its thermal decomposition temperature. This fact makes P3HB hard to be processed by melt-processing machines and limits its potential applications (Asrar et al., 2002). The incorporation of 3HV into P3HB improves its properties, since stiffness is decreased, while its flexibility and toughness are improved. Accordingly, the co-polymer is considered to possess more potential in biomedical and industrial applications than P3HB (Sankhla et al., 2010).

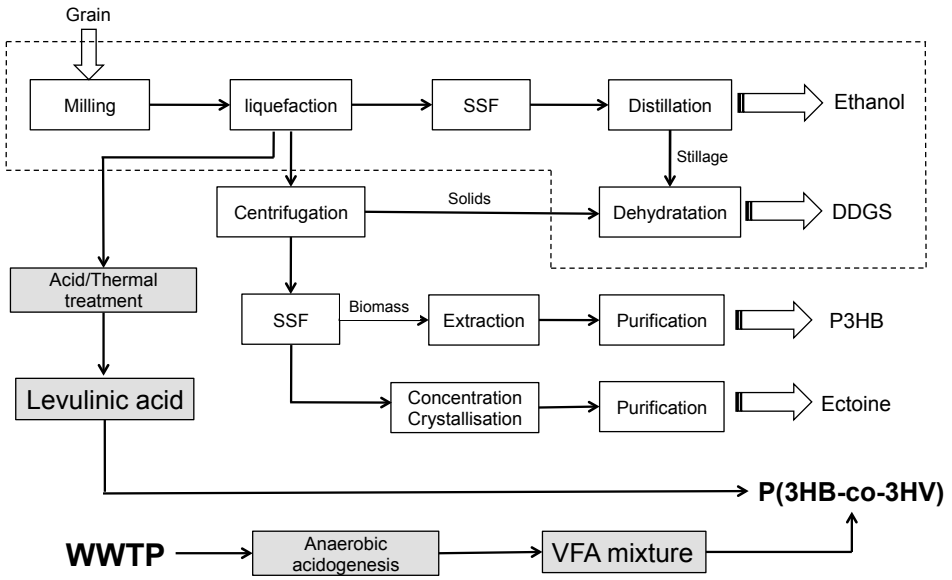

Figure 7.1: Biorefinery scheme. A typical bioethanol process from grain is represented inside the dotted box. Grey boxes show the two alternatives proposed for co-polymer production.

The principal objective in the development of biorefineries is defined by this simple pathway: (biomass) feedstock-mix + process-mix → product-mix (Kamm and Kamm, 2004). The high flexibility of the biorefinery could allow us to obtain different products. In the case of the co-polymer, two different approaches were tested based on the available resources in a whole-crop biorefinery (Figure 7.1). First, starch and sugars are easily converted to levulinic acid (LA) by sulphuric acid with extrusion processing in a pressure reactor (Cha and Hanna, 2002). Levulinic acid is a highly versatile chemical with several industrial uses. It has the potential of a commodity chemical, but it is as well a 3HV precursor. A few studies have shown that LA can be used by *Ralstonia eutropha* as a sole carbon source or as co-substrate for cell growth and PHA formation (Chung et al., 2001; Lee et al., 2009; Yu et al., 2009). And secondly, organic waste from the overall biorefinery process, usually derived to the wastewater treatment plant (WWTP), can be transformed into short-chain carboxylates as intermediate feedstock chemicals, using hydrolysis and fermentation with undefined mixed cultures. The short-chain carboxylates also known as volatile fatty acids (VFA) – acetate,

propionate, butyrate and valerate – are the primary organic products (Agler et al., 2011). There is a vast research on PHA production from VFA with mixed cultures. Due to their metabolic flexibility, they adapt better than pure cultures to non-sterilized complex substrates (Salehizadeh and Van Loosdrecht, 2004). Nevertheless, the main drawback of mixed cultures is the low productivity and biomass concentration that is possible to obtain.

There are several studies about PHA production from single acids, such as acetic (Wang and Yu, 2000), propionic (Kim et al., 1992), butyric (Quillaguamán et al., 2006) and valeric (Page et al. 1992), with pure cultures (mainly with *R. eutropha*). However, the production of a single acid, and its purification, raise the price enormously. The use of a cheap substrate, such as the VFA mixture from anaerobic acidogenesis of waste, will help to reduce this cost (Amache et al., 2013).

Organic acids, such as LA or VFA, often inhibit cell growth at moderate concentrations (Yu et al., 2002). There are two main uptake mechanisms for weak acids (Visser and Postma, 1973), the migration of the lipophilic undissociated form of the acid by simple diffusion and the uptake of the dissociated anion by an antiport mechanism (Figure 7.2). Of these two mechanisms only the last one implies the use of energy by the cell. Nevertheless, the major toxicity effect is due to the lipophilic behaviour of the undissociated form of the acids, which freely diffuse into the cells. It acts as an uncoupling agent, uncoupling electron transport from ATP synthesis (Baronofsky et al., 1984).

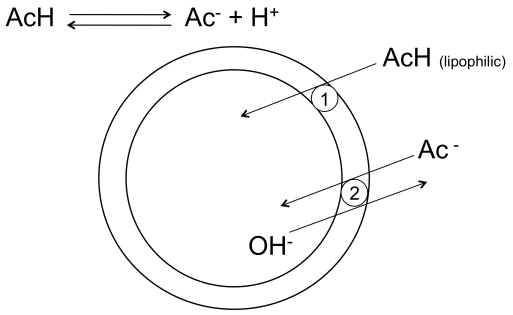

Figure 7.2: Mechanisms of weak acids toxicity in cells. (1) Free diffusion of the undissociated acid form into the cell. (2) Antiport mechanism for the uptake of the dissociated form of the acid.

Uncouplers are lipid-soluble weak acids that act as proton carriers and provide an additional pathway to the ATP synthase for the flow of protons across the cytoplasmic membrane. The proton motive force is dissipated, and ATP cannot longer be synthesised. The inhibition of cell growth by acids can be minimised if the acid can exist in a dissociated anion form in the culture broth (Chung et al., 1997).

Accordingly to the Henderson-Hasselbalch equation and the corresponding pK_a values for LA and VFA (4.6-4.9), the dissociated anion form increases with the increase of the medium pH. *H. boliviensis* is highly tolerant to alkali. Its optimal pH is 7.5-8, then, it is supposed that it could deal better with the acid inhibition.

The aim of this research was to evaluate the performance of the bacterium *H. boliviensis* using LA and VFA as carbon source for producing PHA co-polymers, in order to integrate this new product into a biorefinery scheme.

7.2 Materials and Methods

7.2.1 Flask scale fermentations

LA and three different VFA mixtures were tested. For LA, two different fermentation strategies were followed at flask scale, using the substrate as sole carbon source or as co-substrate with glucose. VFA mixtures were only tested as sole carbon source. Inoculum was prepared as described in Chapter 2.

Sole carbon source fermentation

First, biomass was grown in 2 l flasks, with 200 ml of BC medium. Baffled flasks were used in order to improve the aeration of the biomass and to enhance grow. After 24 h, biomass was harvested by centrifugation and transferred to 250 ml flasks with 50 ml of new BC medium, in which glucose was replaced by 10 g l^{-1} of LA or VFA mixture and NH_4Cl concentration was decreased to 0.25 g l^{-1}, in order to provoke PHA accumulation by nitrogen limitation. After 48 h, biomass and polymer production were quantified.

Co-substrate fermentation

H. boliviensis was grown in 250 ml flasks with 50 ml of BC medium with glucose. After 24 h of fermentation, pulses of LA were added periodically to increase its concentration in 1 or 2 g l^{-1}. In order to quantify biomass and PHA, destructive assays were performed by triplicate for each sampling point.

7.2.2 Bioreactor scale fermentations

Scale-up cultivation was performed in a 2 l bioreactor using a working volume of 1.5 l, as described in Chapter 2. Fed-batch operation was followed applying N-limitation conditions with low O_2 supply, as described in Chapter 4. During the growth stage, BC medium with glucose as carbon source was used until nitrogen exhaustion. The accumulation stage took place under nitrogen limitation, and the FBC medium was fed. In this medium, glucose was replaced by a synthetic mixture of VFA with a total concentration of 250 g l^{-1}.

7.2.3 Polymer characterisation

Extraction of PHA

PHA was isolated from freeze-dried cells with hot chloroform in a Soxhlet extractor. The extract was concentrated by evaporation at the final step of the extraction, and the polymer was precipitated in 10 vol of ice-cold methanol. Upon separation of the PHA from methanol through centrifugation at 1920 x *g* for 20 min, the polymer was left to dry.

Differential scanning calorimetry (DSC)

PHA samples were heated from room temperature to 650°C at a heating rate of 20°C min^{-1} in an N_2 atmosphere. The melting temperature (*Tm*) and enthalpy of fusion (ΔH_f) were calculated from the maximum and the area of the first endothermic peak, respectively, whereas decomposition temperature (*Td*) was calculated from the second endothermic peak.

7.3 RESULTS AND DISCUSSION

7.3.1 Levulinic acid

H. boliviensis was first grown in glucose during 24 h to obtain a high biomass concentration. Despite the absence of nitrogen-limiting conditions, 22.0±2.1% of P3HB was accumulated. After 48 h growing in 10 g l^{-1} of synthetic LA under nitrogen-limiting conditions, biomass and P3HB slightly increased. Final P3HB accumulation was 26.4±1.8%. However, no 3HV peak was detected by GC analysis (Figure 7.3).

Levulinic acid is more hydrophobic than short organic acids such as acetic or propionic. Then, a large proportion of LA removed from the liquid sample could not have been consumed, but adsorbed or absorbed by the wet pellet (Jaremko and Yu, 2011). Although LA was measured by HPLC, the results were not accurate enough neither to confirm nor to calculate its consumption. A control experiment was done to check if the growth observed in Figure 7.3 is due to LA or monosodium glutamate metabolization. When the medium was fed only with LA as carbon source and no MSG was added, no growth was appreciated (data not shown).

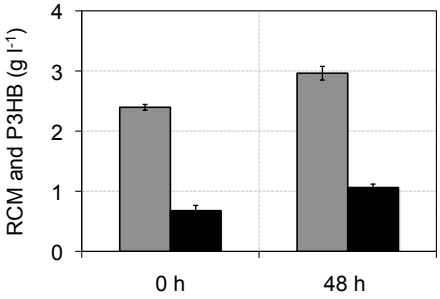

Figure 7.3: Biomass (grey bar) and P3HB production (black bar) growing on levulinic as sole carbon source.

Previous studies have shown that successful co-polymer production has been reached when low LA concentrations were used in combination with other less harmful substrates, such as, glucose (Jang and Rogers, 1996), fructose syrup (Chung et al., 2001), xylose (Keenan et al., 2004) or gluconic acid (Kim et al., 2009). This different fermentation approach was assayed since the previous experiment with LA as sole carbon source was not successful. In this case, glucose was used as the main carbon source and synthetic LA was fed as pulses during bacterial growth. Biomass and P3HB production are shown in Figure 7.4. Although both parameters increased with time and P3HB accumulation reached 33.8±0.6%, 3HV monomer was not detected.

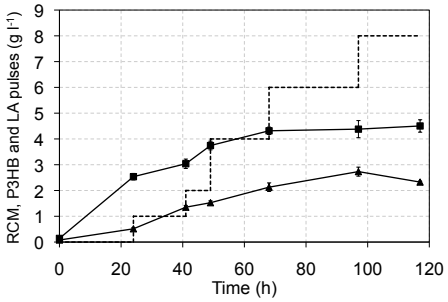

Figure 7.4: Bacterial growth (squares) and P3HB accumulation (triangles) on glucose with LA pulses (dotted line).

In a previous study, Bera et al. (2015) used seaweed-derived crude levulinic acid as substrate with *Halomonas hydrothermalis*, a microorganism closely related to *H. boliviensis*. This complex substrate contained LA, but also formic acid, residual sugars and dissolved minerals. Co-polymer was obtained with this substrate. However, in a control experiment with synthetic LA, PHA and bacterial growth was surprisingly reduced, observing inhibitory effects even at a concentration as low as 0.06%. However, this

study did not clear up if LA is a real 3HV precursor for *H. hydrothermalis* or if any other constituent of the complex substrate acted as a precursor.

Our experiments clearly demonstrate that LA is not a 3HV precursor for *H. boliviensis*. Jaremko and Yu (2011) examined LA metabolism by *R. eutropha* and found that the metabolic route of HV production from LA is based on its activation to form 4-ketovaleryl-CoA and then it is split into propionyl-CoA and acetyl-CoA. These two intermediates are either used for cell growth or condensed into 3-ketovaleryl-CoA and acetoacetyl-CoA, yielding 3HV and 3HB, respectively. Acyl-CoA synthetase is an inducible, not constitutive, membrane-bound enzyme. Since it is known that *H. boliviensis* is able to grow and accumulate PHA with acetyl-CoA and propionyl-CoA, the bottleneck of the pathway may be the first activation step of acyl-CoA synthetase. However, a deeper *in vitro* study of the intermediates in the initial reactions of LA metabolism is necessary to reveal the correct pathway.

7.3.2 Volatile fatty acids

It is known that pH plays a major role in anaerobic acidogenesis. It was previously demonstrated that modifying the pH of the medium it is possible to modulate the profile of the main products obtained during the process (Zoetemeyer et al., 1982). Under acidic and neutral conditions, the main products were butyric acid, while acetic and propionic acids were the main products under basic conditions. In Table 7.1, the compositions of three different VFA mixtures obtained from anaerobic acidogenesis reactors are summarised. Mixtures VFA 1 and 2 were taken from Horiuchi et al. (2002) and VFA 3 was obtained from Palmeiro-Sánchez T. (personal communication).

Table 7.1: Composition of the VFA mixtures (wt. %).

	VFA 1	VFA 2	VFA 3
Acetic acid	53.7	20.9	58.4
Propionic acid	32.7	1.3	24.5
Butyric acid	7.3	74.7	6.2
Ethanol	6.3	3.1	–
Valeric acid	–	–	10.9

For shake flask experiments, *H. boliviensis* was grown first on glucose for 24 h to obtain a high biomass concentration. Although nitrogen was not in limiting concentrations, PHA was accumulated to 29.4±6.1% and only the 3HB monomer was detected. After 24 h, biomass was transferred to a new media with the different VFA mixtures as carbon source. A control experiment, in which VFA was replaced by glucose, was also carried out. In Figure 7.5, the increment of 3HB, the 3HV production between the initial point and the 72 h and the residual biomass increment are represented. During the accumulation phase, the control experiment (growth on glucose) presented the highest P3HB increment, and no co-polymer was obtained.

It was previously reported that acetic and butyric acid mixtures produce higher PHA accumulations than acetic and propionic acid mixtures for *R. eutropha* (Yu et al., 2002), however, in this study, the opposite behaviour was observed with *H. boliviensis* (Figure

7.5A). VFA 1 (rich in acetic and propionic acid) reported a P3HB increment 5 times higher than the obtained with VFA 2 (rich in acetic and butyric acid).

Co-polymer formation by the addition of precursors like propionic or valeric acid was previously studied with other microorganisms (Doi et al., 1988). With *H. boliviensis*, the 3HV formation was obtained with the mixtures VFA 1 and 3, which have both a high propionic acid concentration (Figure 7.5B). However, the highest 3HV fraction (17.5 mol %) was obtained with the VFA 3 mixture, which was the only one that contained valeric acid. With the VFA 1 mixture, a lower 3HV fraction of 2.56 mol % was obtained.

Yu et al., (2002) established that *R. eutropha* prefers propionic acid for cell mass synthesis and butyric acid for polymer synthesis. However, in this study, the VFA 3 mixture reported the highest increase in cell mass (Figure 7.5C).

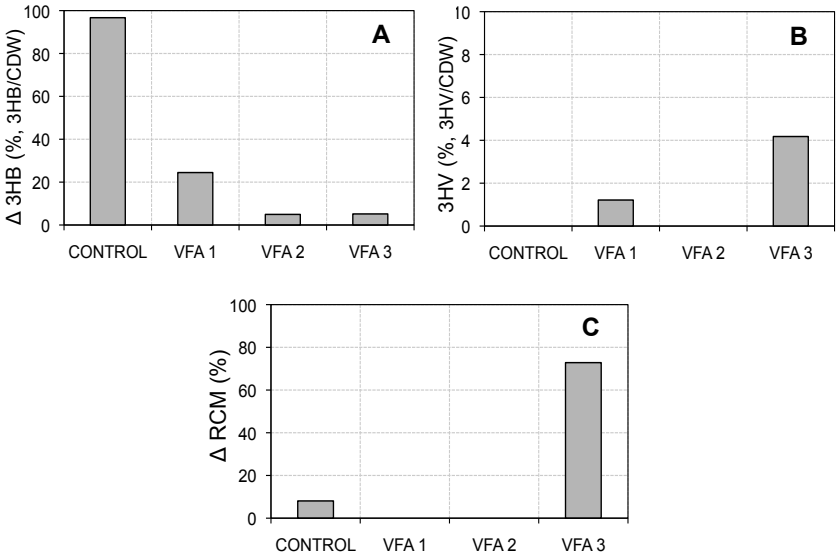

Figure 7.5: Increase in 3HB concentration **(A)**, accumulation of 3HV **(B)** and increase in RCM during the accumulation phase **(C)**, with the different carbon sources tested at flask scale.

Since VFA 3 mixture reported the highest 3HV fraction into the co-polymer accumulation, this substrate was chosen to scale-up the process. Once more, a synthetic mixture was used during the fed-batch operation of the bioreactor in two stages. First of all, glucose was fed into the bioreactor until the nitrogen source was exhausted, between 21 and 24 h, then the VFA 3 mixture replaced glucose in the feed, and it started to be added into the bioreactor (Figure 7.6). PHA accumulation peaked (71%) after 42 h, and it was maintained constant until the end of the fermentation.

As observed in Figure 7.6B, total glucose consumed during the first 27 h reached 50 g l^{-1}, and no remaining glucose was detected afterwards. During the next 38 h, *H. boliviensis* used VFA as carbon source, with a total uptake of 70 g l^{-1}. Acetic acid was the most consumed VFA (46 g l^{-1}), followed by propionic acid (16 g l^{-1}). These two acids were also the most abundant in the VFA mixture.

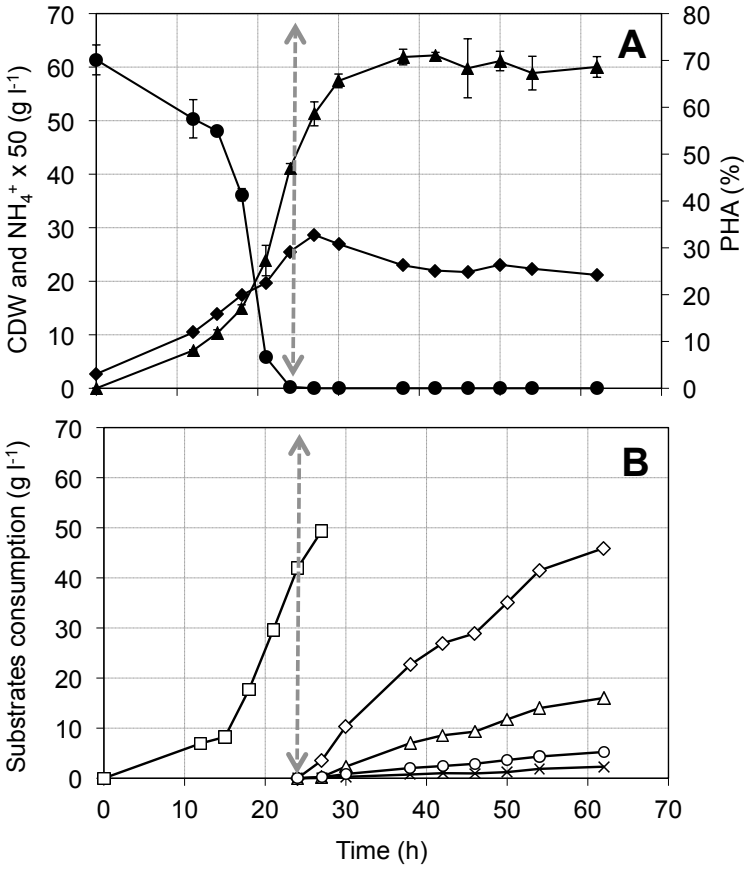

Figure 7.6: Time course of the PHA production at bioreactor scale. Figure A depicts the total cell dry weight production (rhombuses), PHA accumulation (triangles) and ammonia exhaustion (circles). Figure B shows the consumption of carbon sources, glucose (white squares), acetic (white rhombuses), propionic (white triangles), valeric (white circles) and butyric (crosses) acid. Grey arrow indicates the feed switch from glucose to VFA mixture in both cases.

Co-polymer, P(3HB-co-3HV), was also detected at bioreactor scale. As it can be observed in Figure 7.7, 3HV monomer appeared after 24 h, in coincidence with the feed switch from glucose to VFA, and it increased until the end of the fermentation. Contrary to that observed at flask scale, operational conditions were not optimal for *H. boliviensis* maintenance, since residual biomass decreased considerably in the presence of acids, and PHA concentration slightly decreased. The evolution of co-polymer composition and the increase of the HV fraction occurred in parallel during the time course fermentation.

After 62 h of operation in fed-batch mode, 21 g l^{-1} of total biomass was obtained, from which 70% was PHA. The type of PHA accumulated was a copolymer of P(3HB-co-3HV) with an HV content of 8.5 mol %.

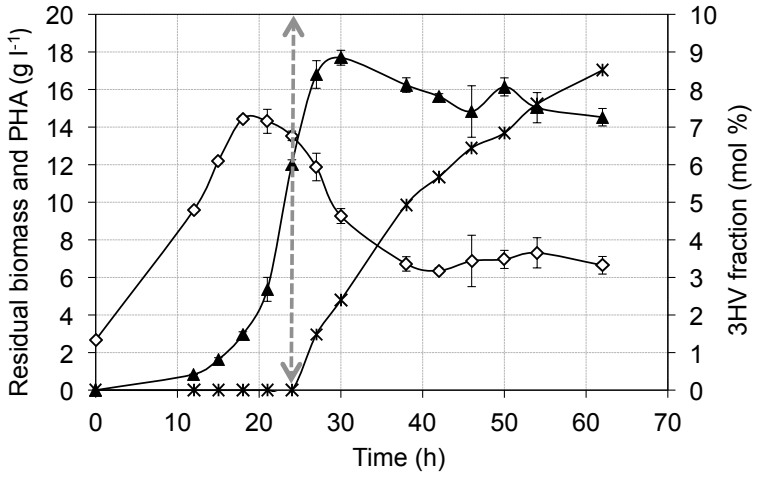

Figure 7.7: Evolution of the residual biomass (white rhombuses), PHA concentration (black triangle) and copolymer 3HV fraction (crosses) evolution during the fed-batch fermentation at bioreactor scale. Grey arrow indicates the feed switch from glucose to VFA mixture.

Table 7.2 shows an overview of various studies, in which PHA was produced from VFA mixtures obtained with anaerobic acidogenesis from wastes or synthetic VFA mixtures that simulate the real ones. The PHA concentration and 3HV fraction obtained in this study are among the highest values published so far, except the recent study of Huschner et al. (2015) that reported amazing higher results than the other studies. Their fermentation strategy is based on a high cell density process with *R. eutropha* H16, using different control techniques.

Table 7.2: Summary of PHA production studies from VFA mixtures as the main carbon sources at bioreactor lab scale.

Microorganism	CDW (g l^{-1})	PHA (%)	PHA (g l^{-1})	3HV (mol%)	Reference
R. eutropha	10.0	63.3	6.3	NG	Jin et al., 1999
R. eutropha	3.5	34.1	1.2	NG	Yu, 2001
R. eutropha	15.9	62.9	10.0	10.7	Ruan et al., 2003
R. eutropha	14.3	48.0	6.9	NG	Yan et al., 2003
R. eutropha	22.7	72.6	16.5	2.8	Du et al., 2004
R. eutropha	12.0	90.0	10.8	NG	Hong et al., 2009
Comamonas sp.	7.0	82.0	5.7	NG	Mumtaz et al., 2010
R. eutropha	21.1	39.5	8.4	NG	Chakraborty et al., 2012
R. eutropha	112.0	83.3	93.3	5.6	Huschner et al., 2015
H. boliviensis	21.0	70.0	16.0	8.5	This study

NG: Not given.

Studies with mixed cultures using real VFA mixtures reported PHA contents as high as 0.75 gPHA $gVSS^{-1}$ or 0.77 gPHA g VSS^{-1} using fermented molasses (Albuquerque et al., 2010) or fermented paper mill wastewater (Jiang et al., 2012), respectively. However, total

biomass concentration (measured as volatile suspended solids, VSS) was much lower (between 5.1 and 2.4 g l^{-1}) than the values obtained in this study. Besides, the downstream process for the PHA recovery of a highly diluted stream will increase production costs.

7.3.3 Polymer characterization

The incorporation of the monomer 3HV into the biopolymer was reported to modify the properties of the PHA (Dai et al., 2008). The PHA obtained in this Chapter using VFA as carbon source was found to be composed by 3HB and 3HV by GC analysis. However, to check if the properties of the PHA were indeed different or affected by the incorporation of the 3HV, the thermoanalytical technique known as differential scanning calorimetry (DSC) was applied. This is an extremely useful tool for the characterization of the PHA in the light of melting temperature, thermal stability, etc. However, the use of this technique for the measurement of crystallinity in PHA copolymers becomes very complex (Barham et al., 1992), since the density and heat of fusion measurements are affected by the partitioning of the HV units between the crystalline and amorphous regions and can only be used for the extreme cases of complete inclusion or exclusion of the comonomers from the crystals.

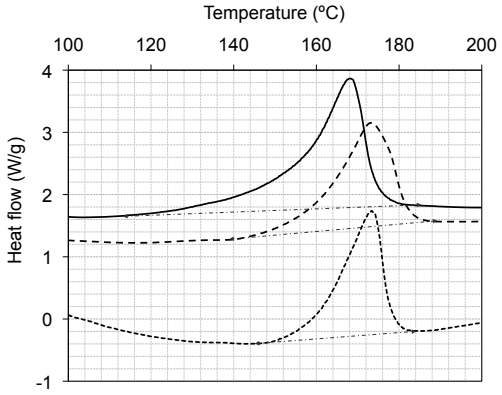

Figure 7.8: Fusion peaks of the biopolymer obtained in this Chapter from VFA 3 (continuous line), and the biopolymer obtained in Chapter 6 from corn juice applying SHF (dashed line) and SSF (dotted line), analysed by DSC.

The P3HB obtained in the Chapter 6, using corn juice as carbon source applying either SHF or SSF, were used as controls. The main difference between the curves of the different samples, analysed by DSC (Figure 7.8), is that the P(3HB-co-3HV) presented a lower initial melting temperature, a longer range of melting temperatures and a longer distance between melting and decomposition temperature (Table 7.3). Both P3HB obtained from corn juice under different fermentation procedures presented similar characteristics.

Table 7.3: Characteristics of different biopolymers: enthalpy of fusion (ΔH_f), melting temperature (T_m), decomposition temperature (T_d) and degree of crystallinity (Xc).

Carbon source	Polymer	T_m (°C)	T_d (°C)	ΔH_f (J g^{-1})
Corn juice (SHF)	P3HB	140-188	230-304	84.7
Corn juice (SSF)	P3HB	148-184	237-315	71.6
VFA 3	P(3HB-co-3HV)	116-185	250-325	76.7

The impact of the 3HV constituents on the thermal characteristics is in good agreement with the previous findings of Abe and Doi (2001) or Dai et al. (2008).

7.4 CONCLUSIONS

The great versatility of the biorefinery allowed us to figure out different operational strategies to obtain a different product. Despite the promising capacity of levulinic acid as platform chemical and as 3HV precursor with other microorganisms, it had null effect in 3HV production with *H. boliviensis*. On the other hand, the flexibility of the anaerobic acidogenesis process is considered as an advantage in this study, since it allows us to obtain different mixtures of acids in different proportions. Thus, according to the PHA producer used, it could be possible to adapt the carbon source composition to the metabolic requirements of the microorganism in order to obtain a PHA co-polymer with a specific composition. In this study, it was demonstrated that the halophilic bacterium, *H. boliviensis*, is able to grow and accumulate different kinds of PHA using such a complex and toxic substrate like VFA. The presence of hydroxyvaleric fraction in the co-polymer P(3HB-co-3HV) changes its properties, and characteristics and this is directly related to the target application of the biopolymer. By applying fed-batch fermentation in two stages, it was possible to increase the 3HV fraction of the copolymer without a significance change in the total PHA content. According to the specific use of the biopolymer, the process could be stopped at any moment, depending on the required 3HV fraction. Our long-term objective is to produce PHA from a real VFA stream obtained from waste in an anaerobic acidogenesis reactor. This would reduce the costs of producing PHA and enlarge the types of PHA produced.

8

General discussion and conclusions

OUTLINE

8.1 Main outcome and positioning of this work

8.2 PHA production from *H. boliviensis*

8.3 Use of biorefinery feedstocks

8.4 Thesis implications and limitations

8.5 General conclusions

8.1 Main outcome and positioning of this work

There is a strong trend towards the use of sustainable, biodegradable and renewable materials across the world nowadays. This is reflected in many recent regulations that, for example, restrict or ban the use of traditional plastic bags (Directive (EU) 2015/720). Among all the known biopolymers that can replace the petroleum based polymers, PHA stands out for many applications due to its special features. PHA production is a well-known process that had kept much attention, however, several issues that often affect the production costs threaten its industrialization. Gaining a better understanding of the PHA accumulation mechanisms of a potentially good PHA producer and the development of detailed methodology to allow the integration of the PHA process into a biorefinery has been the main objective of this PhD research. Different feedstocks, technologies, products and process pathways have been studied in order to obtain the optimal configuration that fits better for each type of industry.

In this Thesis, several PHA production strategies framed into a biorefinery scheme (Figure 8.1) have been developed. Biorefinery has been defined as the main tool to move the present production systems towards a bioeconomy. Despite this transition is necessary, it still requires further research, investment and efforts from different disciplines. The main outcome of this Thesis is focused on solving those limitations.

Halophilic microorganisms have a great potential in biotechnological applications, but they have been scarcely used at industrial scale yet (Yin et al., 2015). For that reason, to increase the knowledge of the PHA production by *H. bolivensis* was the first step previous to the integration of the biopolymers production into a bioethanol plant (Figure 8.1). A rapid and easier method for PHA quantification was developed in order to facilitate the monitorization of the process, looking forward its subsequent evaluation at higher scale. The use of low cost substrates and the development and application of novel processes were carried out with the aim of reducing the production costs. Finally, the use of residues as substrates and the concomitant production of an upgrade copolymer were developed. All this contributions are oriented to develop the future sustainable production of PHA into a biorefinery.

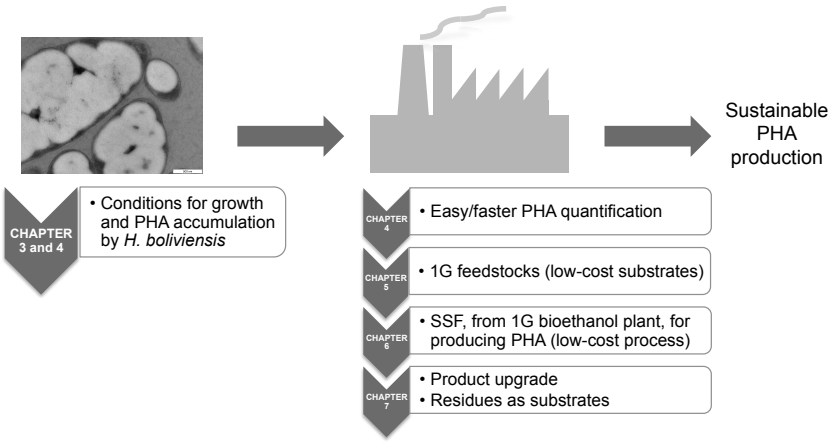

Figure 8.1: General scheme and summary of the main content of the Thesis.

8.2 PHA PRODUCTION BY *H. BOLIVIENSIS*

Several microorganisms possessing the ability to accumulate PHA in satisfactory amounts have been studied in recent years (Table 8.1). The fermentation process with the bacterium *R. eutropha* is one of the most effective. *Burkholderia sacchari* has been reported as a potential PHA producer. In addition to the wild strains, efforts have been made to obtain and use genetically modified microorganisms to produce PHA, such as *Escherichia coli,* that does not normally produce the biopolymer. However, there are still many potential PHA producing strains that remain undiscovered and could produce novel PHA constituents or interesting subproducts. *H. boliviensis* is not a model microorganism for PHA production, such as *R. eutropha*, nevertheless, recent research on halophiles has shown a remarkable potential for the biotechnological production of PHA (Table 8.1). It also presents some attractive advantages (e.g. ectoine production, lower contamination risk, etc.) compared with the previously mentioned strains, which could turn it into the optimal microorganism for some specific applications. For instance, as was described in Chapter 7, its alkalitolerant behaviour and resistence to unbalanced osmotic preassures resulted great advantages to deal with complex substrates such as VFA.

Table 8.1: Comparison of several PHA producer strains.

Microorganism	Carbon source	P3HB (%)	P3HB (g l^{-1})	P3HB (g l^{-1} h^{-1})	Reference
Recombinant *Escherichia coli*	Glucose	73	142	4.63	Choi et al., 1998
R. eutropha	Sucrose	88	99	4.94	Wang and Lee, 1997
R. eutropha	Glucose	74	105	2.63	Lee et al., 1997
Burkholderia sacchari	Sucrose	42	63	1.70	Pradella et al., 2010
Azotobacter vinelandii	Glucose	79	25	1.00	Page and Cornish, 1993
Halomonas TD01	Glucose	80	64	1.14	Tan et al., 2011
Halomonas salina	Glucose	78	35	0.72	Chen et al., 2014
H. boliviensis	Glucose	73	35	0.59	This study (Chapter 3)

H. boliviensis was recently isolated by Quillaguamán et al. (2004) and was the first member of the genus *Halomonas* reported to produce PHA (Quillaguamán et al., 2005). However, the small amount of information available at the beginning of this study, about the PHA accumulation by halophilic microorganisms, supposed the first issue to be faced. In order to accomplish the main aim of this Thesis, the first objective was to determine how the type and severity of the nutrient limitation affects PHA production in *H. boliviensis* to obtain the highest PHA accumulation.

Nitrogen or oxygen are usually chosen as limiting nutrients to trigger PHA accumulation, since their concentrations are easy to control (Kim et al., 1994). *H. boliviensis* metabolism under nutrient balanced growth conditions seems to be driven mainly towards the carbohydrate catabolic pathway considering that no PHA accumulation was detected on that circumstances. This behaviour contrast with that of *R. eutropha*, which is able to accumulate PHA even under nutrient balanced media (Lopar et al., 2013). Moreover, the type and extent of nutrient limitation present a different influence on the PHA accumulation for the different strains tested at the moment. For instance, oxygen can lead to enhancements in PHA production in the case of *P. putida* or *Methylobacterium* (Kim et al., 1997; Nath et al., 2008), but it also can be prejudicial in the case of *Bacillus mycoides* (Borah et al., 2002). This study demonstrates that only when a nitrogen limitation is combined with a low oxygen supply the PHA accumulation is the highest for *H. boliviensis*.

Another special feature of *H. boliviensis* was discovered after evaluating the population dynamics of PHA producing cultures (Chapter 4). With the aim to develop a faster an easier technique for PHA quantification, a heterogenic bacterial culture was distinguished by flow cytometry, in which PHA accumulating and non-accumulating bacteria were coexisting in the same biorreactor. This behaviour was not detected for *R. eutropha* using the same analytical technique (Kacmar et al., 2005), but it was noticed in some cases with recombinant PHA-producers or mutant strains (Lee et al., 2013; Prieto et al., 2016). This heterogeneity in PHA accumulation of the bacterial culture could be explained by the absence of a gene that encodes a protein known as PhaM or PhaF/PhaI for *R. eutropha* and *P. putida*, respectively. However this fact could not be completely claimed.

8.3 Use of biorefinery feedstocks

The industrialization of the PHA production is being hampered by its production costs. However, since biopolymers are commodities with higher added value compared to ethanol, the integration of the PHA production into a bioethanol plant could decrease its production costs and benefit as well the ethanol production (Nonato et al., 2011).

A wide range of substrates has been previously studied for economical production of PHA, a few examples are shown in Table 8.2. Koutinas et al. (2007) evaluated the production of PHA from 1G feedstoks in a wheat-based biorefinery, obtaining satisfactory results. Other lignocellulosic substrates, such as sugarcane bagasse or wheat straw (Lopes et al., 2011; López-Abelairas PhD Thesis, 2014), were as well tested, obtaining lower PHA yields. 2G feedstocks do not compete with food markets as 1G do, however they present several drawbacks i.e. a complex pretreatment of the biomass is mandatory to release sugars before the fermentation, some of these sugars are not so easy to metabolize as glucose, and inhibitory compounds are usually produced due to the severe conditions of the pretreatment.

The use of inexpensive an readily available sub-products or residues, produced in huge quantities, such as glycerol, waste cooking oil, cheese whey or agro-industrial processing waters (Mothes et al., 2007; Lee et al., 2008; Pais et al., 2016; Elain et al., 2016) were as well tested as substrates for PHA production. Besides the reduction of PHA producing costs, the valorisation of this type of residues can avoid pollution when efficient disposal is not suitable or as an alternative to an existing disposal method.

Table 8.2: Comparison of different substrates used for PHA production.

Substrate	Strain	Scale (l)	CDW (g l^{-1})	PHA (%)	PHA (g l^{-1})	Reference
Wheat flour hydrolysates	*R. eutropha*	0.5	73	70[1]	51	Koutinas et al., 2007
Crude glycerol	*R. eutropha*	2	50	48[1]	24	Mothes et al., 2007
Waste cooking oil	*R. eutropha*	0.25	4.3	75[2]	3.2	Lee et al., 2008
Wheat bran hydrolysate and potato waste biodigested	*H. boliviensis*	2	6.6	43[1]	2.8	Van-Thuoc et al., 2008
Sugarcane bagasse hydrolysate	*Burkholderia* sp. F24	0.5	25.8	44[1]	11.3	Lopes et al., 2011
Wheat straw hydrolysate	*H. boliviensis*	4	5.2	68[1]	3.5	López-Abelairas PhD Thesis, 2014
Cheese whey	*Haloferax mediterranei*	2	15.4	53[2]	7.9	Pais et al., 2016
Agro-industrial processing waters	*Halomonas* i4786	5	2.3	78	1.8	Elain et al., 2016

[1]P3HB; [2]P(3HB-co-3HV)

Different type of feedstocks used in the biorefineries, such as cereal mash, sugarcane or VFA derived from waste, were tested as target substrates for PHA production by *H. boliviensis* during this PhD Thesis. The main fermentation results obtained at bioreactor scale with these carbon sources are summarized in Table 8.3. Synthetic glucose reported the highest P3HB accumulation. The bioreactor operation in the case of the cereal mash presented an important influence on biomass growth, and reciprocally, on P3HB production. A poor P3HB production was obtained with sugarcane as substrate at bioreactor scale. While the mixture of VFA fed during the accumulation phase triggered 3HV incorporation into the P3HB at good yields.

Table 8.3: Main fermentation results obtained from different feedstocks with *H. boliviensis* on this Thesis.

Carbon source	Bioreactor operation[1]	CDW (g l^{-1})	RCM (g l^{-1})	PHA (g l^{-1})	PHA[2] (%)
Glucose	FD	48	13	35	73
Cereal mash	FD/SHF	28	12	16	58
	FD/SSF	49	24	26	52
Sugarcane	FD	19	17	2	12
VFA	FD	21	5	16	70

[1]FD: Fed-batch; [2]PHA: Only in the case of VFA as carbon source the PHA obtained was the copolymer P(3HB-co-3HV), for the others carbon sources, P3HB was the PHA obtained.

As far as we know, among all the previous studies about PHA production with *H. boliviensis*, only Van-Thuoc et al. (2008) utilised real agricultural residues as cheap carbon

sources, obtaining low production yields (Table 8.2). More extensive research was performed with other strains, mainly *R. eutropha,* by using renewable biomass or residues as substrates. The PHA production obtained in this Thesis using cereal mash as substrate and following a SSF strategy at bioreactor scale (26 g l^{-1}) is in the range of the best results obtained with complex substrates in previous studies (Table 8.2).

8.4 THESIS IMPLICATIONS AND LIMITATIONS

This Thesis provides insights of the effect of nutrients availability in the culture medium of *H. boliviensis* on PHA accumulation. Moreover, special attention was focused on the development of a faster technique for PHA quantification, which also provided information on the population dynamics of the bacterial culture, and the evaluation of cheap and renewable substrates as carbon source for biopolymer production.

The information presented in this Thesis increases the existing knowledge about halophilic microorganisms and can serve in the future as a starting point for the development of processes that can be integrated into a biorefinery. On the other side, this Thesis also unveils some drawbacks that may limit a more extensive exploitation of the special features of *H. boliviensis*, the maximal integral use of the substrates and the number of products to be obtained.

There is no doubt about the necessity of replacement of the petroleum-based plastics, and PHA is the biopolymer with the highest potential for this substitution. However, much more effort should be done; e.g. proper design of biorefinery systems is needed to avoid the errors involved in the past during petroleum refineries development.

There are alternative processes where *H. boliviensis* could make the difference. The halophilic characteristic of *H. boliviensis* could be a great advantage for the utilization of substrates that contain high intrinsic NaCl concentration. Seafood processing wastewater obtained from canning plants usually presents treatment challenges due to its high NaCl concentration. Mussel farming is extensively established in Galicia (Spain), consequently, mussel processing wastewater is produced in huge quantities. This is a residual material rich in glycogen, besides in NaCl (25-18 g l^{-1}). The integration of PHA and ectoine production in a biorefinery, based on the use of glycogen obtained from a residual industrial stream with high salinity is an alternative that has not been evaluated yet. *H. boliviensis* is a competitive PHA producer that could be the key microorganism for such process, taking profit of its halophilic behaviour. On the other hand, the operational strategy described on this Thesis, based on the simultaneous saccharification and fermentation (SSF), presents the flexibility to be applied with different bacterial strains or even with different substrates, which are susceptible to be hydrolysed.

Two of the potential advantages of *H. boliviensis* that have not been studied on this Thesis are the use of non-sterile conditions during the PHA production and the application of osmotic downshock for PHA recovery. The advantage of using halophilic bacteria in the recovery of PHA using less chemicals or energy than in processes with non-halophiles has been previously use with other strains. For example, Rathi et al (2012) used a simplified downstream processing based on osmotic lysis for recovering PHA produced from oil palm trunk sap and seawater as carbon source. The use of non-sterile conditions could be also an advantage. PHA production with other *Halomonas* strains has been shown to be feasible in

an open and continuous process (Yue et al., 2014). The requirement of sterile conditions is usually argued as a drawback when comparing the use of pure cultures with the production of PHA by mixed cultures (e.g. in wastewater treatment plants). These two topics can be considered as the following steps to be carried out before analysing the feasibility of PHA production from an economical point of view.

Another approach for further continue this work, could be a better exploitation of the streams used as substrates. To carry out this, a detailed fractionation of the substrates before fermentation into fractions that can be considered a valuable product by themselves, or the development of new platforms for obtaining different marketable products, should be implemented. All these improvements could help to decrease the gap between the current petroleum refineries and the biorefineries.

8.5 GENERAL CONCLUSIONS

Most conclusions have been stated in each specific chapter. The following are the most relevant:

On the mechanisms of PHA production by *H. boliviensis*

- PHA production presents a high dependence on the type and degree of nutrient limitation.

- There is no PHA accumulation when this bacterium is cultivated in a balanced nutrient medium.

- The simultaneous limitation by nitrogen combined with a low oxygen supply is more efficient than a single limitation by nitrogen or oxygen.

- Ectoine production was found to be mainly extracellular, despite the fact that this is usually described as an intracellular product.

- The supplementation of the culture medium with MSG enhances the total ectoine production and yield (ectoine/RCM), but it also improves biomass production and PHA concentration.

- A correlation between the PHA accumulation measured by GC and flow cytometry is established. A simplified PHA quantification method is proposed, based on the measurement of the OD and fluorescence of the cells stained with BODIPY 493/503.

- Two different bacterial populations (PHA-producing and non-producing cells) are distinguished during PHA accumulation in the same bioreactor under the same culture conditions.

On the integration of PHA production by *H. boliviensis* into a biorefinery

- 1G feedstocks, such as sugarcane juice and corn syrup, through the carboxylate platform, can be applied directly as the carbon source for growth and P3HB production.

- P3HB production with corn syrup is much higher than with sugarcane juice, at bench-top bioreactor.

- A novel configuration for the PHA production is developed (SSF), based on the industrial bioethanol process.

- Simultaneous saccharification and fermentation (SSF) of the corn juice for PHA production presents higher PH3B yields than the sequential SHF process (23.5 and 9.8%, respectively).

- Levulinic acid does not act as 3HV precursor with *H. boliviensis*.

- 2G feedstocks, through the carbon-rich chains platform (i.e. VFA), can be applied as the carbon source for growth and PHA production.

- *H. boliviensis* is able to grow and accumulate the co-polymer P(3HB-co-3HV) using such a complex and toxic substrate like VFA.

- By applying fed-batch fermentation in two stages, it was possible to increase the 3HV fraction of the copolymer without a significant change in the total PHA content. According to the specific use of the biopolymer, the process could be stopped at any moment, depending on the required 3HV fraction.

References

Abe H., Doi Y. 2001. Crystalline morphology, thermal properties, and enzymatic degradability of (R)-3-hydroxybutyric acid-based copolyesters. Riken Rev 42:7–10.

Agler M.T., Wrenn B.A., Zinder S.H., Angenent L.T. 2011. Waste to bioproduct conversion with undefined mixed cultures: the carboxylate platform. Appl Microbiol 29:70-78.

Anderson A.J., Dawes E.A. 1990. Ocurrence, metabolism, metabolic role and industrial uses of bacterial polyhydroxyalkanoates. Microbiol Rev 54(4):450-472.

Albuquerque M.G.E., Torres C.A.V., Reis M.A.M. 2010. Polyhydroxyalkanoate (PHA) productionby a mixed microbial culture using sugar molasses: effect of the influent substrate concentration on culture selection. Water Res 44:3419-3433.

Altschul S.F., Madden T.L., Schäffer A.A., Zhang J., Zhang Z., Miller W., Lipman D.J. 1997. Gapped BLAST and PSI-BLAST: a new generation of protein database search programs. Nucleic Acids Res 25:3389-3402.

Altschul S.F., Wootton J.C., Gertz E.M., Agarwala R., Morgulis A., Schäffer A.A., Yu Y.K. 2005. Protein database searches using compositionally adjusted substitution matrices. FEBS J 272:5101-5109.

Amache R., Sukan A., Safari M., Roy I., Keshavarz T. 2013. Advances in PHAs production. Chem Eng Trans 32:931-936.

APHA, 1998. Standard Methods for the Examination of Water and Waste Water, 20th Edition. American Public Health Association, Washington DC.

Arnoldini M., Heck T., Blanco-Fernández A., Hammes F. 2013. Monitoring of dynamic microbiological processes using real-time flow cytometry. PLoS ONE 8:80117.

Asrar J., Valentin H.E., Berger P.A., Tran M., Padgette S.R., Garbow J.R. 2002. Biosynthesis and properties of poly(3-hydroxybutyrate-co-3-hydroxyhexanoate) polymers. Biomacromolecules 3:1006-1012.

Barham P.J., Barker P., Organ S.J. 1992. Physical properties of poly(hydroxybutyrate) and copolymers of hydroxybutyrate and hydroxyvalerate. FEMS Microbiol Rev 103:289–98.

Baptist J.N. 1962. Process for preparing poly-3-hydroxybutyric acid. U.S patent 3044942.

Baronofsky J.J., Schreurs W.J.A., Kashket E.R. 1984. Uncoupling by acetic acid limits growth of and acetogenesis by Clostridium thermoaceticum. App Environmental Microbiol 48(6):1134-1139.

Bera A., Dubey S., Bhayani K., Mondal D., Mishra S., Ghosh P.K. 2015. Microbial synthesis of polyhydroxyalkanoate using seaweed-derived crude levulinic acid as co-nutrient. Int J Biol Macromol 72: 487-494

Bergsma M.H., Chotani G.K., Cuevas W.A., Duan G., Lee S.H., Qian Y., Sharma V., Shetty J.K., Strohm B.A., Teunissen P.J., Xu H. 2012. Neutral pH saccharification and fermentation, WO 2012/019159 A1.

Bertrand J.L., Ramsay B.A., Ramsay J.A., Chavarie C. 1990. Biosynthesis of poly-β-hydroxyalkanoates from pentoses by *Pseudomonas pseudoflava*. App Environmental Microbiol 56(10):3133-3138

Bhattacharyya A., Saha J., Haldar S., Bhowmic A., Mukhopadhyay U.K., Mukherjee J. 2014. Production of poly-3-(hydroxybutyrate-co-hydroxyvalerate) by *Haloferax mediterranei* using rice-based ethanol stillage with simultaneous recovery and re-use of medium salts. Extremophiles 18:463-470.

Borah B., Thakur P.S., Nigam J.N. 2002. The influence of nutritional and environmental conditions on the accumulation of poly-β-hydroxybutyrate in *Bacillus mycoides* RLJ B-017. J Appl Microbiol 92:776-783.

Bothast R.J., Schlicher M.A. 2005. Biotechnological processes for conversion of corn into ethanol. Appl Microbiol Biotechnol 67:19-25.

Brennan L., Owende P. 2010. Biofuels from microalgae – a review of technologies for production, processing, and extractions of biofuels and co-products. Renew Sustainable

Energy Rev 14:557-577.

Cavalheiro J.M., de Almeida M.C.M., da Fonseca M.M.R., de Carvalho C.C. 2013. Adaptation of *Cupriavidus necator* to conditions favoring polyhydroxyalkanoate production. J Biotechnol 164:309-317.

Cha J.Y., Hanna M.A. 2002. Levulinic acid based on extrusion and pressurized batch reaction. Ind Crop Prod 16:109-118.

Chakraborty P., Muthukumarappan K., Gibbons W.R., 2012. PHA productivity and yield of *Ralstonia eutropha* when intermittently or continuously fed a mixture of short chain fatty acids. J Biomed Biotechnol. doi:10.1155/2012/506153.

Chanprateep S. 2010. Current trends in biodegradable polyhydroxyalkanoates. J Biosci Bioeng 110(6):621-632.

Chen C.W., Don T-M., Yen H-F. 2006. Enzymatic extruded starch as a carbon source for the production of poly(3-hydroxybutyrate-co-3-hydroxyvalerate) by *Haloferax mediterranei*. Process Biochem 41:2289-2296.

Chen Q., Zhang L., Li X., Liu S., Li D. 2014. Poly-ß-hydroxybutyrate/ectoine co-production by ectoine-excreting strain *Halomonas salina*. Process Biochem 49:33-37.

Choi J-I., Lee S.Y. 1997. Process analysis and economic evaluation for poly(3-hydroxybutyrate) production by fermentation. Bioprocess Eng. 17:335-342.

Choi J., Lee S.Y., Han K. 1998. Cloning of the *Alcaligenes latus* polyhydroxyalkanoate biosynthesis genes and use of these genes for enhanced production of poly(3-hydroxybutyrate) in *Escherichia coli*. Appl Microbiol Biotechnol 64:4897–4903.

Chung Y.J., Cha H.J., Yeo J.S., Yoo Y.J., 1997. Production of poly(3-hydroxybutyric-co-3-hydroxyvaleric)acid using propionic acid by pH regulation. J Ferment Bioeng 83(5):492-495

Chung, S.H., Choi, G.G., Kim, H.W., Rhee, Y.H., 2001. Effect of levulinic acid on the production of poly(3-hydroxybutyrate-co-3-hydroxyvalerate) by *Ralstonia eutropha* KHB-8862. J Microbiol 39:79–82

Dahman Y., Ugwu C.U. 2014. Production of green biodegradable plastics of poly (3-hydroxybutyrate) from renewable resources of agricultural residues. Bioprocess Biosyst Eng 37 (8):1561-1568.

Dai Y., Lambert L., Yuan Z., Keller J. 2008. Characterisation of polyhydroxyalkanoate copolymers with controllable four-monomer composition. J Biotechnol 134:137-145.

Dastgheib S.M.M., Amoozegar M.A., Khajeh K., Shavandi M., Ventosa A. 2012. Biodegradation of polycyclic aromatic hydrocarbons by a halophilic microbial consortium. App Microbiol Biotechnol 95(3):789-798.

Davidov E.R., Kanygin P.S., Frankin O.A., Cheremnov I.V. 2010. Process for production of organic solvents. WO 2010/087737 A2.

Dean P.N., Bagwell C.B., Lindmo T., Murphy R.F., Salzman G.C. 1990. Data file standard for flow cytometry. Cytometry 11:323-332.

Díaz M., Herrero M., García L.A., Quirós C. 2010. Application of flow cytometry to industrial microbial bioprocesses. Biochem Eng J 48:385-407.

DiGregorio B.E. 2009. Biobased performance bioplastic: Mirel. Chem Biol 16(1):1-2.

Doi Y., Tamaki A., Kunioka M., Soga K. 1988. Production of copolyesters of 3-hydroxybutyrate and 3-hydroxyvalerate by Alcaligenes eutrophus from butyric and pentanoic acids. Appl Microbiol Biotechnol 28:330-334

Dong C., Bai X., Sheng H., Jiao L., Zhou H., Shao Z. 2015. Distribution of PAHs and the PAH-degrading bacteria in the deep–sea sediments of the high-latitude Artic Ocean. Biogeosciences 12(7):2163-2177.

Du G-C., Chen J., Gao H-J., Chen Y-G., Lun S-Y. 2000. Effects of environmental conditions on cell growth and poly-beta-hydroxybutyrate accumulation in *Alcaligenes eutrophus*. World J Microbiol Biotechnol 16:9-13.

Du G., Chen L.X.L., Yu J., 2004. High-efficiency production of bioplastics from biodegradable organic solids. J Polym Environ 12:89-94

Elain A., Le Grand A., Corre Y-M., Le Fellic M., Hachet N., Le Tilly V., Loulergue P., Audic J-L., Bruzaud S. 2016. Valorisation of local agro-industrial processing waters as growth media for polyhydroxyalkanoates (PHA) production. Ind Crops Prod 80:1-5.

Ensinas A.V., Nebra S.A., Lozano M.A., Serra L.M. 2007. Analysis of process steam demand reduction and electricity generation in sugar and ethanol production from sugarcane. Energ Convers Manage 48:2978-2987.

Eriksen M., Lebreton L.C.M., Carson H.S., Thiel M., Moore C.J., Borerro J.C., Galgani F., Ryan P.G., Reisser J. 2014. Plastic pollution in the world's oceans: more than 5 trillion plastic pieces weighing over 250,000 tons afloat at sea. PLoS ONE 9(12): e111913.

European Bioplastics http://www.european-bioplastics.org. Last access: 24 March 2017.

European Renewable Ethanol Association (ePURE) http://epure.org/resources/statistics/. Last access: 26 January 2015.

Global Agricultural Information Network (Gain). Brazil Biofuels Annual, 2015, Report Number BR15006,http://gain.fas.usda.gov/Recent%20GAIN%20Publications/Forms/AllItems.aspx. Last access: 26 January 2015.

González-Peñas H., Lu-Chau T.A., Moreira M.T., Lema J.M. 2015. Assessment of morphological changes of *Clostridium acetobutylicum* by flow cytometry during acetone/butanol/ethanol extractive fermentation. Biotechnol Lett 37:577-584.

Gregory M. 2009. Environmental implications of plastic debris in marine settings-entanglement, ingestion, smothering, hangers-on, hitch-hiking and alien invasions. Philos Trans R Soc Lond B Biol Sci 364:2013–2025.

Gullón B., Garrote G., Alonso J.L., Parajó J.C. 2007. Production of L-lactic acid and oligomeric compounds from apple pomace by simultaneous saccharification and fermentation: a response surface methodology assessment. J Agric Food Chem 55:5580-5587.

Guzmán H., Van-Thuoc D., Martín J., Hatti-Kaul R., Quillaguamán J. 2009. A process for the production of ectoine and poly(3-hydroxybutyrate) by *Halomonas boliviensis*. Appl Microbiol Biotechnol 84:1069-1077.

Harding K.G., Dennis J.S., von Blottnitz H., Harrison S.T.L. 2007. Environmental analysis of plastic production processes: Comparing petroleum-based polypropylene and polyethylene with biologically-based poly-β-hydroxybutyric acid using life cycle analysis. J Biotechnol 130:57-66.

Haywood G.W., Anderson A.J., Chu L., Dawes E.A. 1988. The role of NADH- and NADHP-linked acetoacetyl-CoA reductases in the poly-3-hydroxybutyrate synthesizing organism *Alcaligenes eutrophus*. FEMS Microbiol Lett 52:259–264.

Haywood G.W., Anderson A.J., Dawes E.A. 1989. The importance of PHB synthase substrate specificity in polyhydroxyalkanoate synthesis by *Alcaligenes eutrophus*. FEMS Microbiol Lett, 57:1–6.

Herbert D. 1961. The chemical composition of microorganisms as a function of their growth environment. In: Meynell CG, Gooder H (ed) Microbial reaction to the environment pp. 391–416, Cambridge University Press, Cambridge.

Hong S.K., Shirai Y., Nor Aini A.R., Hassan M.A. 2009. Semi-continuous anaerobic treatment of palm oil mill effluent for the production of organic acids and polyhydroxyalkanoates. Res J Environ Sci 3:552-559

Horiuchi J.-I., Shimizu T., Tada K., Kanno T., Kobayashi M. 2002. Selective production of organic acids in anaerobic acid reactor by pH control. Bioresource Technol 82:209-213

Huschner F., Grousseau E., Brigham C.J., Plassmeier J., Popovic M., Rha C., Sinskey A.J. 2015. Development of a feeding strategy for high cell and PHA density fed-batch fermentation of *Ralstonia eutropha* H16 from organic acids and their salts. Process Biochem 50:165-172

International Energy Statistics, http://www.eia.gov/cfapps/ipdbproject/IEDIndex3.cfm Last access: 26 January 2015.

Jaki T., Wolfsegger M.J. 2011. Estimation of pharmacokinetic parameters with the R package PK. Pharm Stat 10:284-288.

Jang J.H., Rogers P.L., 1996. Effect of levulinic acid on cell growth and poly-β- hydroxyalkanoate production by Alcaligenes sp. SH-69. Biotechnol Lett 18:219–224

Jaremko M., Yu J. 2011. The initial metabolic conversion of levulinic acid in *Cupriavidus necator*. J Biotechnol 155:293-298

Jiang Y., Marang L., Tamis J., van Loosdrecht M.C.M., Dijkman H., Kleerebezem R. 2012. Waste to resource: converting paper mill wastewater to bioplastics. Water Res 46:5517-5530.

Jin D., Chen J., Lun S., 1999. Production of poly(hydroxyalkanoate) by a composite anaerobic acidification-fermentation system. Process Biochem 34:829-833

Kacmar J., Carlson R., Balogh S.J. Srienc F. 2005. Staining and quantification of poly-3-hydroxybutyrate in *Saccharomyces cerevisiae* and *Cupriavidus necator* cell populations using automated flow cytometry. Cytometry Part A 69:27-35.

Kamm B., Kamm M. 2004. Principles of biorefineries. Appl Microbiol Biotechnol 64:137-145.

Kedia G., Passanha P., Dinsdale R.M., Guwy A.J., Lee M., Esteves S.R. 2013. Addressing the challenge of optimum polyhydroxyalkanoate harvesting: Monitoring real time process kinetics and biopolymer accumulation using dielectric spectroscopy. Bioresour Technol 134:143-150.

Keenan T.M., Tanenbaum S.W., Stipanovic A.J., Nakas J.P., 2004. Production and characterization of poly-β-hydroxyalkanoate copolymers from *Burkholderia cepacia* utilizing xylose and levulinic acid. Biotechnol Prog 20:1697–1704.

Kessler B., Witholt B. 2001. Factors involved in the regulatory network of polyhydroxyalkanoate metabolism. J Biotechnol 86:97-104.

Kilimann K.V., Doster W., Vogel R.F., Hartmann C., Ganzle M.G. 2006. Protection by sucrose against heat-induced lethal and sublethal injury of Lactococcus lactis: an FT-IR study. Biochim Biophys Acta 1764:1188–1197.

Kim J.H., Kim B.G., Choi C.Y. 1992. Effect of propionic acid on poly(beta-hydroxybutyric-co-beta-hydroxyvaleric) acid production by *Alcaligenes eutrophus*. Biotechnol Lett 14:903-906.

Kim B.S., Lee S.C., Lee S.Y., Chang H.N., Chang Y.K., Woo S.I. 1994. Production of poly(3-hydroxybutyric) acid by fed-batch culture of *Alcaligenes eutrophus* with glucose concentration control. Biotechnol Bioeng 43:892-898.

Kim G.J., Lee I.Y., Yoon S.C., Shin Y.C., Park Y.H. 1997. Enhanced yield and a high production of medium-chain-length poly(3-hydroxyalkanoates) in a two-step fed-batch cultivation of *Pseudomonas putida* by combined use of glucose and octanoate. Enzyme Microb Tech 20:500-505.

Kim D.Y., Park D.S., Kwon S.B., Chung M.G., Bae K.S., Park H.Y., Rhee Y.H. 2009. Biosynthesis of poly(3-hydroxybutyrate-co-3-hydroxyvalerate) copolyesters with a high molar fraction of 3-hydroxyvalerate by an insect-symbiotic Burkholderia sp. IS-01. J. Microbiol 47:651–656.

Koller M., Rodríguez-Contreras A. 2015. Techniques for tracing PHA-producing organisms and for qualitative and quantitative analysis of intra- and extracellular PHA. Eng Life Sci 15:558-81.

Koning G.J.M., Kellerhals M., van Meurs C., Witholt B. 1997. A process for the recovery of poly(hydroxyalkanoates) from Pseudomonads Part 2: Process development and economic evaluation. Bioprocess Eng 17:15-21.

Koutinas A.A., Xu Y., Wang R., Webb C. 2007. Polyhydroxybutyrate production from a novel feedstock derived from a wheat-based biorefinery. Enzyme Microb Technol 40:1035-1044.

Koutinas A.A., Vlysidis A., Pleissner D., Kopsahelis N., Garcia I.L., Kookos I.K., Papanikolaou S., Kwan T.H., Lin C.S.K. 2014. Valorization of industrial waste and by-product streams via fermentation for the production of chemicals and biopolymers. Chem Soc Rev 43:2587-2627

Kshirsagar P., Suttar R., Nilegaonkar S., Kulkarni S., Kanekar P. 2012. Scale up production of polyhydroxyalkanoate (PHA) at different aeration, agitation and controlled dissolved oxygen levels in fermenter using *Halomonas campisalis* MCM B-1027. J Biochem Tech 4:512-517.

Kunte H.J., Lentzen G., Galinski E.A. 2014. Industrial production of the cell protectant ectoine: protection mechanisms, processes and products. Current Biotechnol 3:10-25.

Lang Y-J., Bai L., Ren Y-N., Zhang L-H., Nagata S. 2011. Production of ectoine through a combined process that uses both growing and resting cells of *Halomonas salina* DSM 5928^T. Extremophiles 15:303-310.

Lee I.Y., Kim M.K., Chang H.N., Park Y.H. 1995. Regulation of poly-beta-hydroxybutyrate biosynthesis by nicotinamide nucleotide in *Alcaligenes eutrophus*. FEMS Microbiol Lett 131:35–39.

Lee J.H., Hong J., Lim H.C. 1997. Experimental optimization of fed-batch culture for poly-beta-hydroxybutiryc acid production. Biotechnol Bioeng 56:697-705.

Lee W-H., Loo C-Y., Nomura C.T., Sudesh K. 2008. Biosynthesis of polyhydroxyalkanoate copolymers from mixtures of plant oils and 3-hydroxyvalerate precursors. Bioresour Technol 99:6844-6851.

Lee S.-E., Li Q.X., Yu J. 2009. Diverse protein regulations on PHA formation in *Ralstonia eutropha* on short chain organic acids. Int J Biol Sci 5:215–225.

Lee J.H., Lee S.H., Yim S.S., Kang K.H., Lee S.Y., Park S.J., Jeong K.J. 2013. Quantified high-throughput screening of *Escherichia coli* producing poly (3-hydroxybutyrate) based on FACS. Appl Biochem Biotechnol 170:1767-1779.

Lemoigne M. 1926. Produits de deshydration et de polymerisation de l'acide b-oxybutyric. Bull Soc Chem Biol 8:770 – 782.

Liccioli T., Chambers P.J., Jiranek V. 2011. A novel methodology independent of fermentation rate for assessment of the fructophilic character of wine yeast strains. J Ind Microbiol Biotechnol 38:833-843.

Liu Y-S., Wu J-Y., Ho K-P. 2006. Characterization of oxygen transfer conditions and their effects on *Phaffia rhodozyma* growth and carotenoid production in shake-flask cultures. Biochem Eng J 27:331-335.

Lopar M., Spoljaric I.V., Atlic A., Koller M., Braunegg G., Horvat P. 2013. Five-step continuous production of PHB analyzed by elementary flux, modes, yield space analysis and high structured metabolic model. Biochem Eng J 79:57–70.

Lopes M.S.G., Gosset G., Rocha R.C.S., Gomez J.G.C., da Silva L.F. 2011. PHB biosynthesis in catabolite repression mutant of *Burkholderia sacchari*. Curr Microbiol 63:319-326.

López-Abelairas M. 2014. Bioprocess for production of fuels, chemicals and polymers from lignocellulosic materials. PhD Thesis. University of Santiago de Compostela.

López-Abelairas M., García-Torreiro M., Lú-Chau T., Lema J.M., Steinbüchel A. 2015. Comparison of several methods for the separation of poly(3-hydroxybutyrate) from *Cupriavidus necator* H16 cultures. Biochem Eng J 93:250-259.

Lu-Chau T., Guillán A., Roca E., Nuñez M.J., Lema J.M. 2001. Population dynamics of a continuous fermentation of recombinant *Saccharomyces cerevisiae* using flow cytometry. Biotechnol Prog 17:951-957.

Moncada J.B., Aristizábal V.M., Cardona C.A. 2016. Design strategies for sustainable biorefineries. Biochem Eng J 116:122-134.

Mothes G., Schnorpfeil C., Ackermann J-U. 2007. Production of PHB from crude glycerol. Eng Life Sci 7(5):475-479.

Mozejko-Ciesielska J., Kiewisz R. 2016. Bacterial polyhydroxyalkanoates: still fabulous? Microbiol Res 192:271-282.

Mravec F., Obruca S., Krzyzanek V., Sedlacek P., Hrubanova K., Samek O., Kucera D., Benesova P., Nebesarova J. 2016. Accumulation of PHA granules in *Cupriavidus necator* as seen by confocal fluorescence microscopy. FEMS Microbiol Lett 363(10) doi: 10.1093/femsle/fnw094.

Mumtaz T., Yahaya N.A., Abd-Aziz S., Rahman N.A.A., Yee P.L., Shirai Y., Hassan M.A. 2010. Turning waste to wealth-biodegradable plastics polyhydroxyalkanoates from palm oil mill effluent – a Malaysian perspective. J Clean Prod 18:1393-1402.

Nath A., Dixit M., Bandiya A., Chavda S., Desai A.J. 2008. Enhanced PHB production and scale up studies using cheese whey in fed batch culture of *Methylobacterium* sp. ZP24. Bioresour Technol 99:5749-5755.

Nonato R.V., Mantelatto P.E., Rossell C.E.V. 2001. Integrated production of biodegradable plastic, sugar and ethanol. Appl Microbiol Biotechnol 57:1-5.

Obruca S., Snajdar O., Svoboda Z., Marova I. 2013. Application of random mutagenesis to enhance the production of polyhydroxyalkanoates by *Cupriavidus necator* H16 on waste frying oil. World J Microbiol Biotechnol 29:2417-2428.

Oeding V., Schlegel H.G. 1973. Beta-ketothiolase from *Hydrogenomonas eutropha* H16 and its significance in the regulation of poly-beta-hydroxybutyrate metabolism. Biochem J 134:239-248.

Öhgren K., Bura R., Lesnicki G., Saddler J., Zacchi G. 2007. A comparison between simultaneous saccharification and fermentation and separate hydrolysis and fermentation using steam-pretreated corn stover. Process Biochem 42:834-839.

Onraedt A.E., Walcarius B.A., Soetaert W.K., Vandamme E.J. 2005. Optimization of ectoine synthesis through fed-batch fermentation of *Brevibacterium epidermis*. Biotechnol Prog 21:1206-1212.

Page W.J., Manchak J., Rudy B. 1992. Formation of poly(hydroxybutyrate-co-hydroxyvalerate) by Azotobacter vinelandii UWD. Appl Environ Microbiol 58:2866-2873

Page W.J., Cornish A. 1993. Growth of *Azotobacter vinelandii* UWD in fish peptone medium and simplified extraction of poly-ß-hydroxybutyrate. Appl Environ Microbiol 59:4236–4244.

Pais J., Serafim L.S., Freitas F., Reis M.A.M. 2016. Conversion of cheese whey into poly(3-hydroxybutyrate-co-3-hydroxyvalerate) by *Haloferax mediterranei*. New Biotechnol 33(1):224-230.

Palmeiro-Sánchez T., Personnal communication.

Pastor J.M., Salvador M., Argandoña M., Bernal V., Reina-Bueno M., Csonka L.N., Vargas C., Nieto J.J., Cánovas M. 2010. Ectoines in cell stress protection: uses and biotechnological production. Biotechnol Adv 28:782-801.

Pedrós-Alió C., Mas J., Guerrero R. 1985. The influence of poly-β-hydroxybutyrate accumulation on cell volume and buoyant density in *Alcaligenes eutrophus*. Arch Microbiol 143:178-184.

Pena R. 2009. Alternativas para la optimización de la producción industrial de bioetanol a partir de cereals [Alternatives to optimize the industrial production of bioethanol from cereals]. PhD Thesis. University of Santiago de Compostela.

Peoples O.P., Sinskey A.J. 1989. Poly-β-hydroxybutyrate (PHB) biosynthesis in *Alcaligenes eutrophus* H16. Identification and characterization of the PHB polymerase gene *(phbC)*. J Biol Chem 264:15298–15303.

Pfeiffer D., Wahl A., Jendrossek D. 2011. Identification of a multifunctional protein, PhaM, that determines number, surface to volume ratio, subcellular localization and distribution to daughter cells of poly(3-hydroxybutyrate), PHB, granules in *Ralstonia eutropha* H16. Mol Microbiol 82:936-951.

Philp J.C., Ritchie R.J., Guy K. 2013. Biobased plastics in a bioeconomy. Trends Biotechnol 31(2):65-67.

Plastics Europe – The Facts 2016. http://www.plasticseurope.org/Document/plastics–the-facts-2016-15787.aspx?Page=DOCUMENT&FolID=2. Last access: 16 March 2017

Pradella J.G.C., Taciro M.K., Mateus A.Y.P. 2010. High-cell-density poly(3-hydroxybutyrate) production from sucrose using *Burkholderia sacchari* culture in airlift bioreactor. Bioresour Technol 101:8355-8360.

Prestrelski S.J., Tedeschi N., Arakawa T., Carpenter J.F. 1993. Dehydration-induced conformational transitions in proteins and their inhibition by stabilizers. Biophys J 65:661–671.

Prieto A., Escapa I.F., Martínez V., Dinjaski N., Herencias C., Peña F., Tarazona N., Revelles O. 2016. A holistic view of polyhydroxyalkanoate metabolism in *Pseudomonas putida*. Environ Microbiol 18:341-357.

Quillaguamán J., Hatti-Kaul R., Mattiasson B., Alvarez M.T., Delgado O. 2004. *Halomonas boliviensis* sp. nov., an alkalitolerant, moderate halophile isolated from soil around a Bolivian hypersaline lake. Int J Syst Evol Microbiol 54:721–725.

Quillaguamán J., Hashim S., Bento F., Mattiasson B., Hatti-Kaul R. 2005. Poly(β-hydroxybutyrate) production by a moderate halophile, *Halomonas boliviensis* LC1 using starch hydrolysate as substrate. J Appl Microbiol 99:151–157.

Quillaguamán J., Delgado O., Mattiasson B., Hatti-Kaul R., 2006. Poly(beta-hydroxybutyrate) production by a moderate halophile, *Halomonas boliviensis* LC1. Enzyme Microb Tech 38:148-154.

Quillaguamán J., Muñoz M., Mattiasson B., Hatti-Kaul R. 2007. Optimizing conditions for poly(β-hydroxybutyrate) production by *Halomonas boliviensis* LC1 in batch culture with sucrose as carbon source. Appl Microbiol Biotechnol 74:981-986.

Quillaguamán J., Van-Thuoc D., Guzmán H., Guzmán D., Martín J., Everest A., Hatti-Kaul R. 2008. Poly(3-hydroxybutyrate) production by *Halomonas boliviensis* in fed-batch culture. Appl Microbiol Biotechnol 78:227-232.

Quillaguamán J., Guzmán H., Van-Thuoc D., Hatti-Kaul R. 2010. Synthesis and production of polyhydroxyalkanoates by halophiles: current potential and future prospects. Appl Microbiol Biotechnol 85:1687-1696.

Quintero J.A., Montoya M.I., Sánchez O.J., Giraldo O.H., Cardona C.A. 2008. Fuel ethanol production from sugarcane and corn: comparative analysis for a Colombian case. Energy 33:385-399.

Rathi D-N., Amir H.G., Abed R.M.M., Kosugi A., Arai T., Sulaiman O., Hashim R., Sudesh K. 2012. Polyhydroxyalkanoate biosynthesis and simplified polymer recovery by a novel moderately halophilic bacterium isolated from hypersaline microbial mats. J App Microbiol 114:384-395.

R Core Team, 2015. R: A language and environment for statistical computing. R Foundation for Statistical Computing, Vienna, Austria. URL http://www.R-project.org/.

Reid S.J., Abratt V.R. 2005. Sucrose utilisation in bacteria: genetic organisation and regulation. Appl Microbiol Biotechnol 67:312-321.

Reusch R.N., Sparrow A.W., Gardiner J. 1992. Transport of poly-β-hydroxybutyrate in human plasma. Biochimia et Biophysica Acta 1123:33-40.

Riss V., Mai W. 1988. Gas chromatographic determination of poly-β-hydroxybutyric acid in microbial biomasss after hydrochloric acid propanolysis. J Chromatography 445:285-289.

Rivera-Terceros P., Tito-Claros E., Torrico S., Carballo S., Van-Thuoc D., Quillaguamán J. 2015. Production of poly(3-hydroxybutyrate) by *Halomonas boliviensis* in an air-lift reactor. J Biol Res-Thessalon 22:8 DOI 10.1186/s40709-015-0031-6.

Rochman C.M., Browne M.A., Halpern B.S., Hentschel B.T., Hoh E., Karapanagioti H.K., Rios-

Mendoza L.M., Takada H., Teh S., Thompson R.C. 2013. Classify plastic waste as hazardous. Nature 494:169–171.

Ruan W., Chen J., Lun S., 2003. Production of biodegradable polymer by *A. eutrophus* using volatile fatty acids from acidified wastewater. Process Biochem 39:295-299.

Ryu H.W., Hahn S.K., Chang Y.K., Chang H.N. 1997. Production of poly(3-hydroxybutyrate) by high cell density fed-batch culture of *Alcaligenes eutrophus* with phosphate limitation. Biotechnol Bioeng 55:28-32.

Salehizadeh H., Van Loosdrecht M.C.M., 2004. Production of polyhydroxyalkanoates by mixed cultures: recent trends and biotechnological importance. Biotechnol Adv 22:261-279

Sánchez R.J., Schripsema J., da Silva L.F., Taciro M.K., Pradella J.G.C., Gomez J.G.C. 2003. Medium-chain-length polyhydroxyalkanoic acids (PHAmcl) produced by *Pseudomonas putida* IPT 046 from renewable sources. European Polymer J 39(7):1385-1394.

Sankhla I.S, Bhati R., Singh A.K., Mallick N. 2010. Poly(3-hydroxybutyrate-co-3-hydroxyvalerate) co-polymer production from a local isolate, Brevibacillus invocatus MTCC 9039. Bioresource Technol 101:1947-1953.

Satpute S., Banat I., Dhakephalkar P., Banpurkar A., Chopade B. 2010. Biosurfactants, bioemulsifiers and exopolysaccharides from marine microorganisms. Biotechnol Adv 28:436–50.

Sauer T., Galinski E.A. 1998. Bacterial milking: a novel bioprocess for production of compatible solutes. Biotechnol Bioeng 57:306–313.

Schlegel H.G., Kaltwasser H., Gottschalk G. 1961. Ein Submersverfahren zur Kultur wasserstoffoxidierender Bakterien: Wachstumsphysiologische Untersuchungen. Archiv Für Mikrobiologie 38:209-222.

Schubert P., Steinbüchel A., Schlegel H.G. 1988. Cloning of the *Alcaligenes eutrophus* gene for synthesis of poly-β-hydroxybutyric acid and synthesis of PHB in *Escherichia coli*. J Bacteriol 170:5837–5847.

Setati M.E. 2010. Diversity and industrial potential of hydrolase-producing halophilic/halotolerant eubacteria. Afr J Biotechnol 9:1555–60.

Slater S., Houmiel K.L., Tran M., Mitsky T.A., Taylor N.B., Padgette S.R., Gruys K.J. 1998. Multiple β-ketothiolases mediate poly(β-hydroxyalkanoate) copolymer synthesis in *Ralstonia eutropha*. J Bacteriol 180:1979–1987.

Society for Analytical Cytology. 1990. Data file standard for flow cytometry. Cytometry 11:323-332.

Söderström J., Galbe M., Zacchi G. 2005. Separate versus simultaneous saccharification and fermentation of two-step steam pretreated softwood for ethanol production. J Wood Chem Technol 25:187-202.

Srienc F., Arnold B., Bailey J.E. 1984. Characterization of intracellular accumulation of poly-beta-hydroxybutyrate (PHB) in individual cells of *Alcaligenes eutrophus* H16 by flow cytometry. Biotechnol Bioeng 26:982-987.

Stanbury P.F., Whittaker A., Hall S.J. 1995. Chapter 6, in: Principles of Fermentation Technology, second ed., Butterworth-Heinemann, Jordon Hill, Oxford, pp. 147–164.

Takagi M., Abe S., Suzuki S., Emert G.H., Yata N. 1977. A method for production of alcohol direct from cellulose using cellulase and yeast. In: Process Bioconversion Symposium, 551–71.

Tan D., Xue Y-S., Aibaidula G., Chen G-Q. 2011. Unsterile and continuous production of polyhydroxybutyrate by *Halomonas* TD01. Bioresource Technol 102:8130-8136.

Tracy B.P., Gaida S.M., Papoutsakis E.T. 2010. Flow cytometry for bacteria: enabling metabolic engineering, synthetic biology and the elucidation of complex phenotypes. Curr Opin Biotechnol 21:85-99.

Trinder P. 1969. Determination of blood glucose using 4-amino phenazone as oxygen acceptor. J

Clin Pathol 22(2):246

Uad I., Silva-Castro G.A., Pozo C., González-López J., Calvo C. 2010. Biodegradative potential and characterization of bioemulsifiers of marine bacteria isolated from samples of seawater, sediment and fuel extracted at 4000 m of depth (Prestige wreck). Int Biodeter Biodegr 64(6):511-518.

U.S. Department of Energy, http://www.afdc.energy.gov/fuels/ethanol_feedstocks.html Last access: 26 January 2015.

Van-Thuoc D., Quillaguamán J., Mamo G., Mattiasson B. 2008. Utilization of agricultural residues for poly(3-hydroxybutyrate) production by *Halomonas boliviensis* LC1. J App Microbiol 104:420-428.

Van-Thuoc D., Guzmám H., Quillaguamán J., Hatti-Kaul R. 2010. High productivity of ectoines by *Halomonas boliviensis* using a combined two-step fed-batch culture and milking process. J Biotechnol 147:46-51.

van't Riet K. 1979. Review of measuring methods and results in nonviscous gas-liquid mass transfer in stirred vessels. Ind Eng Chem Proc DD 18(3):357-364.

Visser A.S., Postma P.W. 1973. Permeability of *Azotobacter vinelandii* to cations and anions. Biochimica et Biophysica Acta 298:333-340.

Wahl A., Schuth N., Pfeiffer D., Nussberger S., Jendrossek D. 2012. PHB granules are attached to the nucleoid via PhaM in *Ralstonia eutropha*. BMC Microbiol 12:262.

Wang F., Lee S.Y. 1997. Poly(3-hydroxybutyrate) production with high productivity and high polymer content by a fed-batch culture of *Alcaligenes latus* under nitrogen limitation. Appl Environ Microbiol 63:3703–3706.

Wang J., Yu J., 2000. Kinetic analysis on inhibited growth and poly(3-hydroxybutyrate) formation of *Alcaligenes eutrophus* on acetate under nutrient-rich conditions. Process Biochem 36:201-207.

Ward A.C., Rowley B.I., Dawes E.A. 1977. Effect of oxygen and nitrogen limitation on poly-β-hydroxybutyrate biosynthesis in ammonium-grown *Azotobacter beijerinckii*. J Gen Microbiol 102:61-68.

Witholt B., Lageveen R.G. 1992. Process for producing polyesters by fermentation; a process for producing optically active carboxylic acids and esters. US Patent No. 5,135,859. Washington, DC: U.S. Patent and Trademark Office.

Yan Q., Du G., Chen J. 2003. Biosynthesis of polyhydroxyalkanoates (PHAs) with continuous feeding of mixed organic acids as carbon sources by *Ralstonia eutropha*. Process Biochem 39:387-391.

Yin J., Chen J-C., Wu Q., Chen G-Q. 2015. Halophiles, coming stars for industrial biotechnology. Biotechnol Adv 33(7):1433-1442.

York G.M., Stubbe J., Sinskey A.J. 2001. New insight into the role of the PhaP phasin of *Ralstonia eutropha* in promoting synthesis of polyhydroxybutyrate. J Bacteriol 183:2394-2397.

Yu J. 2001. Production of PHA from starchy wastewater via organic acids. J Biotechnol 86:105-112.

Yu J., Si Y., Wong W.K.R. 2002. Kinetics modeling of inhibition and utilization of mixed volatile fatty acids in the formation of polyhydroxyalkanoates by *Ralstonia eutropha*. Process Biochem 37:731-738.

Yu J., Chen L.X.L., Sato S. 2009. Biopolyester synthesis and protein regulations in *Ralstonia eutropha* on levulinic acid and its derivatives from biomass refining. J Biobased Mater Bio 3:113–122.

Yue H., Ling C., Yang T., Chen X., Chen Y., Deng H., Wu Q., Chen J., Chen G-Q. 2014. A seawater-based open and continuous process for polyhydroxyalkanoates production by

recombinant *Halomonas campaniensis* LS21 grown in mixed substrates. Biotechnol Biofuel 7:108-120.

Zhang L-H., Lang Y-J., Nagata S. 2009. Efficient production of ectoine using ectoine-excreting strain. Extremophiles 13:717-724.

Zinn M., Witholt B., Egli T. 2001. Occurrence, synthesis and medical application of bacterial polyhydroxyalkanoate. Adv Drug Deliver Rev 53:5-21.

Zoetemeyer R.J., Heuvel J.C., Cohen A. 1982. pH influence on acidogenic dissimilation of glucose in anaerobic digester. Wat Res 16:303–311.

List of Tables

Chapter 8

8.1: Comparison of several PHA producer strains.
8.2: Comparison of different substrates used for PHA production.
8.3: Main fermentation results obtained from different feedstocks with *H. boliviensis* on this Thesis.

List of Figures

3.7: Different production yields: (A) residual biomass; and (B) P3HB, on consumed glucose during fermentations with nitrogen limitation (black triangles), oxygen limitation (black squares) and nitrogen limitation with low oxygen supply (black rounds).

3.8: A. Glucose consumption during fermentations with nitrogen limitation (black triangles), oxygen limitation (black squares) and nitrogen limitation with low oxygen supply (black rounds). B. Global carbon balance, percentage of the carbon source distributed in P3HB (black), RCM (grey), estimated CO_2 (hatched) and other byproducts (white).

Chapter 4

4.1: Scheme of a typical flow cytometer. Source: Thermo Fisher Scientific.

4.2: Forward and side scattering signals measured by flow cytometry for different P3HB accumulation states of *H. boliviensis*: (A) 7% and (B) 67.5% w/w P3HB/CDW. And TEM photographs of the bacteria observed at the same accumulation states: (C) 7% and (D) 67.5% w/w P3HB/CDW. Samples at 7 and 67.5% w/w P3HB/CDW were taken at 24 and 64 h of growth, respectively, during fermentation with nitrogen limitation and low oxygen supply.

4.3: Different FC signals obtained from *H. boliviensis* culture with 67.5% w/w P3HB/CDW: (A) fluorescence histogram; (B) fluorescence versus forward scatter dot plot and (C) forward scatter histogram. The sample was taken at 64 h of growth, during fermentation with nitrogen limitation and low oxygen supply.

4.4: Calibration curve for *H. boliviensis* cells stained with BODIPY 493/503. The mean value of the fluorescence signal for the population PHB^+ minus its intrinsic fluorescence obtained by FC is represented *versus* the mass of P3HB per mass of cells determined by gas chromatography and gravimetrically, respectively. The regression line obtained is: $FL1_{PHA}{}^+ - FL1_0 = 83.94 \cdot P3HB/RCM + 29.21$; with a correlation factor (R^2) of 0.975.

4.5: Calibration curves for biomass growth measured gravimetrically (CDW) or by the optical density (OD) of the sample. Biomass modification due to bacterial division (white rhombuses) presented a different correlation than biomass modification by PHA accumulation (black circles). The respective regression lines and correlations factors obtained were: $CDW_{growth} = 1.3297 \cdot OD + 0.7294$; $R^2 = 0.943$ and $CDW_{accumulation} = 0.2007 \cdot OD + 9.4985$; $R^2 = 0.965$.

4.6: Validation of the FC correlations (dotted line and white symbols) with the experimental data (solid line and black symbols) obtained from bioreactor fermentations at two different conditions: nitrogen limitation (A and C) and nitrogen limitation with low oxygen supply (B and D). The parameters represented are P3HB percentage (square), P3HB concentration (rhombuses), RCM concentration (circle) and P3HB productivity (triangle).

4.7: Mean value of fluorescence from PHA^+ cells region (asterisk and dotted line), percentage of PHA^+ cells (crosses), RCM (white circles) and P3HB concentration measured by GC (rhombuses) for bioreactor fermentations at two different conditions: nitrogen limitation and nitrogen limitation with low oxygen supply.

Chapter 5

5.1: Process scheme for bioethanol production from grain.

5.2: Process scheme for bioethanol production from sugarcane.

5.3: Main steps in corn pretreatment.

5.4: P3HB accumulation (white squares), RCM (black crosses) and P3HB concentration (black triangles) during flask scale fermentation using corn syrup (A) and glucose (B) as carbon sources.

5.5: P3HB accumulation (white squares), RCM (black crosses) and P3HB concentration (black triangles) during flask scale fermentation using sugarcane juice (A) and sucrose (B) as carbon sources.

5.6: Sucrose (grey bar) and fructose (white bar) consumption profile in flask scale.

Chapter 6

Chapter 7

List of publications

Journal publications

García-Torreiro M., López-Abelairas M., Lú-Chau T., Lema J.M. 2016. Application of flow cytometry for monitoring the production of poly(3-hydroxybutyrate) by *Halomonas boliviensis*. Biotechnology Progress. DOI: 10.1002/btpr.2373

García-Torreiro M., López-Abelairas M., Lú-Chau T., Lema J.M. 2016. Production of poly(3-hydroxybutyrate) by simultaneous saccharification and fermentation of cereal mash using *Halomonas boliviensis*. Biochemical Engineering Journal, 114:140-146.

García-Torreiro M., Lú-Chau T., Lema J.M. 2016. Effect of nitrogen and/or oxygen concentration on poly(3-hydroxybutyrate) accumulation by *Halomonas boliviensis*. Bioprocess Biosystems Engineering, 39(9):1365-1374.

García-Torreiro M., Lú-Chau T., Steinbüchel A., Lema J.M. 2016. Waste to bioplastic conversion by the moderate halophilic bacterium *Halomonas boliviensis*. Chemical Engineering Transactions, 49:163-168.

Patent

García-Torreiro M., López-Abelairas M., Lú-Chau T., Lema J.M. 2016. Procedimiento para la producción de polihidroxialcanoatos y de ectoína mediante sacarificación y fermentación simultánea a partir de hidrolizados de grano de cereal. ES 2 562 377 B2.

Conference papers

Oral contributions

García-Torreiro M., López-Abelairas M., Lú-Chau T., Lema J.M. 2016. Simultaneous saccharification and fermentation for poly(3-hydroxybutyrate) production from cereal mash. Bio.Iberoamérica 2016: Biotecnología Integrando Continentes. Salamanca (Spain).

García-Torreiro M., Lú-Chau T., Steinbüchel A., Lema J.M. 2016. Waste to bioplastic conversion by the moderate halophilic bacterium *Halomonas boliviensis*. 5th International Conference on Industrial Biotechnology. Bologna (Italy).

García-Torreiro M., López-Abelairas M., Lú-Chau T., Lema J.M. 2014. Production of polyhydroxyalkanoates by *Halomonas boliviensis* from first generation bioethanol streams. 10th International Conference on Renewable Resources and Biorefineries. Valladolid (Spain).

García-Torreiro M., López-Abelairas M., Lú-Chau T., Lema J.M. 2013. Application of flow cytometry for monitoring the production of poly-3-hydroxybutyrate (PHB) by halophilic bacterium. European Symposium on Biopolymers. Lisbon (Portugal).

López-Abelairas M., García-Torreiro M., Lú-Chau T., Lema J.M. 2013. Producción de polihidroxialcanoatos (PHAs) a partir de hidrolizado de paja de trigo. Red Lignocel 2013. Pontevedra (Galicia), Spain.

Poster

García-Torreiro M., López-Abelairas M., Lú-Chau T., Lema J.M. 2016. Integrated production of polyhydroxyalkanoates into 1G and 2G biorefineries. 15th International Symposium on Biopolymers. Madrid (Spain).

López-Abelairas M., García-Torreiro M., Lú-Chau T., Lema J.M. 2013. Production of polyhydroxyalkanoates from biological pretreated wheat straw. European Symposium on Biopolymers. Lisbon (Portugal).